# FLAME DRIVING OF LONGITUDINAL INSTABILITIES IN LIQUID FUELED DUMP COMBUSTORS

Final Report

Prepared for

Office of Naval Research

by

Ben T. Zinn, Uday G. Hegde, Dierk Reuter and B. R. Daniel

Georgia Institute of Technology

School of Aerospace Engineering

Atlanta, GA 30332



Contract No. SFRC #N00014-84-K-0470

October 1988

UNCLASSIFIED

SECURITY CLASSIFICATION OF THIS PAGE

AD-A202 292

# REPORT DOCUMENTATION PAGE

| | |
|---|---|
| 1a. REPORT SECURITY CLASSIFICATION: Unclassified | 1b. RESTRICTIVE MARKINGS |
| 2a. SECURITY CLASSIFICATION AUTHORITY | 3. DISTRIBUTION/AVAILABILITY OF REPORT: Approved for public release; Distribution is unlimited |
| 2b. DECLASSIFICATION/DOWNGRADING SCHEDULE | |
| 4. PERFORMING ORGANIZATION REPORT NUMBER(S) | 5. MONITORING ORGANIZATION REPORT NUMBER(S) |
| 6a. NAME OF PERFORMING ORGANIZATION: Georgia Institute of Technology School of Aerospace Engr. / 6b. OFFICE SYMBOL (If applicable) | 7a. NAME OF MONITORING ORGANIZATION: Office of Naval Research |
| 6c. ADDRESS (City, State and ZIP Code): Atlanta, Georgia 30332 | 7b. ADDRESS (City, State and ZIP Code) |
| 8a. NAME OF FUNDING/SPONSORING ORGANIZATION / 8b. OFFICE SYMBOL (If applicable) | 9. PROCUREMENT INSTRUMENT IDENTIFICATION NUMBER: SFRC N00014-84-K-0470 |
| 8c. ADDRESS (City, State and ZIP Code) | 10. SOURCE OF FUNDING NOS. — PROGRAM ELEMENT NO. / PROJECT NO. / TASK NO. / WORK UNIT NO. |
| 11. TITLE (Include Security Classification): Flame Driving of Longitudinal Instabilities in Liquid Fueld ... | |
| 12. PERSONAL AUTHOR(S): Ben T. Zinn and Uday G. Hegde | |
| 13a. TYPE OF REPORT: Final Report / 13b. TIME COVERED: FROM 7/1/84 TO 2/29/88 | 14. DATE OF REPORT (Yr., Mo., Day): October 1, 1988 / 15. PAGE COUNT: 119 |
| 16. SUPPLEMENTARY NOTATION | |
| 17. COSATI CODES — FIELD / GROUP / SUB. GR. | 18. SUBJECT TERMS (Continue on reverse if necessary and identify by block number): Coaxial dump type ramjet, flame driving, combustion, acoustics longitudinal instability, vortex shedding, shear layer instability |

19. ABSTRACT (Continue on reverse if necessary and identify by block number)

See reverse side

| | |
|---|---|
| 20. DISTRIBUTION/AVAILABILITY OF ABSTRACT: UNCLASSIFIED/UNLIMITED ☒ SAME AS RPT. ☐ DTIC USERS ☐ | 21. ABSTRACT SECURITY CLASSIFICATION |
| 22a. NAME OF RESPONSIBLE INDIVIDUAL | 22b. TELEPHONE NUMBER (Include Area Code) / 22c. OFFICE SYMBOL |

DD FORM 1473, 83 APR — EDITION OF 1 JAN 73 IS OBSOLETE.

UNCLASSIFIED

SECURITY CLASSIFICATION OF THIS PAGE

This report describes the results of experimental and theoretical investigations of the mechanisms by which the core flow combustion process in coaxial, single inlet, dump type ramjet engines drives longitudinal combustion instabilities. To this end, the behavior of V-shaped flames, similar to those often occurring in ramjet combustors, stabilized in longitudinal acoustic fields has been studied. The presence of burning vortical structures is observed in the flame region. These structures appear at frequencies close to the first natural acoustic frequency of the combustor and are believed to be connected with a shear layer type of instability of the flame. Experiments conducted show that the unsteady combustion in these structures is capable of driving the acoustics at the fundamental acoustic mode frequency. With increase in fuel air ratio, a spontaneous instability involving the fundamental mode is observed and explained in terms of increased driving associated with the higher, unsteady heat release rates. The results of experiments conducted with external acoustic excitation of the flame at different frequencies are also reported and confirm the idea that the vortical structures arise due to a fluid mechanical instability of the flame. It is shown that the interactions between the vortical structures and the system's acoustic field affect the heat release rates from the flame and provide a mechanism for the driving of longitudinal mode instabilities.

TABLE OF CONTENTS

# PREFACE

This report describes research conducted under Contract No. SFRC N00014-84-K-0470 during the period 7/1/84 - 2/29/88. The report consists of two parts:

(a) Part I describes the results obtained during the original contract period 7/1/84 - 6/30/87.

(b) Part II consists of the paper "Flowfield Measurements in an Unstable Ramjet Burner" and it provides results obtained during the contract extension period 7/1/87 - 2/29/88.

## ABSTRACT

This report describes the results of experimental and theoretical investigations of the mechanisms by which the core flow combustion process in coaxial, single inlet, dump type ramjet engines drives longitudinal combustion instabilities. To this end, the behavior of V-shaped flames, similar to those often occurring in ramjet combustors, stabilized in longitudinal acoustic fields has been studied. The presence of burning vortical structures is observed in the flame region. These structures appear at frequencies close to the first natural acoustic frequency of the combustor and are believed to be connected with a shear layer type of instability of the flame. Experiments conducted show that the unsteady combustion in these structures is capable of driving the acoustics at the fundamental acoustic mode frequency. With increase in fuel air ratio, a spontaneous instability involving the fundamental mode is observed and explained in terms of increased driving associated with the higher, unsteady heat release rates. The results of experiments conducted with external acoustic excitation of the flame at different frequencies are also reported and confirm the idea that the vortical structures arise due to a fluid mechanical instability of the flame. It is shown that the interactions between the vortical structures and the system's acoustic field affect the heat release rates from the flame and provide a mechanism for the driving of longitudinal mode instabilities.

PART I

(7/1/84 - 6/30/87)

# Chapter I

## INTRODUCTION

The primary objective of the research program described in this report was the determination of the characteristics of the driving by the combustion process which is responsible for the occurrence of low frequency longitudinal instabilities in liquid fueled, single inlet, coaxial dump type ramjet engines (see Fig. 1). Recent developments of such ramjet engines, as part of integral rocket-ramjet propulsion systems[1-3], have been hindered by the occurrences of destructive combustion instabilities[4-11]. These instabilities are characterized by either low frequency (i.e., rumble) or high frequency (i.e., screech) pressure and velocity oscillations[4,12]. The low frequency rumble is in the range of 50-500 Hertz and it is generally characterized by longitudinal acoustic oscillations in the inlet section and the combustor[11,13,14] or a combination of a longitudinal acoustic oscillation in the inlet section and a bulk-mode type oscillation in the combustor[8]. In contrast, the high frequency screech occurs when one of the tangential acoustic modes of the combustor is excited (e.g., see Table I in Ref.5). Of the two, the low frequency, longitudinal instability presents a more serious problem because the interaction of the resulting pressure oscillations with the inlet shock system may result in inlet unstarting and loss of engine performance. In addition, this type of instability may result in excessive vibrational loads on the system. On the other hand screech type instabilities result in an increase in heat transfer rates to engine components which may shorten the engine's life time and compromise its performance. This type of instability can, however, be controlled by use of acoustic liners, unless the

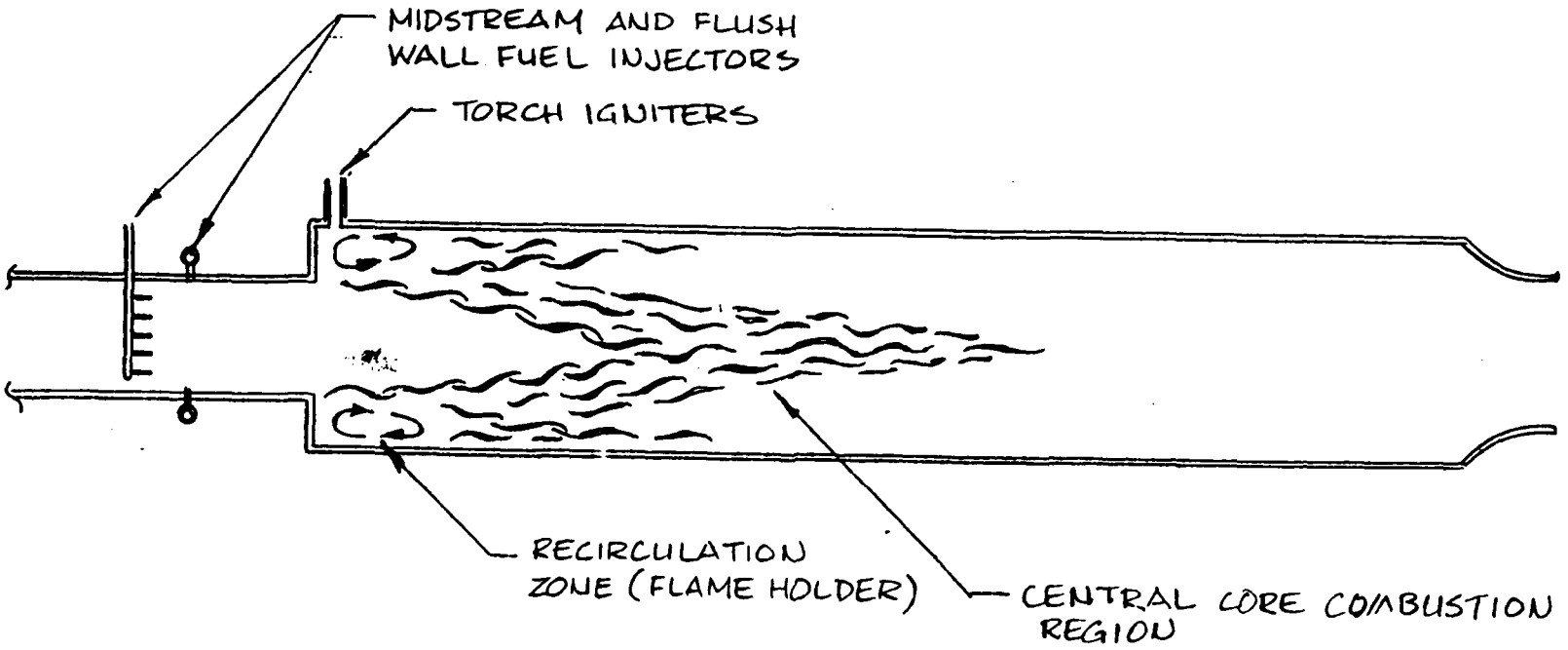


Figure 1. Schematic of a Typical Liquid Fueled, Single Inlet, Coaxial, Dump Type Ramjet Engine.

engine is large and the transverse modes are characterized by low frequencies[5].

While both types of instabilities have the potential for severely hindering the development of present and future ramjet engine programs, of the two, the low frequency, longitudinal instability is potentially more troublesome because of the lack of effective means for its suppression. At present there is no proven model capable of predicting the conditions under which such an instability may occur and its elimination often involves a costly and time consuming trial and error approach. To develop a more rational approach for the treatment of low frequency ramjet instabilities, understanding of the processes responsible for their occurrence needed to be extended. This problem was addressed in the research program described in this report.

To date, combustion instabilities have appeared in almost every type of propulsion system, including liquid[15] and solid[16] rocket motors, air breathing engines[17], ramjets[18] and so on. In the majority of cases the combustion process provides the energy required for the excitation and maintenance of the observed oscillations. These oscillations also experience energy losses due to viscous dissipation, heat conduction, acoustic energy radiation and convection through the exhaust nozzle[19,20]. During an instability, the amplitude of the combustor oscillation grows in time as long as the energy added to the oscillation per cycle is larger than the energy lost per cycle due to the above mentioned loss processes. As the amplitude grows, some or all of the energy gain and loss processes become amplitude dependent and an amplitude is reached at which the energy added to the

oscillation per cycle equals the energy lost per cycle. When a balance between the energy addition and removal processes is established, the amplitude of the oscillation remains constant as long as the above mentioned balance is not disturbed.

An unstable engine can be stabilized by either decreasing the energy supplied to the oscillation by the combustion process (or any other process) or increasing the disturbance losses or by doing both. To accomplish either of these steps, a thorough understanding of the processes in question is required.

According to Rayleigh's criterion[21,22], driving of the combustor's oscillations by the combustion process will occur if

$$E = \int_V \int_0^T p\, Q\, dt dV \qquad > 0 \qquad (1)$$

In the above integral, E,p,Q,t,T, and V represent the total energy added to the system per cycle, the pressure oscillation, the oscillatory heat addition by the combustion process, time, period of the oscillation and volume of the system, respectively. The integration is performed over the volume of interest to account for all possible energy addition processes. When p and Q are in phase, the above integral is positive and vice versa. Also, p and Q might be in phase in some portion of V and out of phase in the remainder of V. In such a case, the sign of E will depend upon the relative contributions of the "driving" and "damping"(i.e., sections where p and Q are out of phase) fractions of V. Combustion instability will occur when the integral E,

Eq.(1), is larger than some quantity L which describes the total losses experienced by the system's oscillation per cycle.

In coaxial, single inlet, dump type ramjet combustors (see Fig. 1), liquid fuel is injected into the air flow in the inlet section upstream of the dump plane. The liquid fuel drops evaporate and mix with the air as they both move towards the combustor. The flow expands as it enters the combustor and a recirculation region, which serves as a flame holder, is established near the step. While it is not clear what fraction of the fuel burns in the recirculation zone, it is expected that most of the fuel burns in the flame around the central, jet-like, core flow ( see Fig. 1) which disappears within a few inlet section diameters downstream of the dump plane. The resulting ramjet flow field is extremely complex involving turbulent mixing, a recirculating flow region, a jet flow region and finite width combustion zones. In addition, shear layers are formed by the flow at the dump as well as by the flame itself which separates the relatively low speed unburned flow from the relatively higher speed burned (reacted) flow. These shear layers, via a fluid mechanical instability mechanism, may roll up into vortices as has been confirmed in the present[23,24] ramjet studies described in this report as well as by other research groups[25,26]. Hence, it is not surprising that, to date, attempts to model steady state ramjet flows have only met with limited success and they have involved some empiricism as well as the latest advances in computational modelling techniques[27-30]. This complexity increases considerably when one attempts to model the unsteady operation of a ramjet engine, as is required in combustion instability analyses.

The question of whether periodic heat release by the combustion process in a ramjet occurs and if so whether it occurs in phase with the pressure oscillation as required by Rayleigh's criterion for combustion instability (i.e., see Eq.(1)) depends upon the response of the combustion process to local pressure and velocity oscillations. For example, local pressure and velocity oscillations may initiate a fluid dynamical instability of the flame causing it to roll up into vortices. If this vortex shedding becomes periodic, the unsteady combustion in the vortices would also become periodic. If the resulting periodic heat release rate is in phase with the local pressure oscillation, an amplification of the oscillation will occur as indicated by Eq. (1) above. Consequently, it is important to develop an understanding of the combustion process response to local oscillations (or disturbances) as such an understanding may lead to means for reducing or minimizing combustion instabilities in ramjets.

The current research program has been concerned with this understanding of the basic mechanisms of ramjet instability. The evidence to date supports the idea that a major culprit causing ramjet instabilities is the unsteady heat release from large scale coherent vortical structures that exist in the core flame region of the ramjet combustor. A sequence of frames taken by means of high speed shadowgraphy in the experimental set up developed at Georgia Tech to study ramjet instabilities is shown in Fig.2. The flame is stabilized in a rectangular combustor by a heated,thin nichrome wire (see Fig.3). The vortical structures are clearly visible. Note also that the vortical structures arise symmetrically on the top and lower flame fronts and cause finite width combustion zones. As will be discussed in the next chapter, it is believed that these vortical structures arise by means of a

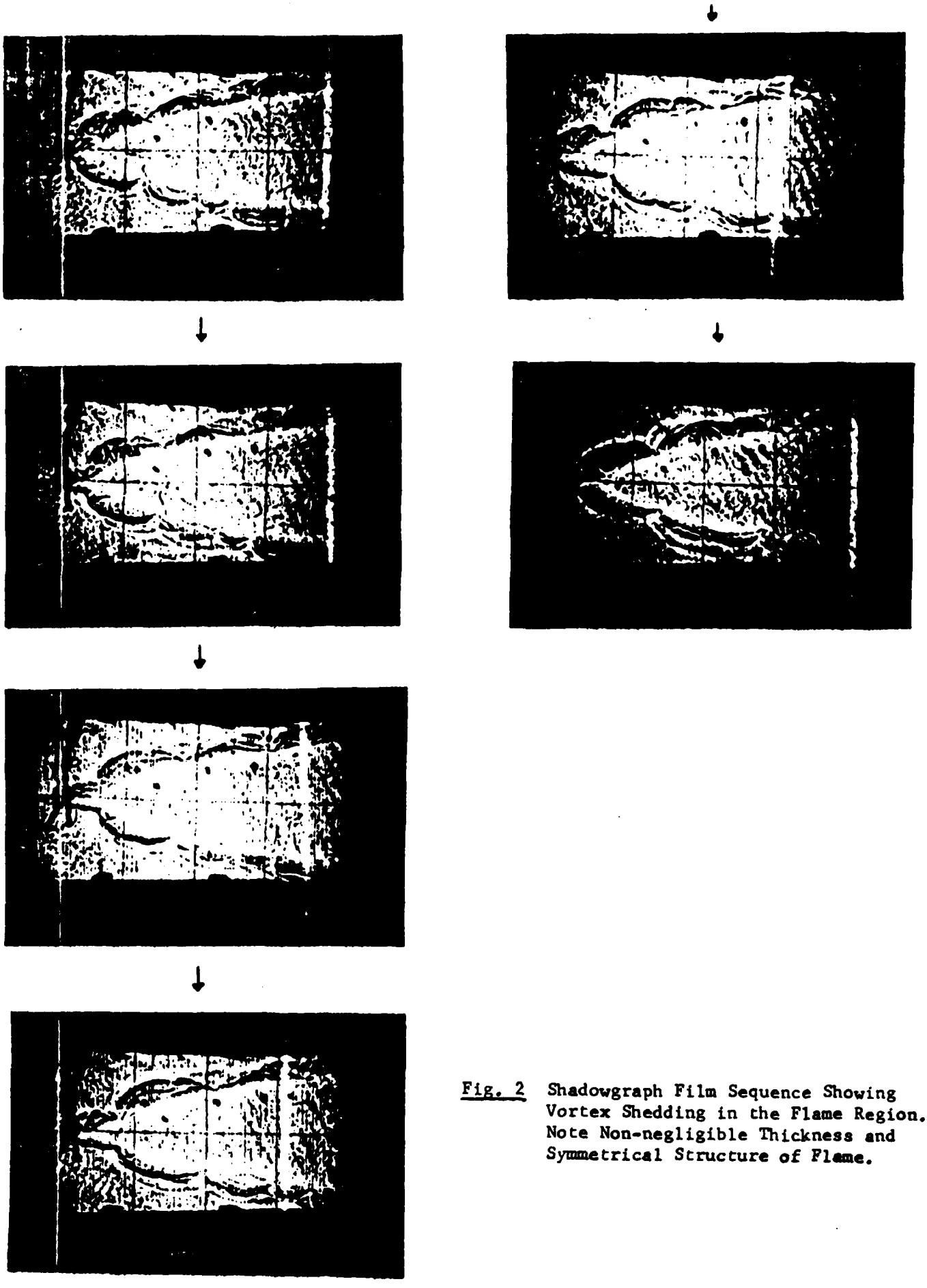

Fig. 2 Shadowgraph Film Sequence Showing Vortex Shedding in the Flame Region. Note Non-negligible Thickness and Symmetrical Structure of Flame.

shear layer type of instability mechanism of the flame region. These vortices are convected along the flame front at approximately the local flow velocity. The phase of the unsteady heat release from the combustion in these vortices is related to their convection velocity. As the flow in the combustor section is, generally, of low Mach number the convection velocity is small compared to the local speed of sound which determines the phase of the acoustic oscillations. Hence, the phase of the acoustic pressure oscillation changes slowly as compared to the phase of the unsteady heat release. Thus, over certain regions of the flame the unsteady heat release and the pressure oscillation are in phase while over other regions they are out of phase. Details are provided in the next chapter and in Appendices B and C. The important fact is that when any significant pressure oscillations (100 dB or more) are measured in the set up it is found that the "driving" or the in phase part of the flame exceeds the "damping" or out-of-phase part of the flame. Therefore, in accordance with Eq. (1), the unsteady heat release from the combustion in the vortical structures inputs energy into the acoustic oscillations. However, this by itself does not mean that the sole cause of the observed pressure oscillations is the unsteady heat release from the vortical structures.

To determine whether the observed pressure fluctuations are indeed caused by the unsteady heat release from the vortical structures a theory has also been developed for predicting the pressure oscillations from the unsteady heat release from the flame. Briefly, the pressure spectrum is constructed from the heat release rate by means of the following equation (derived in Appendix D)

$$S_{pp} = S_{qq} |G|^2 \frac{\omega^2}{c_p^2} \qquad (2)$$

Here, $S_{pp}$ is the pressure spectrum, $S_{qq}$ is the unsteady heat release spectrum and G is the relevant Green's function which describes how an unsteady heat source gets "converted" into pressure. Now, if the predicted spectrum from Eq. (2) agrees with the experimentally measured pressure spectrum in the set up then it may be concluded that indeed the unsteady heat release from the vortical structures is the main cause of the observed acoustic oscillations. That this is the case is confirmed by comparisons between the two spectra (an example is presented in Fig. 10).

Further details of the investigations carried out under the research program are described in this report. In Chapter II, the major results of the experimental and theoretical efforts are documented. The short comings of recent theoretical models of ramjet instability are also considered there. Conclusions and suggestions for further research are presented in Chapter III. The report closes with a number of appendices.

## Chapter II

## REVIEW OF RAMJET INSTABILITY STUDIES AT GEORGIA TECH

The primary objectives of the ramjet combustion instability research program at Georgia Tech described herein were: (i) to determine the characteristics of the combustion process in ramjet combustors responsible for the occurrence of low frequency, longitudinal instabilities in liquid fueled, coaxial, dump type ramjet engines and (ii) to investigate the validity of previously developed linear combustion instability models, such as the model developed by Yang and Culick[31].

To meet these objectives the set up shown in Fig. 3 was developed (see also Appendices B and C). It consists of an inlet, combustor and exhaust sections. The inlet contains a movable injector through which a mixture of propane and air is introduced into the combustor. The flame is stabilized in the 7.5 x 5 $cm^2$ combustor section on a 0.8 mm diameter nichrome wire. The wire is attached to the combustor windows at half combustor height and it is heated electrically to improve the steadiness of the stabilized v-shaped flame. The exhaust section is equipped with two acoustic drivers which are used to excite a standing acoustic wave of desired amplitude and frequency in the set up. This allows the study of the effects of known, external excitation on the flame. In addition, the movable injector provides a capability for "placing" the stabilizing wire (and hence, the flame) on any part of the excited standing wave; that is, at a pressure maximum, minimum or in between. The maximum length, l, available between the injector face and the exhaust section is 3 meters. The flow approaching the stabilizing wire is

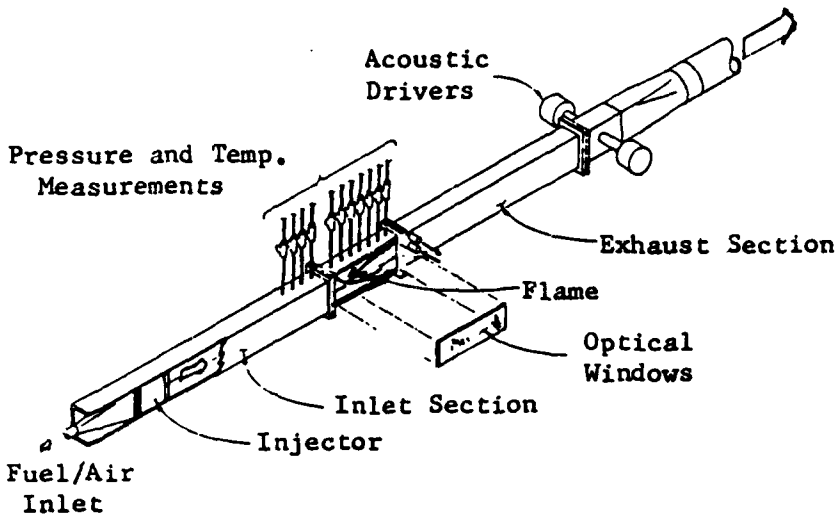


Figure 3. Developed Experimental Set Up.

parallel and uniform and disturbances are damped out by means of a fine wire mesh grid located 8 cm. upstream of the stabilizing wire. This wire mesh also serves as a flame arrestor in case of flash back. The combustor walls are water cooled enabling wall mounted pressure transducers to be used to monitor the acoustic pressure field. Capabilities for time and space resolved measurements of CH species radiation from the flame have also been developed. The concentrations of these species are a measure of the reaction rate[32] and, thus, the heat release rate and are useful in describing the unsteady combustion field.

The acquired pressure and radiation signals are digitized and stored in computer memory prior to their fourier analyses. The developed fourier analysis program yields both auto spectra and cross spectra of the signals. This facilitates determination of relationships between the pressure and the unsteady heat release including their relative phases. Also, capabilities for identifying specific frequency components and their amplitude and phase behavior have been developed.

The acoustic nature of the set up was first investigated under cold flow conditions. It was determined that the injector, whose face is made of sintered stainless steel, could be well approximated as an acoustically rigid surface. Thus, since the exhaust end of the set up is open, the developed set up behaves as an acoustically closed-open organ pipe. The natural acoustic frequencies of this system are, therefore, given by the quarter wave mode[33], the three quarter wave mode and so on.

The behavior of the flame has been investigated under conditions of (i) no driving by the acoustic drivers, (ii) with driving provided by the acoustic drivers at different frequencies and (iii) in a shortened version of the setup which was considered due to reasons set forth shortly. The behavior of the flame under each of these conditions is described below.

(i) Results Obtained with No External Driving: Spontaneous instabilities involving the set up's fundamental acoustic mode (i.e., the quarter wave mode) have been observed in certain fuel/air ratio ranges. When the mixture composition is close to the lean stability limit, the flame is thin and can be readily stabilized on the heated wire. However, as the fuel fraction is increased, instability sets in as indicated by the wall mounted pressure transducers which record an increase in amplitude of the fundamental acoustic mode. With further increase in the fuel fraction (while the mixture remains in the fuel lean range) the flame flashes back from the wire to the screen and the sound pressure levels in the combustor approach 140-150 db. As the mixture becomes fuel rich, not all the fuel can be burned within the combustor and part of the fuel burns outside the set up. When the mixture approaches the rich flammability limit the flame is blown back to the wire where it stabilizes again. Under these conditions the instability subsides and the flame is again stable.

As observations of the flame indicated that an instability (as recorded by the increasing pressure levels with increase in fuel air ratio) set in while the flame was still held at the wire, experiments were undertaken under these conditions to investigate the cause of the instability. These were investigated by use of CH radiation measurements. By a suitable arrangement

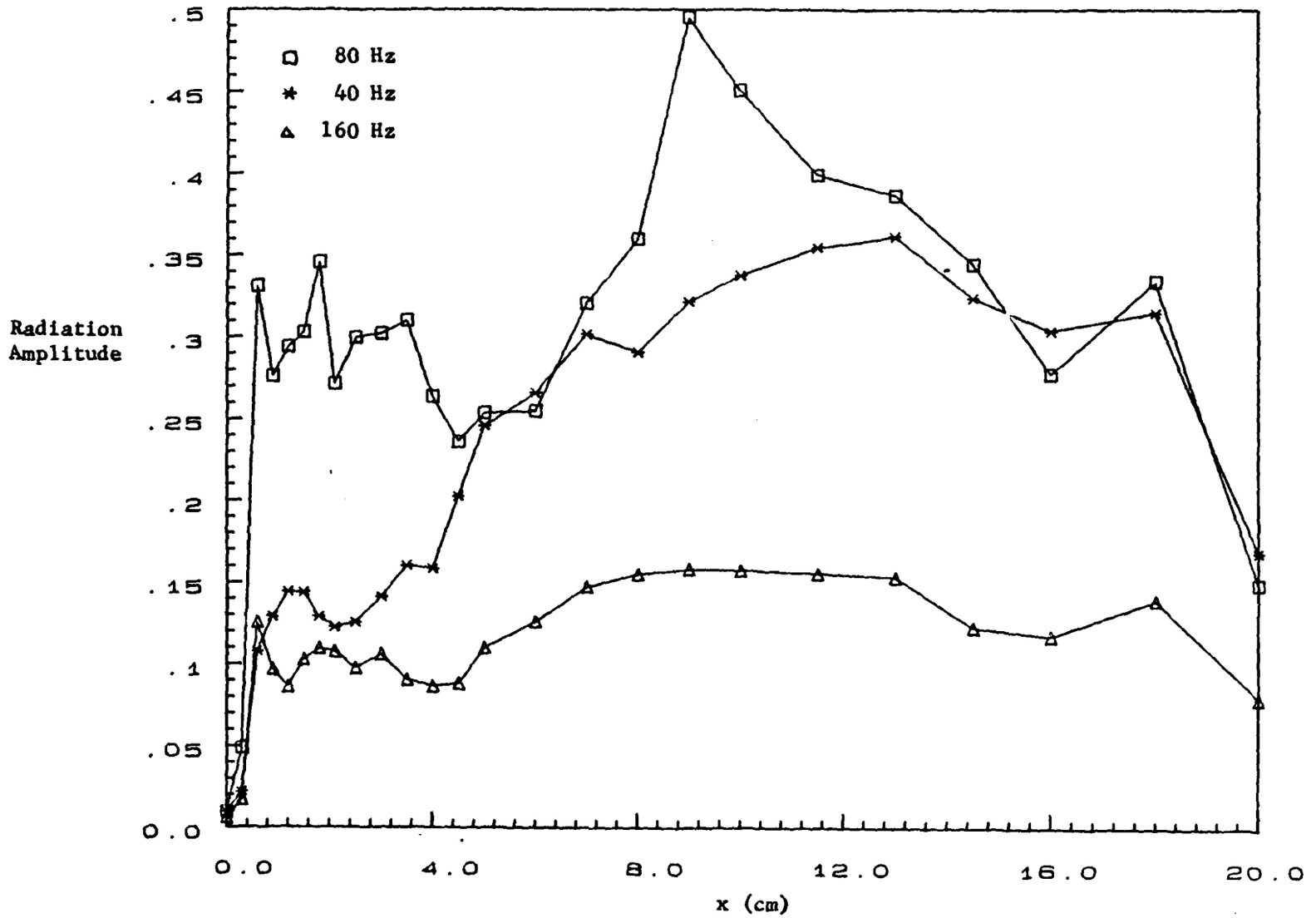


Figure 4. Radiation Amplitudes as a Function of Axial Distance from Flame Holding Wire.

of the optical elements, the radiation from vertical 2 mm wide strips of the flame were measured. The optics could be moved axially so that the radiation from different parts of the flame could be measured. Figure 4 presents the axial dependences of the radiation amplitudes, along the flame front (the wire corresponds to x=0) for three different frequencies of 40 Hz, 80 Hz and 160 Hz. Note the sharp increase in amplitude of all three frequencies just downstream of the wire. The first natural acoustic frequency is 80 Hz and it is clear that the signal at this frequency dominates the local unsteady radiation (and, thus, also the unsteady heat release).

To link this behavior to a shear layer type of instability, some of the features of shear layer instabilities will now be considered. Shear layer instabilities have primarily been investigated for non reacting flows[34], in particular for incompressible flows and this discussion will ,therefore, be limited to such flows. However, as such instabilities are primarily fluid mechanical in nature, it is expected that their major features will also be present even under reacting flow conditions. When a shear layer instability sets in, the amplitudes of the disturbance (e.g., the disturbance velocity) increases exponentially. Also, the instability is confined to a limited frequency range (i.e., the Strouhal number range). Disturbances at frequencies in this limited range are amplified whereas disturbances at other frequencies are not and may, instead, be damped. A typical plot of the growth parameter, which is related to the disturbance growth rate, as a function of the relevant Strouhal number is shown in Fig. 5 taken from Ref. 34. Note that the growth parameter is non zero only in a limited frequency range. The frequency at which the growth parameter maximizes is the most unstable frequency.

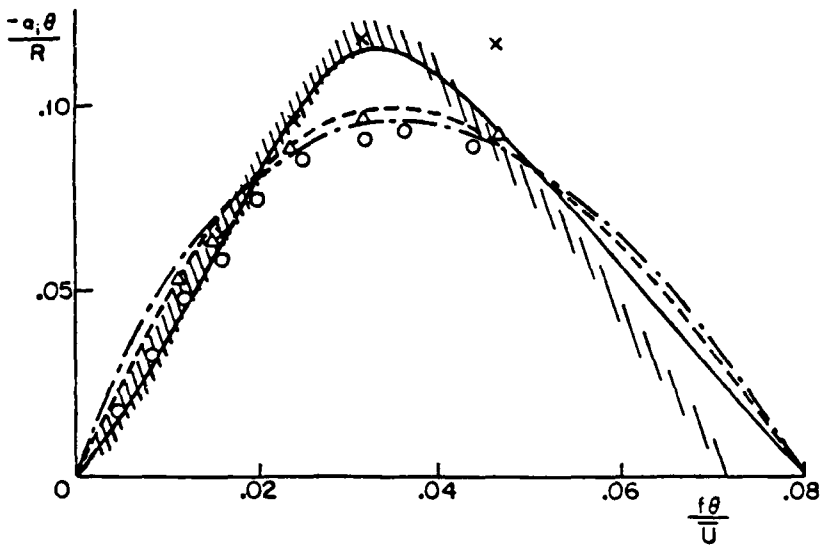


Figure 5. Typical Variations of the Nondimensional Growth Rate with Strouhal Number (taken from Ref. 34).

Looking at the radiation measurements from this point of view, the sharp increase in the radiation measurements just downstream of the wire could indicate a similar instability behavior of the flame shear layer. More evidence to this effect is obtained by noting the relative amplitudes of the different frequency components. While the signal at the first natural frequency of 80 Hz dominates, the signal at 40 Hz is also significant. However, the signals at frequencies higher than 80 Hz start diminishing in magnitude. For example, the signal at 160 Hz is much smaller than both the 80 and 40 Hz components. It was found that signals at higher frequencies (greater than 160 Hz ) rapidly diminished in magnitude. Thus, it is possible that the flame in the set up exhibits a shear layer type of instability which is confined to frequencies up to approximately, 160 Hz.

Additional supporting evidence is obtained by considering the phase of the radiation signal with respect to the pressure oscillations. Figure 6 presents the phase of the radiation signal at the first natural frequency of 80 Hz as a function of the axial location along the flame. Note the smooth monotonic variation of the phase. The smoothness of the phase curve indicates that the disturbances at 80 Hz are well correlated and coherent over the entire flame as would be expected if they were the result of a shear layer type instability. It was found that such smooth phase curves could only be obtained for the frequencies under approximately 160 Hz which, as estimated earlier, was the extent of the frequency range for the shear layer type of instability of the flame. Although it will be discussed under the results obtained with external driving, it may be pointed out that disturbances imposed upon the flame by the acoustic drivers in the frequency range of

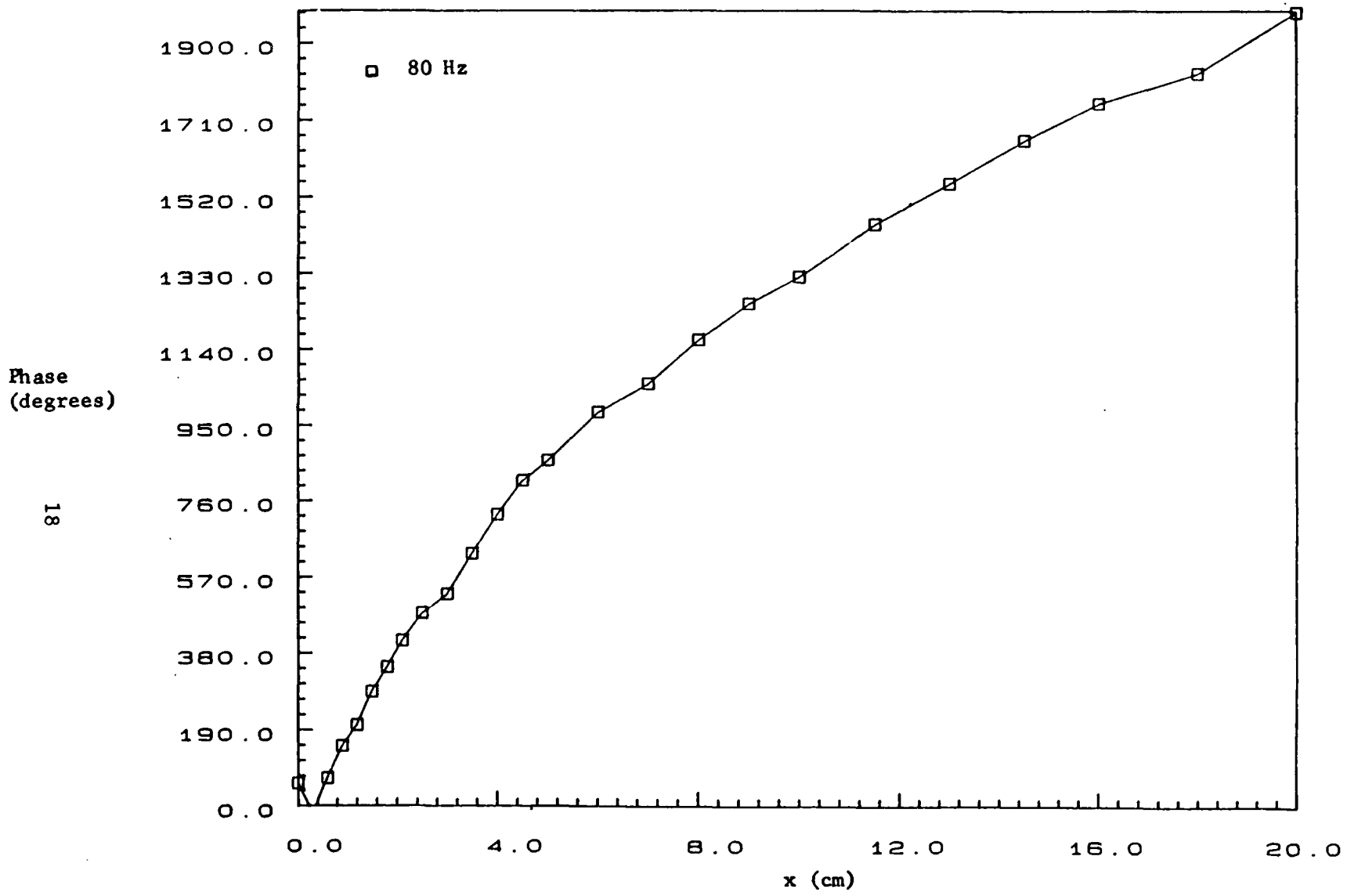


Figure 6. Phase of Radiation Signal (at 80 Hz) with Respect to Pressure.

160-500 Hz were rapidly damped out by the flame. This result also confirms the limited frequency range of the flame shear layer instability.

The phase variation of the low frequency components may be related to the phase velocity of the disturbances. This is done by noting that a phase change of $2\pi$ radians (i.e., $360^{o}$) occurs over a distance that may be regarded as one disturbance wavelength. The convection velocity $\bar{u}_c$ is then given by the product of the relevant frequency with the corresponding disturbance wavelength, provided they remain constant. In the more general case, when these quantities vary over the flame, it is more appropriate to consider the convection velocity between neighboring points along the flame. In such a case the convection velocity $(\bar{u}_c)_{ij}$ between two points $x_i$ and $x_j$ on the flame is given by

$$(\bar{u}_c)_{ij} = \frac{2\pi f[x_j - x_i]}{\theta_j - \theta_i} \qquad (3)$$

where $\theta_i$ and $\theta_j$ are the phases at $x_i$ and $x_j$, respectively.

The convection velocity at 80 Hz, derived from the above equation is plotted in Fig. 7 as a function of the axial distance along the flame. The value at the flame stabilizing wire is about 1.5 m/sec which is equal to the unburned mixture flow velocity. Its value at the downstream end of the flame is about 6 m/sec which is equal to the burned flow velocity calculated on the basis of the density drop across the flame. Thus, the disturbance at 80 Hz is convected along the flame at approximately the average of the local unburned and burned (i.e.,reacted) flow velocities. This fact also implies that the disturbances in the flame are fluid mechanical in nature. If they had been

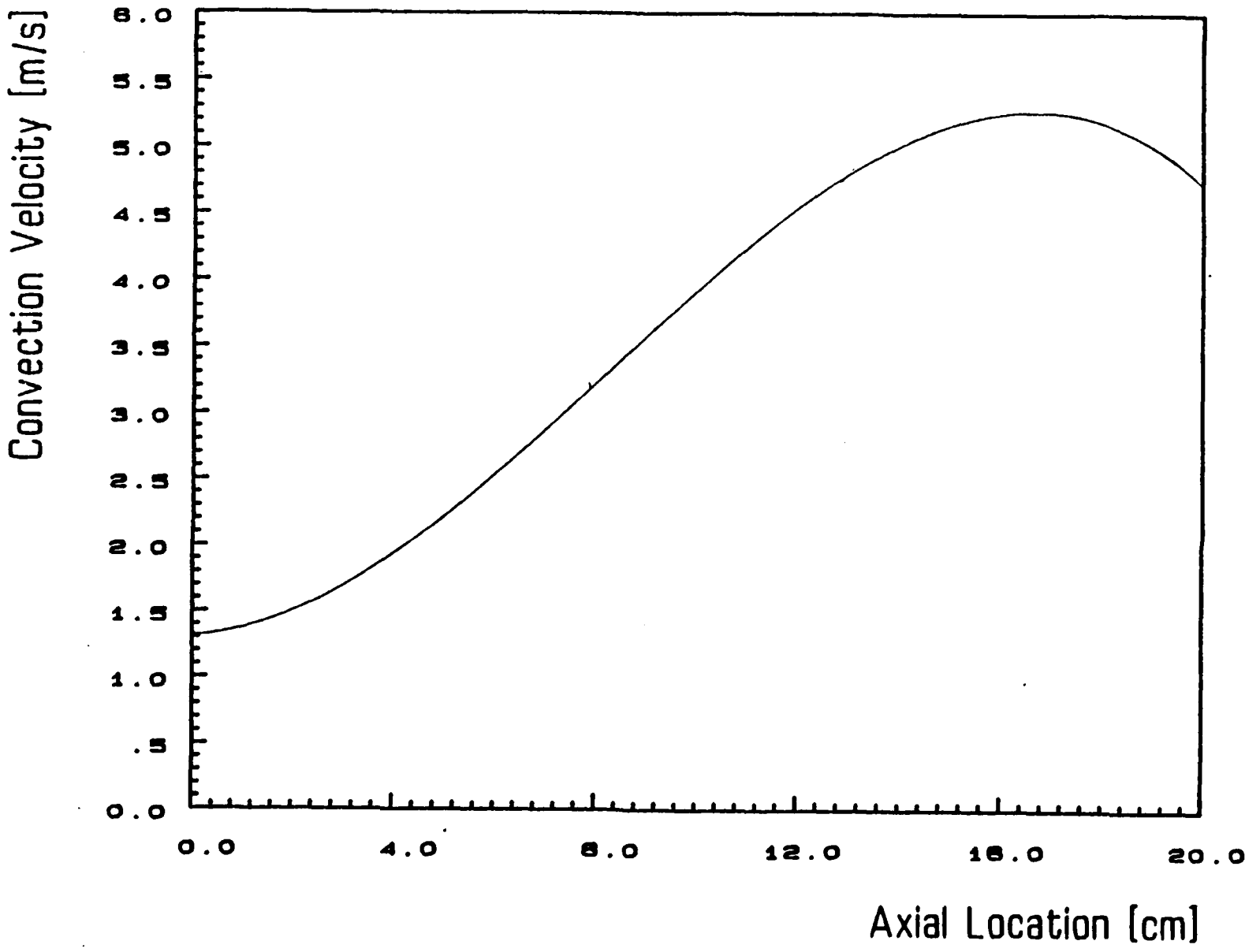


Figure 7. Convection Velocity at 80 Hz.

purely acoustic, their convection or propagation velocity would have been the local speed of sound and not the local flow speed. The other disturbances in the frequency range up to 160 Hz also behave similarly, thus demonstrating their fluid mechanical nature.

These fluid mechanical disturbances have been identified as burning vortical structures that are shed from the flame holding wire by means of high speed (6000 frames/sec) shadowgraphy and schlieren photography performed on the flame. It was found that the frequencies of shedding favored predominantly frequencies around the first natural frequency of the set up. This was found to be true even when external driving by means of the acoustic drivers was provided as will be described shortly (see also Fig. 2).

Thus, the results of these experiments demonstrate that the flame region is fluid dynamically sensitive in a limited frequency range (approximately up to 160 Hz in the developed set up) and is involved in a shear layer type of instability in this frequency range. This results in the formation of vortical disturbances which are convected along the flame front. The unsteady combustion in these structures favors frequencies in the same frequency range that the flame exhibits the shear layer type of instability. The question now arises whether the unsteady combustion is responsible for the pressure oscillations that lead to the observed spontaneous instability.

To answer this question it was checked whether the unsteady heat release in the sensitive frequency range satisfied Rayleigh's criterion for flame driving of the acoustics (i.e., see Eq. (1)). For convenience, Eq. (1) may be rewritten in the frequency domain in the following form

$$\int_{V_{flame}} |S_{pq}| \cos \theta_{pq} \, dV_{flame} > 0 \qquad (4)$$

where

$S_{pq}$ = the cross spectrum between the unsteady heat release and the pressure oscillations at a given frequency and

$\theta_{pq}$ = the corresponding phase between the pressure and the heat release

and $V_{flame}$ is the volume of the flame region.

The integrand of the above equation is plotted in Fig. 8 for the first natural frequency of 80 Hz. As the flame length is much smaller than the acoustic wavelength at 80 Hz the pressure is constant over the flame region. Thus, the oscillatory nature of the integrand is related to the wavelength of the disturbance or vortical structures at 80 Hz. Since the integral was found to be positive, these results indicate that the unsteady heat release at 80 Hz drives the acoustic oscillations at that frequency. The Rayleigh criterion was also found to be satisfied at other low frequency components indicating that the flame also inputs energy into the acoustic oscillations (i.e., drives) at these frequencies.

Satisfying the Rayleigh criterion does not exclude, however, the presence of other important acoustic energy sources in the experimental set up. For example, impingement of the convected vortices against a solid surface (e.g., the duct walls) could also contribute to the excitation of

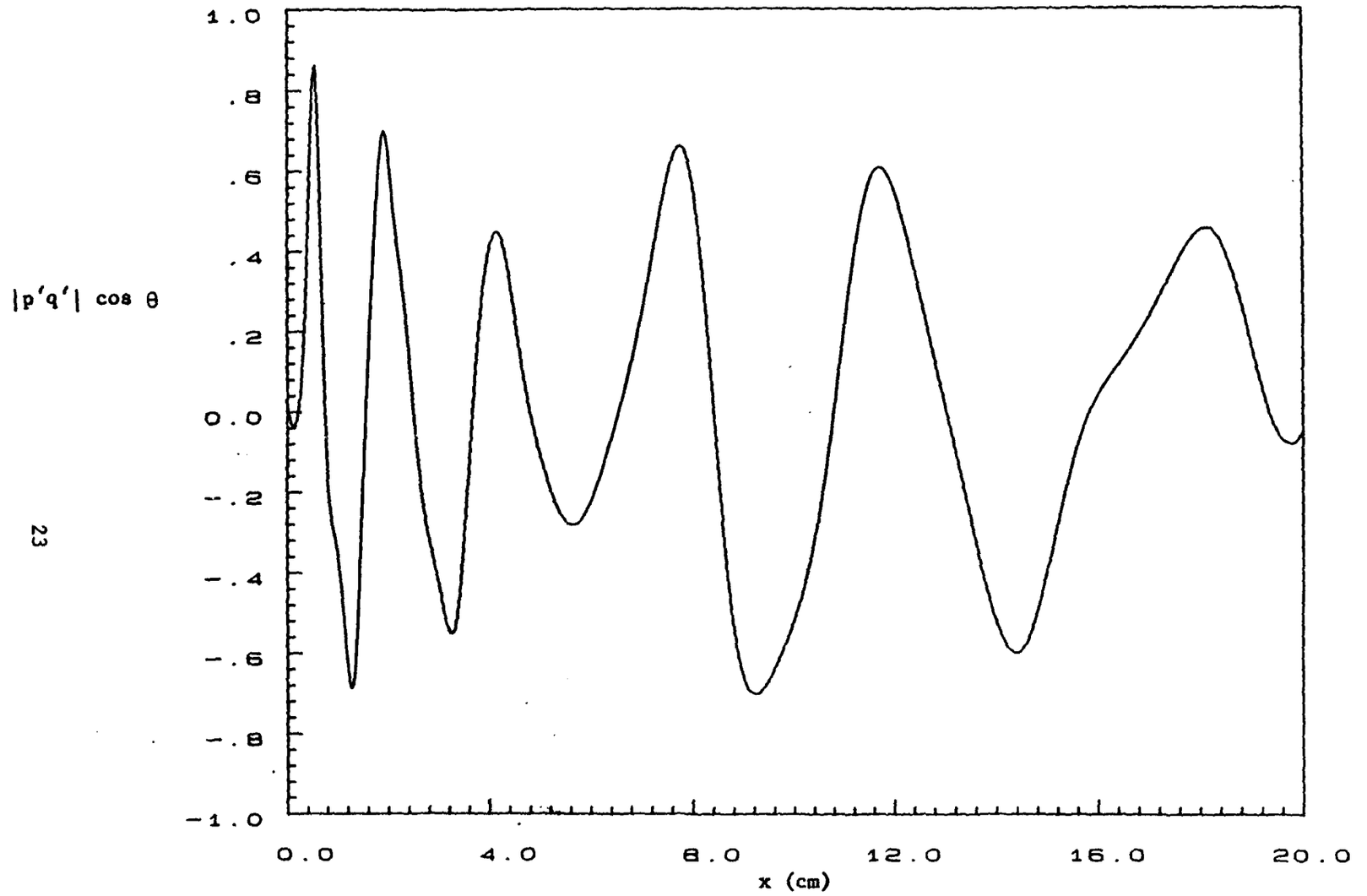




Figure 8. Plot of the Integrand of Eq. (5) which Determines the Flame Driving at 80 Hz According to Rayleigh's Criterion.

duct acoustic oscillations as has been suggested to occur in segmented solid propellant rocket motors[35]. Thus, it becomes necessary to predict the acoustic pressure spectrum by considering the unsteady heat release as the primary acoustic source and comparing this prediction with measured pressure spectra. If satisfactory agreement is obtained, then the unsteady heat release may be taken to be the primary acoustic source.

A theory was, therefore, developed to predict the pressure spectrum from the unsteady heat release. According to this theory, valid for low frequencies for which the flame zone may be taken to be compact compared to the acoustic wavelength (see derivation in Appendix D).

$$S_{pp} = \frac{\omega^2}{c_p^2} |G|^2 S_{qq} \qquad (2)$$

Here, $S_{pp}$ is the acoustic pressure spectrum, $S_{qq}$ is the net or integrated heat release spectrum from the entire flame and G is the relevant Green's function which describes how an unsteady heat source excites acoustic pressure oscillations.

The integrated heat release spectrum was obtained by measuring the CH radiation from the entire flame. The result is shown in Fig. 9. Note that now the radiation at the first natural frequency does not dominate the spectrum as it did for the local heat release at different locations along the flame. The reason for this is that the flame length is equivalent to several vortical wavelengths as is evident from Fig. 8. This means that when the signal is integrated over the entire flame, a lot of cancellation occurs from the positive and negative portions of the unsteady heat release. When lower

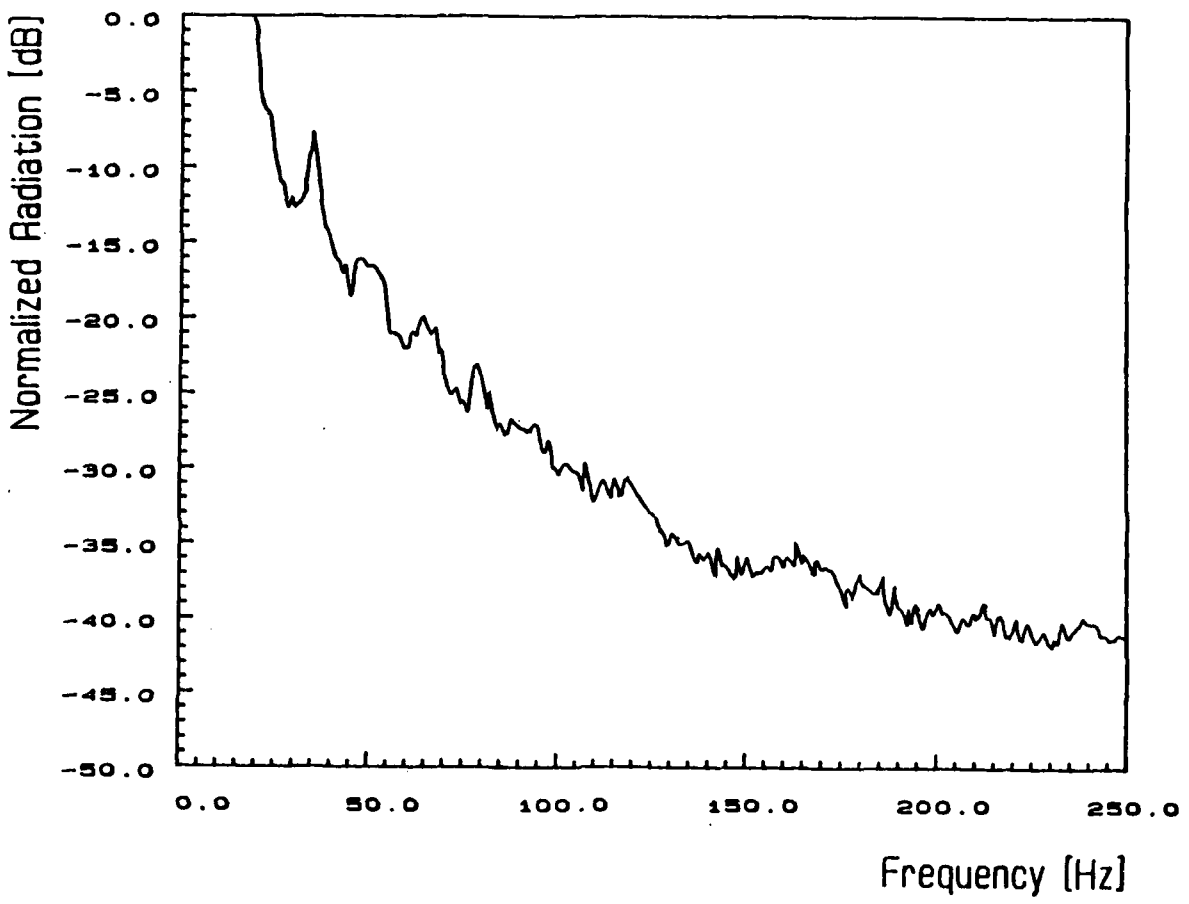


Figure 9. Measured Radiation Spectrum from Entire Flame.

frequencies are considered, due to their greater wavelength, this cancellation is smaller. As a result , it is the frequencies lower than 80 Hz and, in particular, frequencies under 50 Hz that dominate the spectrum.

A typical comparison of the predicted and measured pressure spectra is shown in Fig. 10. The comparison is excellent and, thus, confirms that the unsteady heat release is the primary acoustic source in the set up. It may be noted that although there are substantial levels of pressure oscillations at frequencies lower than 80 Hz, the dominant peak in the pressure spectrum occurs at the first natural frequency of 80 Hz. This takes place because the Green's function acts like a filter and favors frequencies close to the natural acoustic frequencies of the duct (see Appendix D). Thus, although the source strengths at the lower frequencies are higher (see Fig. 10) the pressure oscillations favor the natural acoustic frequencies of the experimental setup.

It was also found that with increase in the fuel/air ratio the magnitude of the unsteady heat release (the source for the pressure oscillations) also increases. For example, Fig. 11 plots the measured radiation signal as a function of the burned gas temperature for the natural frequency of 80 Hz. The measurement was made 3 cm downstream of the flame holding wire and the temperatures are normalized by the temperature at which flash back occurs. Note the sharp increase in the signal as the burned gas temperature (fuel fraction) increases.

Hence, the spontaneous instability observed in the set up can be explained. The shear layer formed by the flame undergoes a fluid mechanical

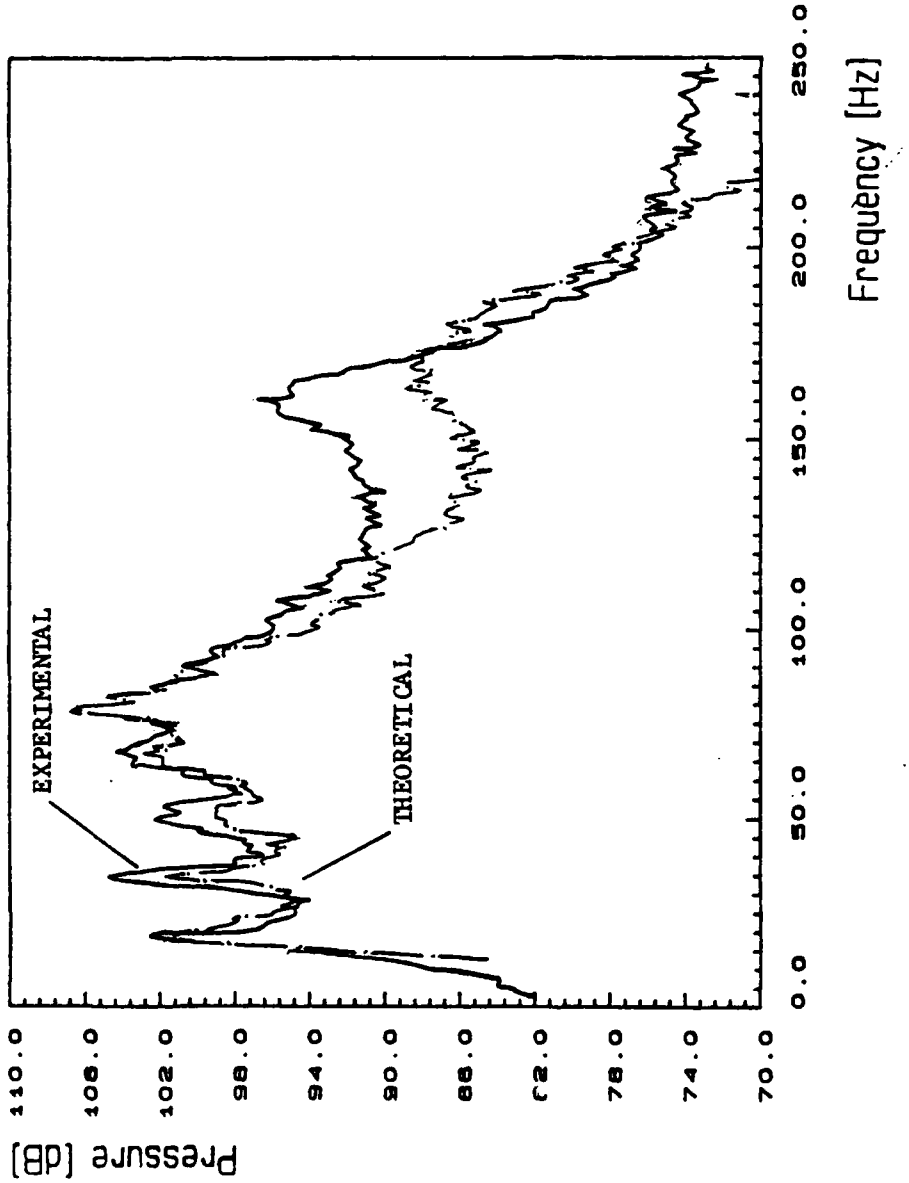


Figure 10. Comparisons of Predicted and Measured Pressure Spectra.

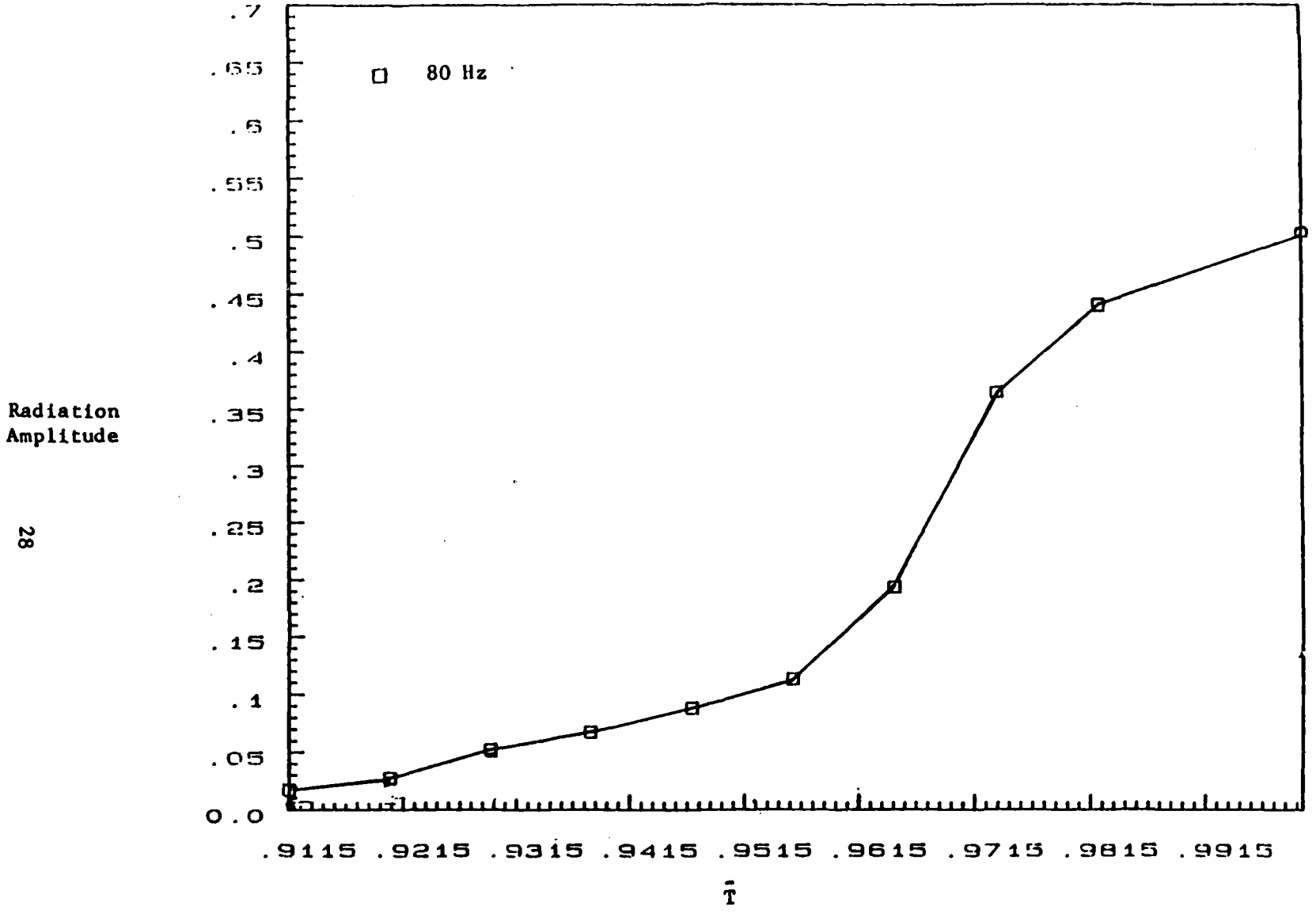


Figure 11. Radiation Levels as a Function of Burned Gas Temperature (Fuel/Air Ratio).

type of instability causing the shedding of vortices from the flame holding wire. The shear layer type of instability is confined to a certain frequency range. The resulting unsteady combustion drives the acoustic oscillations in the set up. With increase in the fuel fraction the unsteady heat release rates increase. The consequent increase in the flame driving then leads to the observed instability.

(ii) Results Obtained with External Driving: Experiments were conducted to study the effects of external excitation, provided by the acoustic drivers, on the flame behavior. These reinforced the concept of a shear layer type of instability of the flame which is confined to a limited frequency range. The driving was provided at different frequencies in the range of 160-500 Hz.

It was found in all these cases that the flame could be divided into two regions, that is, (a) a region close to the flame holding wire, called the near wake region, where the dominant radiation signal is at the driving frequency and (b) a region downstream of the near wake region, called the far wake region where the lower frequency components, in particular the signal at the first natural frequency, dominate. Thus, even under external driving, the flame region exerts a dominating influence in causing the decay of the non sensitive or stable frequency disturbances. An example is shown in Fig. 12 where the near wake and far wake regions for driving at 385 Hz are shown. The near wake and far wake behavior was found to be independent of the location of the flame holding wire on the excited standing wave; i.e., at a pressure maximum, a pressure minimum or in between.

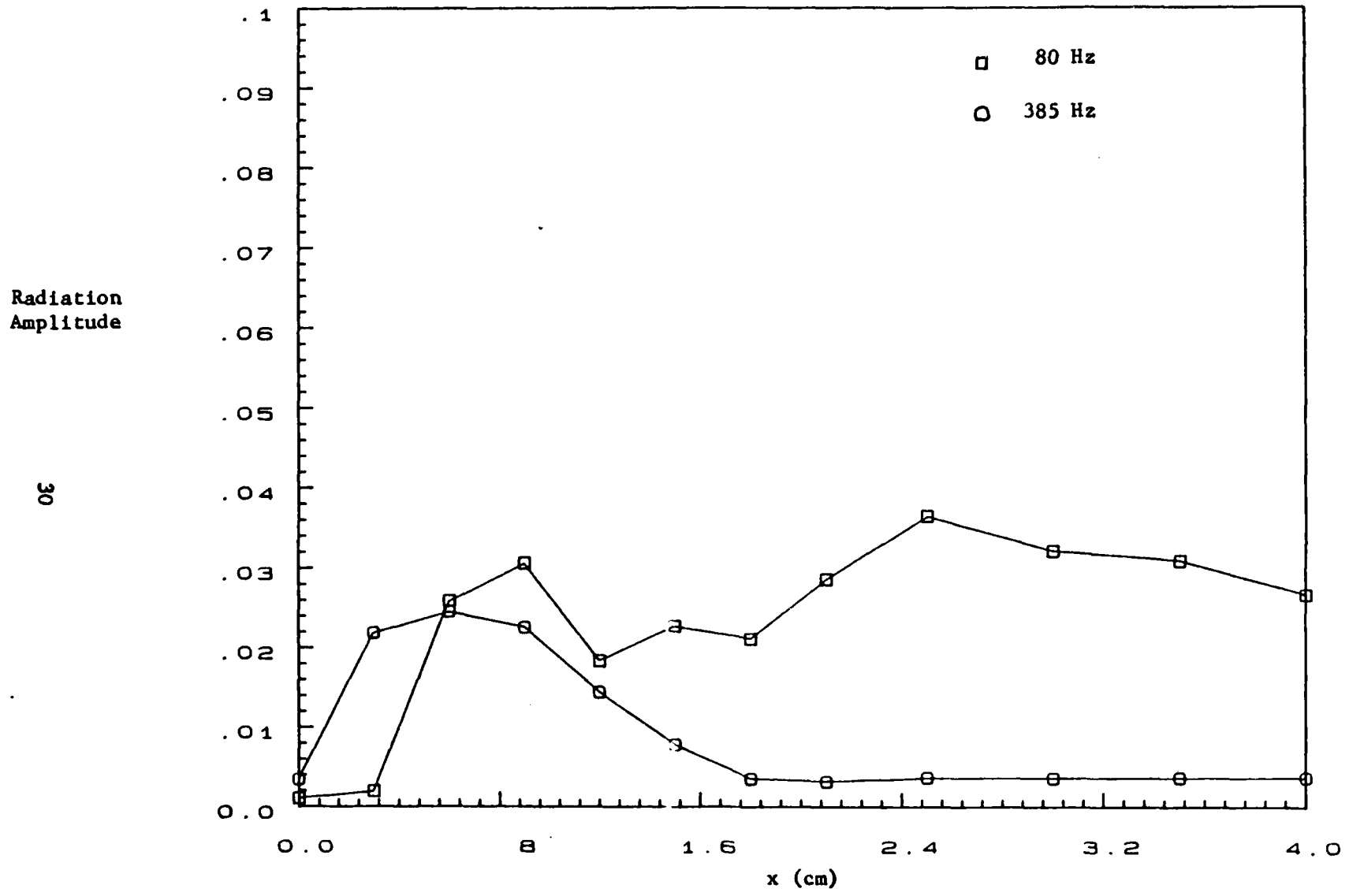


Figure 12. Radiation Amplitude at 80 Hz and 385 Hz with Driving at 385 Hz. Note the Near Wake - Far Wake Behavior of the Flame.

These results were confirmed by high speed schlieren and shadow photography (6000 frames/sec) of the flame under external excitation. A sequence of frames taken from the shadow graph movie is shown in Fig. 2. The vortical structures were still found to formed around the first natural frequency of the set up. Visually, the only effect of the external driving was an oscillation of the vortical structures, as they were convected along the flame front, at the driving frequency.

(iii) Results Obtained in a Shorter Version of the Setup: As the experiments described above indicated that the unstable Strouhal number range for the flow conditions utilized in the setup and the first natural frequency of the setup overlapped, it was felt that a situation where this did not occur should also be investigated. Hence, a shorter version of the setup was considered. The exhaust section, downstream of the combustor section, was removed. This shortening resulted in an increase in the first natural frequency of the setup. Depending upon the injector location upstream of the flame holding wire, the first natural frequency of the setup could be increased to about 200 Hz which was outside the sensitive Strouhal number range.

As before, radiation measurements at different locations along the flame as well as integrated radiation measurements from the entire flame were obtained. A strong radiation component at the first natural frequency was found to be present only very close to the flame holding wire. Downstream of this region, the signal at the first natural frequency decayed and the low frequency components dominated (see Fig. 13). In this respect, the first natural frequency behaved like an externally driven frequency outside the

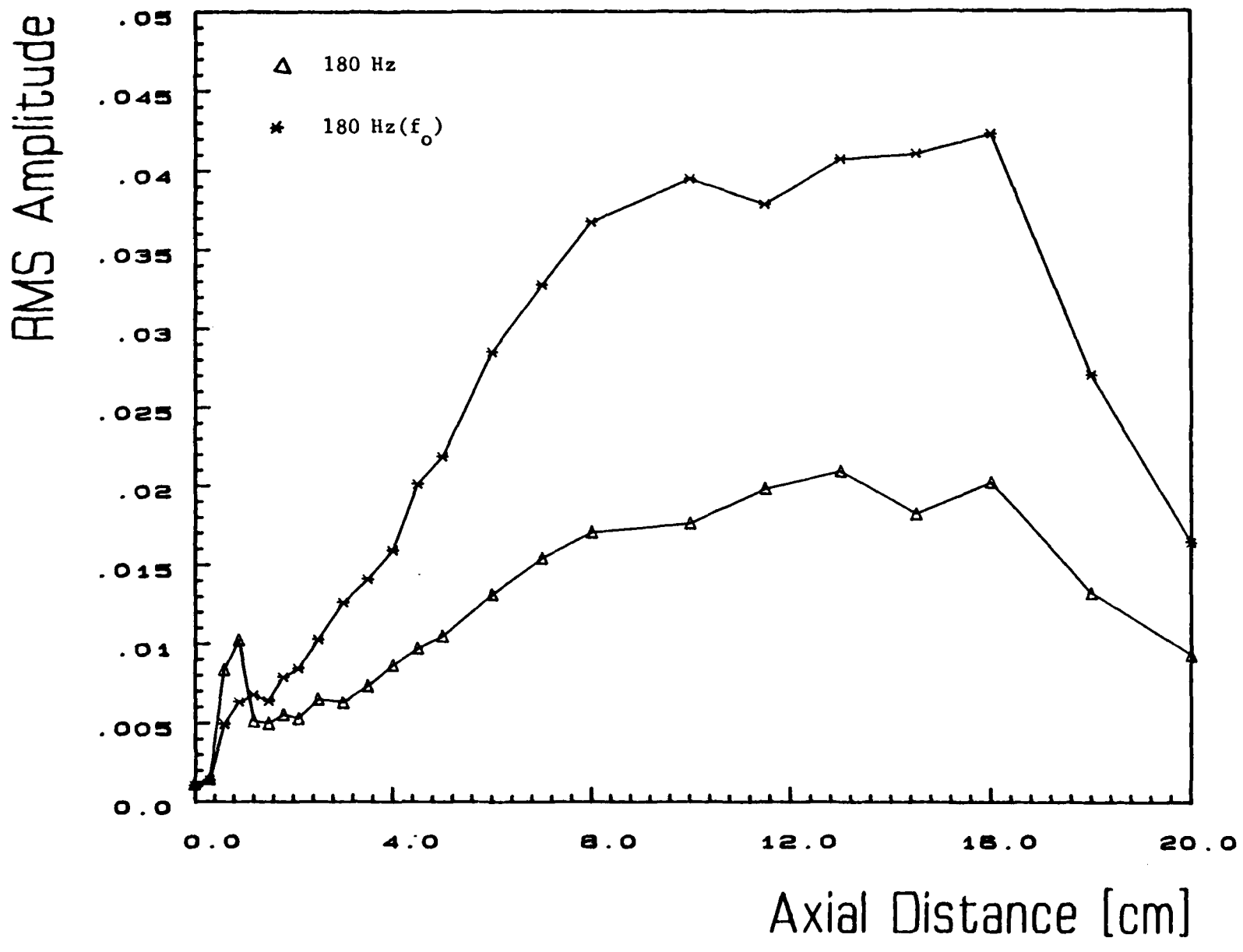


Figure 13. Radiation Amplitudes as a Function of Axial Distance from Flame Holding Wire - (Shortened Set Up, No External Driving).

sensitive Strouhal number range, in the longer setup as described in (ii). However, it was found that unlike in the longer setup, the low frequency components in the sensitive Strouhal number range were not well correlated over the flame front. In particular, a well defined convection velocity could not be obtained at these low frequencies. For the signal at the first natural frequency also, a well defined convection velocity did not exist over the entire flame. A convection velocity could be calculated at the first natural frequency, $f_o$, in this case only in the near portion. This is shown in Fig. 14, for $f_o$ = 180 Hz. However, this velocity seems to bear little, if any, relation to the mean flow velocity as in the longer setup. In the far wake region, moreover, the convection velocity is not calculable to any reasonable precision due to uncorrelated changes in the phase behavior of the signal.

A possible explanation for this behavior is that some amount of acoustic feedback is necessary to correlate disturbances over the entire flame even for those frequencies which lie in the Strouhal number range for the shear layer instability. As shown in Appendix D, the amount of acoustic feedback from the flame at a given frequency is dependent upon

a) the source strength; i.e., the integrated unsteady heat release from the entire flame at the given frequency and

b) how far is this given frequency from the nearest natural acoustic frequency.

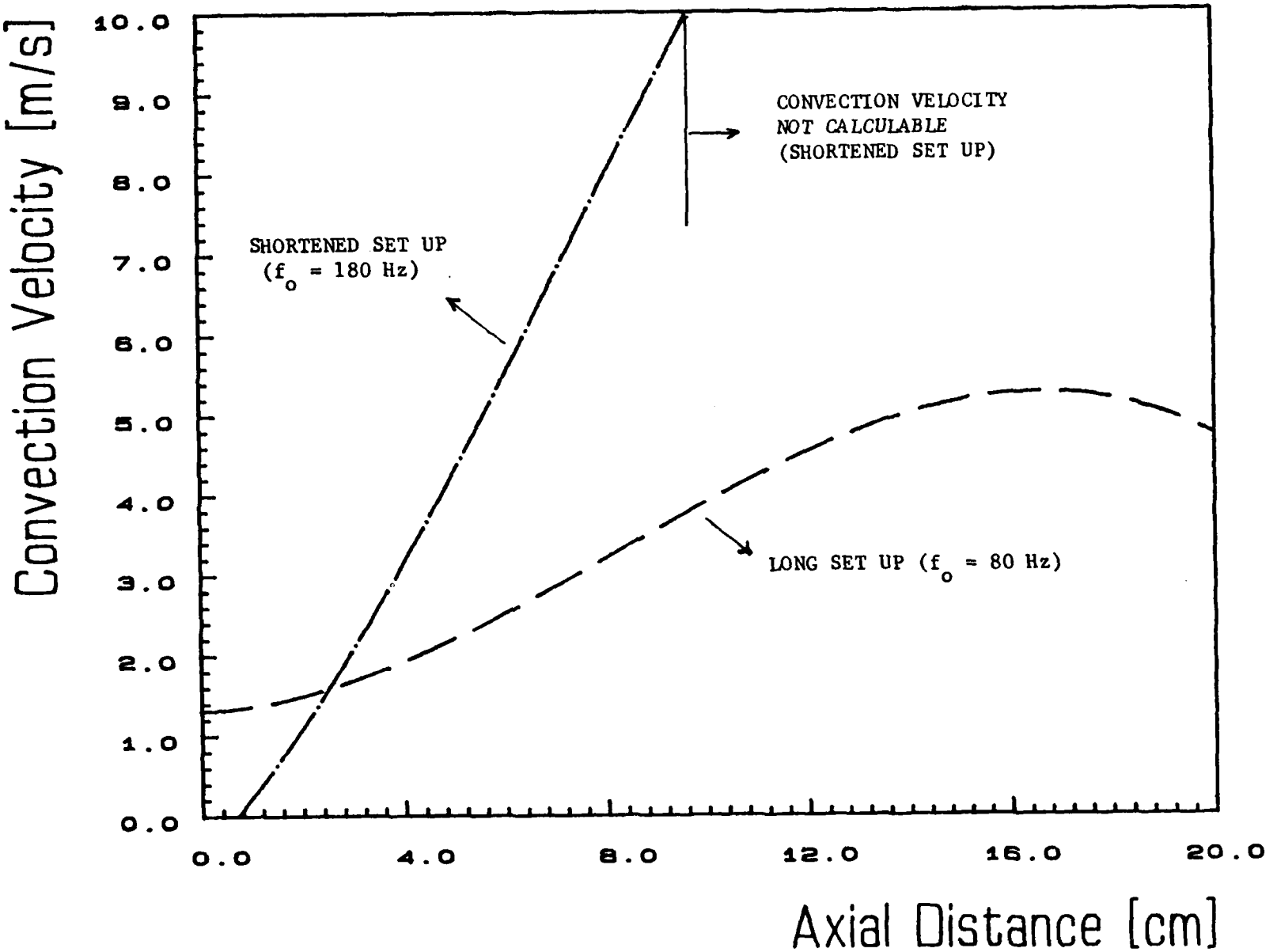


Figure 14. Convection Velocities at the First Natural Frequencies in the Long and Shortened Set Ups (No External Driving).

Thus, when the first natural acoustic frequency becomes removed from the shear layer instability regime, the acoustic feedback at these frequencies will decrease according to b) above.

To test the effect of acoustic feedback, the shortened setup was excited by the acoustic drivers at the natural frequency of $f_o$ = 180 Hz. Figures 15 and 16 show the effect of this driving. Note the sharp increase in the amplitude of the radiation at 180 Hz in the near wake (Fig. 15). It is also seen that the extent of the near wake has increased compared to the no driving case (compare Figures 13 and 15). Also, from Fig. 16, it is clear that with the driving, a well defined convection velocity which is close to the velocity of the mean flow, exists over the entire flame. This confirms the importance of an adequate amount of acoustic feedback to correlate unsteady disturbances over the flame.

(iv) Implications for Ramjet Combustion Instability Models:

The results of the experiments described above shed light on the deficiencies of current ramjet combustion instability models. These aspects will now be discussed.

Referring to Fig.1 it is clear that the ramjet flow field is extremely complex involving turbulent mixing, a recirculating flow region in the vicinity of the dump plane, a jet flow region, shear layers and finite width combustion zones. Thus, even the modeling of only steady state ramjet combustor flow fields presents the investigator with a myriad of challenging problems which are related, in one way or another, to the lack of complete

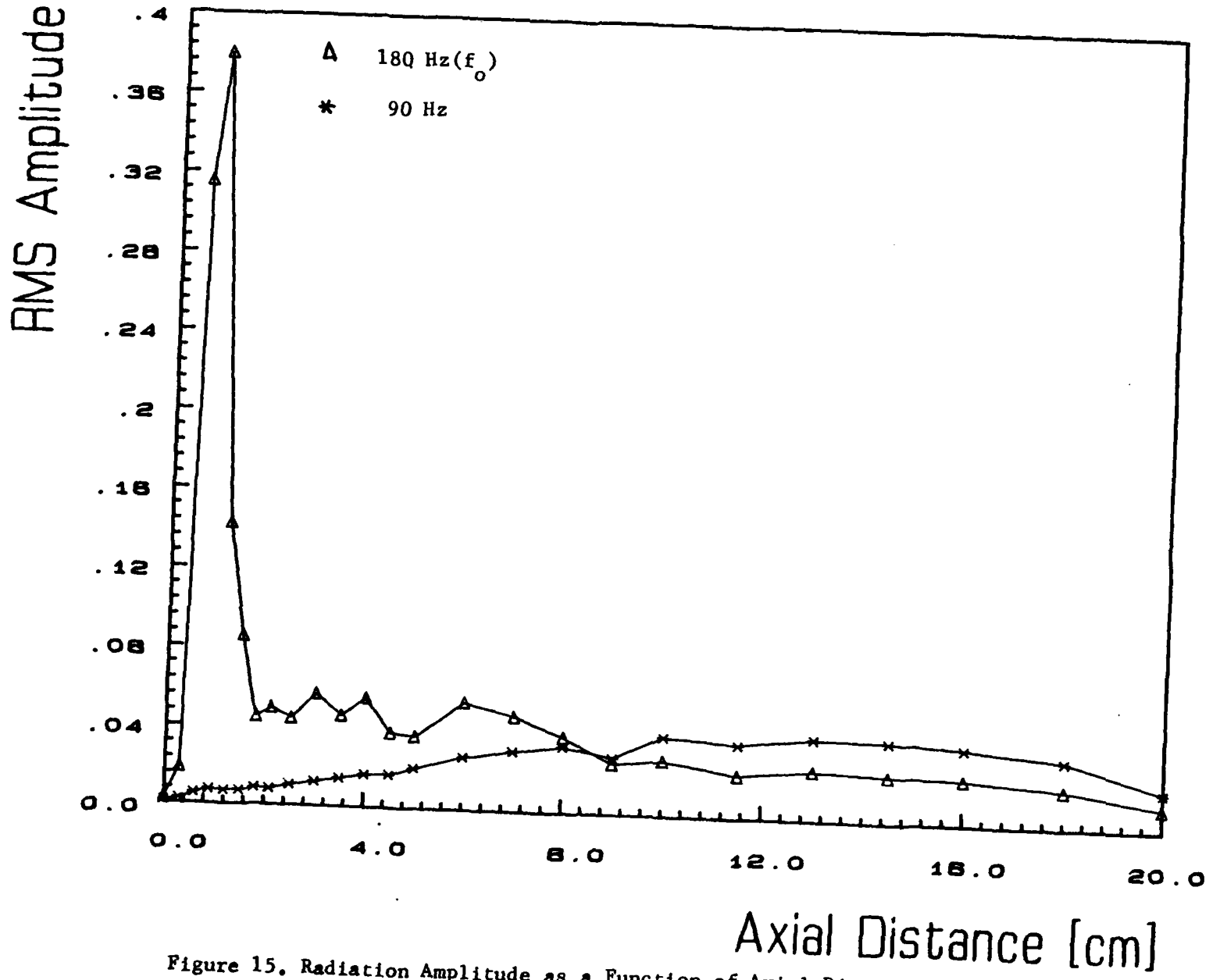


Figure 15. Radiation Amplitude as a Function of Axial Distance from Flame Holding Wire with Driving at 180 Hz (Shortened Set Up).

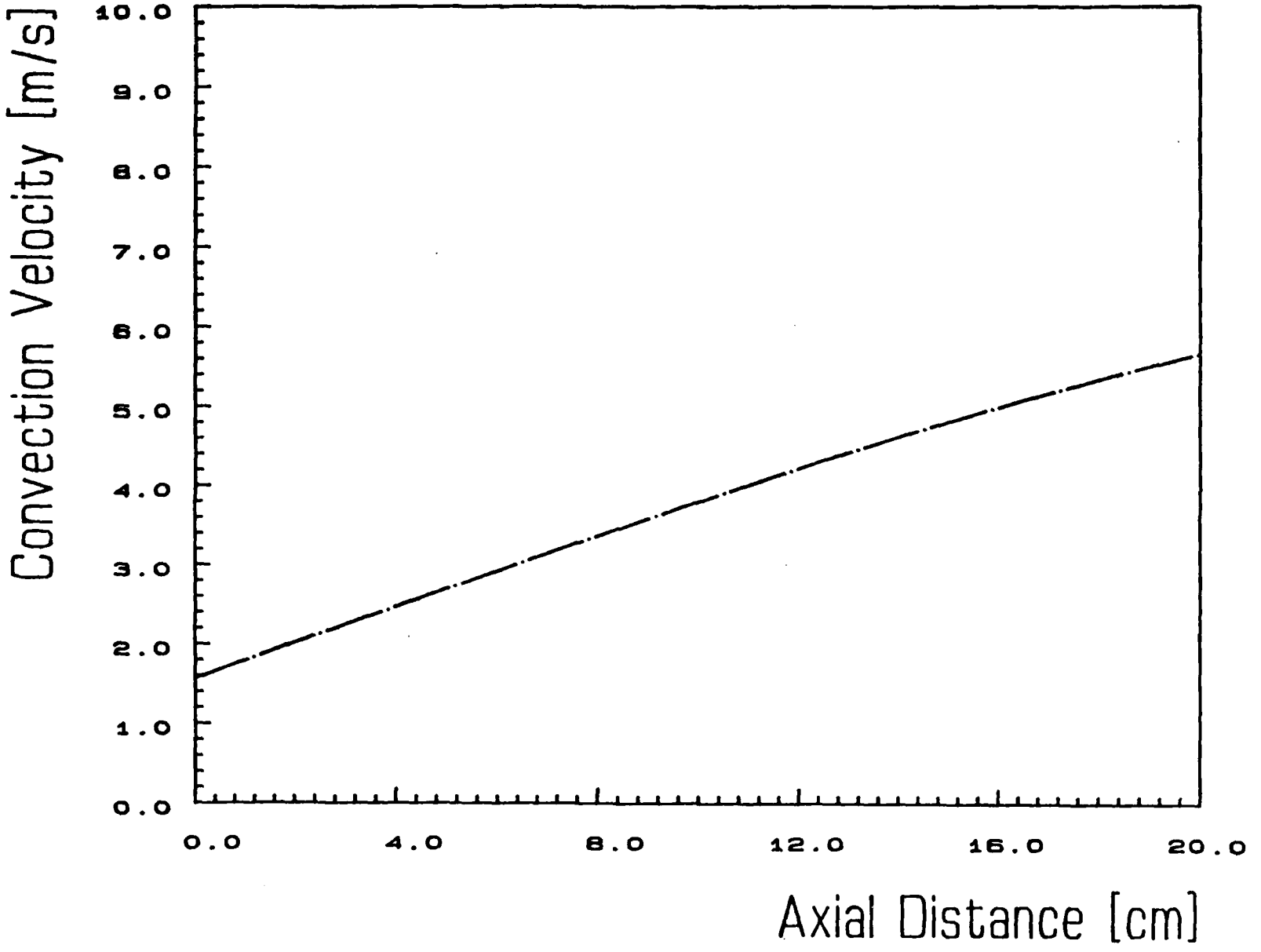


Figure 16. Convection Velocity at 180 Hz with Driving at 180 Hz (Shortened Set Up).

understanding of the complex ramjet combustion and flow processes. These difficulties increase when attempts are made to model the unsteady operation of a ramjet engine as is required in combustion instability analyses.

Notwithstanding these complexities, efforts have been made by some investigators[31,36,37] to develop ramjet combustion instability models. Here, the model developed by Yang and Culick[31] will be discussed to assess the applicability of such models. This model appears to reasonably predict the acoustic wave structure in the combustor but fails to predict stability limits. In the Yang and Culick model (to be denoted henceforth by YCM) considerable simplification is achieved by assuming that the amplitude of the disturbance is small, which reduces the mathematics to the solution of a system of linear differential equations. As a result of these simplifications the model can only hope to predict the operating conditions under which spontaneous combustion instability may occur and the wave structure of the small amplitude oscillations. The model requires that a solution (or a description) of the steady ramjet combustor flow field be available because the steady state solutions appear in the coefficients of the equation which describe the behavior of the instability.

To make the problem tractable, a number of assumptions are made in the YCM. Notable among these is the assumption that all of the combustion in the ramjet combustor takes place inside a thin flame sheet. The model assumes that when an oscillation occurs in the combustor, the flame sheet gets distorted by the perturbations, but remains infinitesimally thin. The flame area is a measure of the amount of combustibles consumed by the flame and periodic variation in the flame area may result in a periodic heat release

rate which, in turn, may drive acoustic pressure oscillations when the proper phase relationship between the heat release rate and the local pressure oscillations is satisfied. This is the primary acoustic driving mechanism considered in the YCM.

While the experiments conducted during this investigation do not negate the idea that the oscillatory heat release from the flame arises due to periodic variations in flame area they do demonstrate that any variations in the flame surface are caused by the presence of vortical structures in the combustion zone. There is no consideration of vortical structures in the flame zone in the YCM. Also, as is clear from the shadowgraph film sequence in Fig 2 the combustion zone is not a zero thickness flame sheet so that the concept of flame surface area must be carefully defined.

The longitudinal acoustic instability of the combustor is linked to the unsteady combustion rate at an axial acoustic natural frequency in the vortical structures. The unsteady combustion rate favors those frequencies to which the flame shear layer is fluid mechanically unstable. Thus, if an axial acoustic natural frequency of the combustor overlaps the unstable frequency range of the flame shear layer high rates of unsteady combustion may be obtained at this frequency which, in turn, could lead to high levels of acoustic oscillations or the onset of longitudinal combustion instability.

Thus, it is clear that the acoustic or longitudinal combustion instability of the ramjet must be considered in conjunction with the fluid mechanical type of instability of the flame shear layer. So far, fluid dynamicists have focussed on shear layer instabilities in non reacting flows

with much of the work being done in incompressible flows. A fluid dynamic instability theory for a chemically reacting shear layer does not exist at present. Such a theory is needed to predict the frequency range in which the burning vortical structures appear and to understand their response to changes in the flow and chemical composition of the combustible mixture.

Chapter III

## CONCLUSIONS

From the results of the experimental studies described earlier, the importance of vortex shedding and the unsteady combustion in these vortices in causing and maintaining ramjet combustor instabilities is evident. The unsteady combustion in the shed vortices feeds energy into the combustor acoustics if the following inequality (i.e., Rayleigh's criterion) is satisfied (Eq. (4))

$$\int_{V_{flame}} |S_{pq}| \cos \theta_{pq} \, dV_{flame} > 0 \qquad (4)$$

where $S_{pq}$ = cross spectrum between pressure and the unsteady heat release

$\theta_{pq}$ = phase between the pressure and the unsteady heat release and

$V_{flame}$ = volume of the flame region

As $|S_{pq}| > 0$, the sign of the above integral is largely determined by the variation of the phase angle $\theta_{pq}$ over the flame region. Thus, over some regions, the flame may be driving while over other regions the flame may be damping.

The spectrum of the pressure fluctuations $S_{pp}$ is related to the spectrum of the unsteady heat release $S_{qq}$, at least for compact flames, by the following equation (Eq. (2))

$$S_{pp} = \frac{\bar{\rho}^2}{c_{\bar{p}}^2} |G|^2 S_{qq} \qquad (2)$$

where G is the relevant Green's function and describes how an unsteady heat source excites pressure oscillations.

Since G is maximized at the natural acoustic frequencies of the combustor (Appendix D), then Eq. (2) indicates that if high values of unsteady heat release occurs at a natural acoustic frequency of the combustor, large pressure fluctuations will also occur at that frequency. If vortex shedding occurs at a natural frequency of the combustor, then, large values of $S_{qq}$ may be obtained at this frequency.

From these considerations it is clear that to suppress combustion instabilities one or more of the following approaches should be undertaken:

(i) vortex shedding ( at a natural frequency) must be suppressed and/or

(ii) the phase angle $\theta_{pq}$ must be so controlled that the inequality, Eq. (2) is not satisfied and/or

(iii) the magnitude of $S_{qq}$ must be reduced.

Further research is needed to understand how best these approaches may be incorporated in dump type ramjet combustors. For example, the shear layer instability of the flame should be investigated to determine the conditions under which vortex shedding may occur at an acoustic natural frequency of the combustor. This could lead to guidelines for designing the flame holder

region to suppress vortex shedding at an acoustic natural frequency. The fundamental aspects of the interaction between the geometry of the flame zone and its fluid mechanics should also be studied to gain understanding of how the magnitude and phase of the unsteady heat release may be controlled.

In conclusion, it is believed that this research program has been successful in identifying one, if not the major, source of longitudinal instabilities in ramjet like combustors; that is, the modification of combustion rates in the ramjet flame zone by vortical structures arising as a result of the fluid mechanical instability of the flame.

## REFERENCES


1. Belding, J. A. and Coley, W. B., "Integral Rocket/Ramjets for Tactical Missiles," Astronautics and Aeronautics, Vol. II, pp. 20-26, Dec. 1973.

2. Curran, E. T. and Stull, F. D., "Ramjet Engines: Highlights of Past Achievements and Future Promise," Proceedings of Second International Symposium on Airbreathing Engines, International Council of the Aeronautical Sciences, March 1974.

3. Drewry, J. E., "Fluid Dynamic Characterization of Sudden-Expansion Ramjet Combustor Flowfields," AIAA Journal, Vol. 16, No. 4, pp. 303-319, April 1978.

4. Waugh, R. C., Brown, R. S., Hood, T. S., Flandro, G. A., Oates, G. C. and Reardon, F. H., "Ramjet Combustor Instability Investigation Literature Survey and Preliminary Design Study," Interim Report, UTC/CSD-2770-IR, Oct. 1, 1981 - Dec. 31, 1981.

5. Waugh, R. C. and Brown, R. S., "A Literature Survey of Ramjet Combustor Instability," CPIA Publication No. 375, pp. 1-13, April 1983.

6. Rogers, T., "Ramjet Inlet/Combustor Pulsations Study," Final Report, Naval Weapons Center, S-1463 A, Sept. 1977 - May 1978.

7. Rogers, T., "Ramjet Inlet/Combustor Pulsations Analysis and Test," Final Report, Naval Weapons Center, S-1508 A, Sept. 1978 - Sept. 1979.

8. Rogers, T., "Pressure Oscillations in a Small Ramjet Engine," Source of publication unknown; Work supported by Naval Weapons Center, Contract N00123-77-C-0541.

9. Clark, W. H., "Experimental Investigation of Pressure Oscillations in a Side Dump Ramjet Combustor," Jr. of Spacecraft and Rockets, Vol. 19, No. 1, Jan. - Feb. 1982, p. 47.

10. Clark, W. H. and Schadow, K. C., "Recent Liquid Fuel Ramjet Research and Development Programs," CPIA Publication No. 375, pp. 89-114, April 1983.

11. Crump, J. E., Schadow, K. C., Bloomshield, F. S., Culick, F. E. C. and Yang, V., "Combustion Stability in Dump Combustors: Acoustic Mode Determinations," CPIA Publication No. 366, Vol. 1, pp. 617-644, Oct. 1982.

12. Chamberlain, J., "Combustion Instability in Turbine Engine Afterburners and Ramjets," CPIA Publication No. 375, pp. 63-70, April 1983.

13. Schadow, K. C., Clark, W. H., Crump, J. E., Culick, F. E. C., and Yang, V., "Combustion Instability in Liquid Fuel Ramjets," Proceedings of the 6th International Symposium on Air Breathing Engines, June 6-11, 1983.

14. Culick, F. E. C. and Rogers, T., The Response of Normal Shocks in Diffusers," Source of publication unknown; publication available upon request.

15. Crocco, L. and Cheng, S. I., "Theory of Combustion Instability in Liquid Propellant Rocket Motors," Pergamon Press, The Macmillan Co., N. Y., 1957.

16. Technical Panel on Solid Propellant Instability of Combustion: Scientific Papers, 1960-1963, The Johns Hopkins University, Applied Physics Laboratory, Silver Spring, MD.

17. Dix, D. M., and Smith, G. E., "Analysis of Combustion Instability in Aircraft Engine Augmenters," AIAA Paper No. 71-700, AIAA/SAE 7th Propulsion Joint Specialist Conference, Salt Lake City, Utah, June 14-18, 1971.

18. "Proceedings of the ONR/AFOSR Workshop on Mechanisms of Instability in Liquid-Fueled Ramjets," Atlanta, GA, 16-18 March 1983, CPIA Publication No. 375, April 1983.

19. Zinn, B. T., "Review of Nozzle Damping in Solid Rocket Instabilities," AIAA Paper No. 72-1050 and AIAA Journal, Vol. 11, No. 11, pp. 1492-1497, Nov. 1973.

20. Zinn, B. T., "Nozzle Effect upon Combustor Stability," CPIA Publication No. 375, pp. 247-276, April 1983.

21. Lord Rayleigh, "The Theory of Sound," Vol. II, Dover, pp. 224-235, 1945.

22. Putnam, A. A., Non-Steady Flame Propagation: Chapters F, G and H. Pergamon Press, The Macmillan Co., N. Y., 1964.

23. Hegde, U. G., Reuter, D., Daniel, B. R. and Zinn, B. T., "Flame Driving of Longitudinal Instabilities in Dump Type Ramjet Combustors," AIAA 24th Aerospace Sciences Meeting, Paper No. 86-0371, 1986.

24. Hegde, U. G., Reuter, D., Zinn, B. T. and Daniel, B. R., "Fluid Mechanically Coupled Combustion-Instabilities in Ramjet Combustors," AIAA 25th Aerospace Sciences Meeting, Paper No. 87-0216, 1987.

25. Smith, D. A. and Zukoski, E. E., "Combustion Instability Sustained by Unsteady Vortex Combustion," AIAA/SAE/ASME/ASEE 21st Joint Propulsion Conference, AIAA Paper No. 85-1248, 1985.

26. Sterling, J. D. and Zukoski, E. E., "Longitudinal Mode Combustion Instabilities in a Dump Combustor," AIAA 25th Aerospace Sciences Meeting, Paper No. 87-0220, 1987.

27. Harsha, P. T., Edelman, R. B., Schmotolacha, S. N., and Pederson, R. J., "Combustor Modeling for Ramjet Development Programs," AGARD Conference Proceedings No. 307, pp. 29-1/29-17, March 1982.

28. Candel, S. M., Darabiha, N. and Esposito, E., "Models for a Turbulent, Premixed Dump Combustor," AIAA Paper No. 82-1261, AIAA/SAE/ASME 18th Joint Propulsion Conference, June 21-23, 1982.

29. Lilley, G. D., "Computer Modeling of Ramjet Combustors," AIAA Journal, Vol. 19, No. 12, pp. 1562-1563, 1981.

30. Schmotolacha, S. N. and Phung, P. V., "Characteristics of Dump Combustor Flow Fields with and without Chemical Reactions," CPIA Publication No. 329, pp. 547-584, Nov. 1980.

31. Yang, V. and Culick, F. E. C., "Linear Theory of Pressure Oscillations in Liquid Fueled Ramjet Engines," AIAA Paper No. 83-0574, AIAA 21st Aerospace Sciences Meeting, 1983.

32. Gaydon, A. G. and Wolfhard, H. G., "Flames: Their Structure, Radiation and Temperature," 4th Edition, John Wiley & Sons, N. Y. 1979.

33. Pierce, A. D., "Acoustics," McGraw Hill Inc., N. Y., 1981.

34. Ho, C. M. and Huerre, P., "Perturbed Free Shear Layers," Annual Review of Fluid Mechanics, Vol. 16, pp. 365-424, 1984.

35. Flandro, G. A. and Finlayson, P. A., "Nonlinear Interactions between Vortices and Acoustic Waves in a Rocket Combustion Chamber," 21st JANNAF Combustion Meeting, 1984.

36. Abouself, G. E., Keklak, J. A., and Toong, T. Y., "Ramjet Rumble: The Low Frequency Instability Mechanism in Coaxial Dump Combustors," Combustion Science and Technology, Vol. 36, pp. 83-108, 1984.

37. Dowling, A. P. and Bloxsidge, G. J., "Reheat Buzz - An Acoustically Driven Combustion Instability," AIAA 9th Aeroacoustics Conference, AIAA Paper No. 84-2321, 1984.

# APPENDIX A

## Appendix A

## Professional Interactions

1) Professional Personnel:

Dr. B. T. Zinn, Regents' Professor

Dr. U. G. Hegde, Research Engineer

Dr. J. I. Jagoda, Associate Professor

Mr. B. R. Daniel, Senior Research Engineer

Mr. D. M. Reuter, Graduate Research Assistant

Mr. Andy Chuang, Graduate Research Assistant

2) Degrees Awarded:

Mr. Andy Chuang, M.S.

Mr. D. M. Reuter, M.S

3) Refereed Publications:

i) "Flame Driving of Longitudinal Instabilities in Dump Type Ramjet Combustors," submitted to Combustion Science and Technology.

ii) "Sound Generation by Ducted Flames," submitted to the AIAA Journal.

4) Other Publications:

i) "Fluid Mechanically Coupled Combustion Instabilities in Ramjet Combustors," AIAA Paper No. 87-0216, January 1987.

ii) "Combustion Instabilities in Dump Type Ramjet Combustors," Proceedings of the 23rd JANNAF Combustion Meeting, October 1986.

iii) "Flame Driving of Longitudinal Instabilities in Dump Type Ramjet Combustors," AIAA Paper No. 86-0371, January 1986.

iv) "Flame Driving of Longitudinal Instabilities in Dump Type Ramjet Combustors," Proceedings of the 22nd JANNAF Combustion Meeting, CPIA Publication No. 432, Vol. I, October 1985.

5) Presentations:

i) "Fluid Mechanically Coupled Combustion Instabilities in Ramjet Combustors," AIAA 25th Aerospace Sciences Meeting, Reno, Nevada, January 1987.

ii) "Combustion Instabilities in Dump Type Ramjet Combustors," 23rd JANNAF Combustion Meeting, NASA Langley Research Center, Hampton, VA, October 1986.

iii) "Flame Driving of Longitudinal Instabilities in Dump Type Ramjet Combustors," AIAA 24th Aerospace Sciences Meeting, Reno, Nevada, January 1986.

iv) "Combustion Instability in Ramjets," Seminar presented at the Combustion Workshop held at the Brasilian Space Research Institute, Sao Jose dos Campos, Sao Paulo, Brasil, December 1985.

v) "Flame Driving of Longitudinal Instabilities in Liquid Fueled Dump Ramjet Combustors," ONR/NAVIER Contractors Review Meeting, Washington, DC, October 1985.

vi) "Flame Driving of Longitudinal Instabilities in Dump Type Ramjet Combustors," 22nd JANNAF Combustion Meeting, Jet Propulsion Laboratory, Pasadena, CA, October 1985.

vii) "Flame Driving of Longitudinal Instabilities in Liquid Fueled Dump Ramjet Combustors," ONR/NAVAIR Sponsored Meeting on Compact Ramjet Combustion at Naval Postgraduate School, Monterey, CA, October 1984.

viii)"Flame Driving of Longitudinal Instabilities in Liquid Fueled Dump Ramjet Combustors," Naval Air Systems Command Meeting, Washington, DC, September 1984.

APPENDIX B

AIAA'86

AIAA-86-0371

# Flame Driving of Longitudinal Instabilities in Dump Type Ramjet Combustors

U. G. Hegde, D. Reuter, B. R. Daniel and B. T. Zinn, Georgia Institute of Technology, Atlanta, GA

**AIAA 24th Aerospace Sciences Meeting**

January 6-9, 1986/Reno, Nevada

# FLAME DRIVING OF LONGITUDINAL INSTABILITIES IN DUMP TYPE RAMJET COMBUSTORS#

U.G. HEGDE,* D. REUTER,** B.R. DANIEL*** AND B.T. ZINN****

School of Aerospace Engineering
Georgia Institute of Technology
Atlanta, Georgia

## ABSTRACT

Coaxial, dump type ramjet combustors are often prone to combustion instability problems that can seriously affect their performance. This study is concerned with the highly detrimental low frequency instabilities which represent one of the most common types of the encountered instabilities. In particular, the coupling between the cone-like flames which are stabilized at the entrance of the dump combustor and longitudinal acoustic fields is studied in an experimental set up specifically developed for this purpose. It consists of a rectangular tube having an injector plate at one end and acoustic drivers at the opposite end. A combustible mixture enters through the injector and a conical flame is stabilized on a thin wire attached to the side walls of the tube. The behavior of this flame in various longitudinal acoustic fields generated by the acoustic drivers is studied. A variety of experimental techniques, including high speed Schlieren and shadow photography, CH radiation emission and acoustic pressure measurements are used. Investigations were undertaken at two experimental set up lengths. A strong coupling between the flame response and certain natural acoustic frequencies is observed in the longer set up. For the shorter set up, the coupling is seen to be intense when the flame stabilization region is located near an acoustic pressure minimum. These observations shed new light on flame/acoustic mode interactions in a ramjet combustor-like environment and the limitations of current state of the art theoretical models of this phenomenon.

## INTRODUCTION

Recent developments of coaxial dump type ramjet engines have been hindered by occurrences of destructive combusion instabilities [1]. These instabilities are characterized by either low frequency (i.e. rumble) or high frequency (i.e. screech) pressure and velocity oscillations. The low frequency rumble is in the range of 100-500 Hertz and is generally characterized by longitudinal acoustic oscillations in the inlet section and the combustor. In contrast, the high frequency screech occurs when one of the tangential acoustic modes of the combustor is excited. In the present study the low frequency type of instability is considered. This type of instability can interfere with the shock system in the ramjet inlet resulting in loss of engine performance as well as imposing excessive vibrational loads on the system.

Combustion instabilities have appeared in a variety of propulsion systems including liquid and solid propellant rocket motors, air breathing engines, ramjets and so on. In the majority of cases the combustion process provides the energy required for the excitation and maintenance of the observed oscillations. According to Rayleigh's criterion [2], driving of the pressure oscillations by the combustion process occurs if the oscillating heat release from the combustion process is in phase with the pressure oscillations. Under these conditions, energy is added to the oscillations during each cycle. However, the acoustic field also loses energy due to viscous dissipation, heat conduction and the convection and radiation of acoustic energy through the exhaust nozzle. During an instability, the amplitude of the combustor oscillation grows in time as long as the energy added to the oscillations per cycle is larger than the energy lost per cycle due to the above mentioned loss processes. As the amplitude grows, some or all of the energy gain and loss processes become amplitude dependent and an amplitude is reached at which the energy added to the oscillation per cycle equals the energy lost per cycle. When this condition is established, the amplitude of the oscillations remains constant.

To date, there has been a paucity of experimental data relating to the coupling between the combustion processes and acoustic oscillations in a ramjet engine like environment. Recent studies include those of Davis [3] and Heitor et al [4]. With the help of high speed photography Davis categorized two modes of low frequency instability in dump type combustors. In the first mode, the entire combustion zone underwent a cyclic oscillation while in the second mode regular shedding of hot spots from the recirculation zone at the dump plane was observed. Heitor, et al measured the frequency and strength of combustion induced oscillations for premixed methane air flames stabilized on baffles located on the axis of a pipe. They found that instability involving the first natural mode (quarter wave type) occurred for a wide range of fuel to air ratios. More recently, Smith and Zukoski [5] studied combustion instability involving a flame stabilized behind a rearward facing step. They report that under conditions of

# Research supported by the Office of Naval Research, under Contract No. SFRC No. N00014-84-K-0470

* Research Engineer
** Graduate Research Assistant
*** Senior Research Engineer
**** Regents' Professor, Associate Fellow AIAA

instability large vortical structures were formed downstream of the step at an acoustic resonant frequency. These were subsequently convected away from the step and the resulting unsteady combustion was found to feed energy into the acoustic oscillations. Keller, et al [6] identified three modes of instability in a similar set up in an effort to understand the mechanisms responsible for flashback. They attributed this phenomenon to the action of vortices in the recirculation zone of the step. These studies indicate that the fluid mechanics of the flame stabilization region plays an important role in combustion instability.

Theoretical efforts to model combustion instabilities in dump type combustors may be broadly classified into two types. The first type assumes the flame zone to be compact relative to the acoustic wavelength. The governing flow equations on either side of the flame zone are matched by making several assumptions about the combustion process. The analyses of Abouseif et al [7] and Dowling and Bloxsidge [8] exemplify this approach. The second type of analysis, as developed by Yang and Culick [9], investigates the combustion region in more detail. They used an idealized description of the flow field inside a ramjet. Their model assumes the combustion to take place in an infinitely thin flame sheet which is distorted by the presence of pressure and velocity oscillations. Using integral forms of the conservation equations Yang and Culick obtained solutions for both the combustor acoustic wave structure and the complex frequency of oscillation whose imaginary part determines whether an instability will occur or not.

Unfortunately, neither of these approaches have been totally successful. Whereas proponents of the first approach claim to be able to predict instability no understanding of the coupling between the acoustic field and the unsteady combustion process is obtained since the combustion zone acoustic wave structure is ignored. The Yang-Culick model on the other hand appears to reasonably predict the acoustic pressure structure in the combustor but fails to predict stability limits. Thus, there is a need to understand in more detail the complex processes that link the acoustic field to the unsteady combustion field. The present study focuses on this interaction.

## EXPERIMENTAL EFFORTS

The set up described in Fig. 1 has been developed. It consists of an inlet, combustor and exhaust sections. The inlet contains a movable injector through which a mixture of propane and air is introduced into the combustor. The flame is stabilized in the 7.5 x 5 $cm^2$ combustor section on a 0.8 mm diameter nichrome wire chosen to reduce vortex shedding tendencies. The wire is attached to the combustor windows at half combustor height and it is heated electrically to improve the steadiness of the stabilized V-shaped flame. The exhaust section is equipped with two acoustic drivers which are used to excite a standing acoustic wave of desired amplitude and frequency in the set-up. The movable injector provides a capability for "placing" the stabilizing wire on any part of an excited standing wave; that is, at a pressure maximum, minimum or in between. The maximum length, $L_{max}$, available between the injector face and the exhaust section exit plane is 3 meters. The flow approaching the stabilizing wire is parallel and uniform and disturbances are damped out by means of a fine wire mesh grid located 8 cm. upstream of the stabilizing wire. The cold flow Reynolds number is kept below 10,000 in the interest of maintaining a disturbance free flow. The combustor walls are water cooled enabling wall mounted pressure transducers to be used to monitor the acoustic pressure field. Capabilities for time and space resolved measurements of CH species radiation from the flame have also been developed. The concentrations of these species is a measure of the reaction rate [10], and, hence, the heat release rate and are useful in describing the unsteady combustion field.

Experiments have been performed in the set up described above and in a modified version in which the exhaust section was removed and the acoustic driver section was attached directly at the combustor exit. The consequent shortening of the tube results in higher values for the fundamental acoustic frequencies of the set up. Striking differences were observed in the flame response to acoustic excitation in the two set ups. These are described later.

The injector plate is made of sintered stainless steel and it acts, approximately, as an acoustically rigid termination so that the acoustic behavior of the experimental set-up approximates that of a closed-open organ pipe. During tests in both set ups, spontaneous instabilities involving the tube's fundamental acoustic mode (i.e., the quarter wave mode) have been observed in certain fuel/air ratio ranges. When the mixture composition is close to the lean stability limit, the flame is thin and can be readily stabilized on the heated wire. However, as the fuel fraction in increased, instability sets in as indicated by the wall mounted pressure transducers which record an increase in amplitude of the fundamental acoustic mode. With further increase in the fuel fraction (while the mixture remains in the fuel lean range) the flame flashes back from the wire to the screen and the sound pressure levels in the combustor approach 140-150 dB. As the mixture becomes fuel rich, not all the fuel can be burned within the combustor and part of the mixture burns outside the set-up. When the mixture approaches the rich flammability limit the flame is "blown back" to the wire where it stabilizes again. Under these conditions the instability subsides and the flame is again stable and thin.

Observations of the flame indicated that the instability originates at the wire. Thus, experiments conducted to date have been carried out with the flame stabilized at the wire. These included visualization studies with high speed Schlieren and shadow photography, CH radiation measurements from the flame and measurements of acoustic pressure distributions along the flame. These have been carried out with acoustic excitation provided by the drivers at different frequencies.

High speed (6000 frames/second) Schlieren and shadowgraph films were taken in the longer tube with acoustic excitation at a frequency of 385 Hz and acoustic pressure amplitudes of the order of 130 dB. By varying the injector location, tests were conducted with the stabilizing wire placed at a pressure maximum, a minimum and in between. The fuel mass fraction was 2.2% and the burned gas temperature as measured by a thermocouple was 1325 °K. The acoustic pressure along the flame was simultaneously monitored. The films reveal that there is a periodic shedding of flamelets from the wire. As one flamelet is shed another is formed at its tail so that the flame is continuous. These flamelets move along what may be called, approximately, the steady flame front, stretching as they proceed. A sequence from the shadowgraph film taken with the wire at a pressure maximum is presented in Fig. 2. While the mixture injection velocity was 1.5m/sec, the convection velocity of the flamelets was of the order of 2.5m/sec. indicating that the flamelets are convected at the local flow velocity. The surprising fact is that, except when the stabilizing wire was at a pressure minimum (i.e. acoustic velocity maximum) for the driving frequency of 385 Hz. the shedding was at frequencies corresponding to the first natural acoustic mode of the experimental set-up and not at the driving frequency. However, the pressure amplitudes of the first natural mode were at least 7db below those of the acoustically driven signal at 385 Hz. When the wire was moved to the location of the pressure minimum for the driven signal, the shedding frequency increased, but still remained lower than the driving frequency. The only effect characterized by the driving frequency in all the investigated cases was an observed oscillation of the flamelets, as they moved, at the driving frequency. This was most evident in the film with the wire located at the pressure minimum (i.e., a velocity antinode).

To investigate this phenomenon further CH radiation measurements were carried out in the long tube. By a suitable arrangement of the optical elements, the radiation from vertical 3 mm wide strips of the flame were made. The optics could be moved axially so that the radiation from different parts of the flame could be measured. Initially, the measurements were carried out under conditions similar to those under which the high speed films were taken. It was found in these cases that even though the pressure spectra were dominated by the contribution of the 385 Hz oscillation, the radiation spectra were dominated by the frequencies corresponding to the first natural frequency for each case. For example, in Fig. 3 the amplitude of the radiation is plotted as a function of the axial distance from the stabilizing wire. It is seen that the magnitudes of the signals at the first natural frequencies are an order of magnitude larger than those at the driven frequency. Figure 4 describes the frequency spectrum of the radiation 1 cm. downstream of the wire for the case when the wire was between a minimum and maximum for the driving frequency. It is seen that the radiation spectrum contains peaks at frequencies that are multiples of the first natural frequency. For the ideal case of an acoustically closed-open organ pipe, which the system approximates, the nth longitudinal acoustic mode is $f_n = (2n + 1) f_o$ where $f_o$ is the frequency of the first mode ($n = 0$). With the addition of heat due to combustion and the resulting spatial dependence of the speed of sound this relationship becomes only approximate. Therefore, it should be noted that multiples of the first natural mode frequency which are seen in the radiation spectrum are not, in general, natural acoustic frequencies of the system. The pressure spectrum for this case, at the location of the wire is plotted in Fig. 5. It is seen to be dominated by the signal at 385 Hz.

The phase of the radiation signal at the natural frequencies with respect to the pressure at the same frequencies for the above cases is plotted in Fig. 6. A mean curve has been drawn through the points to emphasize the nature of the data. The slope of the phase curve is inversely proportional to the convection velocity of the flamelets. It is seen to decrease with increasing axial distance along the flame, indicating an increase in the convection velocity with distance. This is reasonable because of the increase in temperature that occurs along the flame which results in an acceleration of the flow.

Whereas the phase of the radiation signal changes due to convection by the local flow, the phase of the acoustic pressure changes according to the local speed of sound and these changes are negligible over the length of the flame for the first natural frequency. Thus, over certain regions of the flame the radiation and the acoustic pressure are in phase and over other regions of the flame they are out of phase. It is interesting to note that the maximum of the amplitudes of the radiation signal occur, approximately, 1-2 cm downstream of the stabilizing wire. A comparison of Figures 3 and 6 shows that in this region there is a component of the radiation at the natural frequency which is in phase with the pressure thus satisfying Rayleigh's condition for driving.

It should be noted that the above tests were carried out near the fuel lean flammability limit with the fuel mass fraction between 2.0 to 2.3%. When the fuel fraction is increased beyond this level, spontaneous instability occurs as described earlier. This spontaneous instability begins even as the flame is attached to the wire and with a further (small) increase in the fuel mass fraction the flame flashes back to the screen.

Spectra of pressure and radiation of the unexcited flame are shown in Figures 7 and 8 for different fuel-air ratios. It is clearly seen that the signal strength at the fundamental acoustic frequency (in this case about 63 Hz) increases as the fuel-air ratio increases.

The above discussed data, obtained in the "longer" experimental configurations, indicate that there is a strong coupling between the radiation oscillations, which are a measure of the unsteady heat release rate in the flame, and the fundamental acoustic natural mode frequency. In an effort to establish whether a strong coupling

between the acoustics and the flame also occurs at other frequencies, tests were carried out with different driven frequencies with the injector location fixed. The first four acoustic modes were determined to be at 63 Hz, 168 Hz, 282 Hz and 364 Hz, respectively. Since the drivers are not efficient at frequencies below 200 Hz where a lot of the acoustic power is supplied to higher harmonics, tests were run at frequencies close to the third and fourth natural frequencies.

When the experimental set up was driven at the fourth mode frequency the response of the flame was still at the fundamental frequency. However, for excitation at 282 Hz (the third natural frequency) the major response of the flame was at 282 Hz. However, a slight shift in the driving frequency was sufficient to change this response. For example, for excitation at 280 Hz, the major response of the flame was no longer around the third natural frequency. This is clearly shown in Fig. 9 where the radiation signals for acoustic excitations at 282 Hz and 280 Hz are compared. Thus, a response at the same frequency between the acoustics of the system and the unsteady behavior of the flame occurs, for this set up, only at a few selected frequencies which are close to only certain natural frequencies of the system; that is, in the above case, the first and third and not at all the natural frequencies.

Experiments have also been conducted with the shorter version of the set up with the exhaust section removed and the acoustic drivers located directly at the combustor exit. The original reason for making this modification was to get the fundamental natural frequency in a range where the acoustic drivers are reasonably efficient thus enabling the study of the flame response when excited at this frequency. Surprisingly, it was found that in the short tube the flame response did not always occur at the fundamental natural frequency when the excitation was at different frequencies. Instead the response of the flame depended strongly upon the location of the stabilizing wire on the generated acoustic wave in the range 200-500 Hz in which the tests were carried out. For example, when the stabilizing wire was near a pressure minimum there was a large radiation signal at the driving frequency. On the other hand, when the stabilizing wire was near a pressure maximum the flame response was not at the driving frequency. It appears that the acoustic velocity, dominant at a pressure minimum and small at a pressure maximum, may be important in determining the flame response. Experimental work on the two set ups is continuing.

Some comments on stabilizing the flame on the heated wire are also in order. Originally, the purpose of the wire was to both ignite and stabilize the flame. However, igniting the mixture by heating the wire proved to be quite tricky. Hence, ignition was achieved by use of a propane torch introduced from a port located above the wire. Flames stabilized in this manner on the cold wire exhibited a great degree of unsteadiness. It was found that the heating of the wire greatly reduced this tendency and also helped in avoiding blow off of the flame. It did not, however, appear to have any effect on the flame flashing back under spontaneous instability. The wire was heated by an alternating current at 60 Hz. The fluctuating component of the wire temperature, due to ohmic squaring, was therefore at 120 Hz. No signals in the pressure or radiation spectra were found at this frequency that could be attributed to this fluctuating temperature component of the wire. It is therefore believed that heating of the wire did not interfere with any of the phenomena described here.

## THEORETICAL CONSIDERATIONS

A computer program, based on the Yang-Culick model [9], was developed to solve for the flow variables in the combustion zone. Briefly, it considers the flame as a flow discontinuity separating the unburned and burned flows. Conservation equations are developed and solved for both the upstream and downstream regions of the flame. A kinematic description of the flame front and specification of the flame velocity complete the formulation. The assumption of small perturbations in the flow variables allows the split of the governing equations into a set of nonlinear differential equations for the steady, time independent part and a set of linear differential equations for the unsteady part. Whereas the Yang-Culick model obtains the natural frequencies as eigenvalues of the time dependent equations, the model developed for the present study assumes external excitation by the acoustic drivers and, hence, a known frequency of oscillations.

Observations and photography of the flame indicate that under steady state conditions, the assumptions of the Yang-Culick model appear valid; that is, the flame is thin and may be considered as a discontinuity. Under these conditions the flame shape can be reasonably predicted. An example is shown in Fig. 10. The experimental flame shape was determined by direct photography. The theoretical calculation requires the values of the upstream velocity $u_0$ and pressure, the flame velocity W (assumed constant) and the ratio of the temperature across the flame. The flame velocity W was measured from the photograph with the knowledge of the upstream velocity $u_0$ and the flame length. In all cases, it was found that the theory underpredicted the flame length. This may be due to the neglect of viscous and thermal conduction effects in the model. These effects become important near the wall and tend to lower the flame velocity in that region which, in turn, would cause lengthening of the flame.

The unsteady problem, however, poses numerous hurdles. The Yang-Culick model assumes that in the unsteady case the flame front remains thin though it undergoes perturbations. Viewing of the shadowgraph films and the phenomenon of the flamelet shedding makes this assumption questionable. Secondly, the distortion of the thin flame front signifies the effect of the combustion-acoustic interaction in the model. Experimentally, the convection of the flamelets appears to play a major role in the driving of the tube's acoustic modes. The assumption of a constant flame velocity may also be erroneous. Finally, the response of the flame at a frequency

other than the driving frequency cannot be predicted by a linear model.

## CONCLUSION

The response of wedge shaped flames, similar to those often occuring in ramjet combustors, to acoustic excitation has been studied in two set ups which differed by the length of their exhaust sections. For the longer tube, the flame responds strongly to imposed excitation only at certain preferred frequencies. These frequencies are close to the first and third natural acoustic frequencies of the set up. The phenomenon of flamelet shedding has been observed at these frequencies. The radiation emission from the flame, and presumably the fluctuating heat release rate, undergo phase changes along the flame on the scale of a wavelength, $\lambda$, based on the convection velocity of the flamelets; i.e. $\lambda = u_c/f$ where $u_c$ is the convection velocity. The acoustic pressure, on the other hand, undergoes phase changes based on the speed of sound. Thus, in certain regions of the flame, the heat release and the pressure are in phase and in other regions they are out of phase. For the flamelet shedding at a preferred frequency, the amplitude of the radiation maximizes in a region where there is a component of it in phase with the pressure, thus satisfying Rayleigh's criterion for flame driving of the acoustics. On the other hand, the flame in the tube with the shorter exhaust, is able to respond to the imposed excitation at the driving frequency. The radiation signals from the flame are higher when the stabilizing wire is near a pressure minimum.

Consideration of the acoustic velocity and its relation to the pressure and heat release is also believed to be important. Some of the limitations of current theoretical models were also underlined.

## REFERENCES


1. Waugh, R.C. and Brown, R.S., "A Literature Survey of Combustor Instability", CPIA Publication No. 375, pp. 1-13, April 1983.

2. Lord Rayleigh, "The Theory of Sound," Vol. II., Dover, pp. 224-235.

3. Davis, D.L., "Coaxial Dump Combustor Combustion Instabilities, Part I - Parametric Test Data," Aero Propulsion Laboratory, Air Force Wright Aeronautical Laboratories, Wright-Patterson AFB, Ohio, Interim Report, 1981.

4. Heitor, M.V., Taylor, A.M.K.P. and Whitelaw, J.H., "Influence of Confinement on Combustion Instabilities of Premixed Flames Stabilized on Axisymmetric Baffles," Combustion and Flame, Vol, 57, pp. 109-121, 1984.

5. Smith, D.A. and Zukoski, E.E., "Combustion Instability Sustained by Unsteady Vortex Combustion," AIAA/SAE/ASME/ASEE 21st Joint Propulsion Conference, AIAA Paper No. 85-1248, 1985.

6. Keller, J.O., Vanveld, L., Korschelt, D., Hubbard, G.L., Ghoniem, A.F., Daily, J.W., and Oppenheim, A.K., "Mechanism of Instabilities in Turbulent Combustion Leading to Flashback," AIAA Journal, Vol. 20, No. 2., pp. 254-262, 1982

7. Abouseif, G.E. Keklak, J.A., and Toong, T.Y., "Ramjet Rumble: The Low Frequency Instability Mechanism in Coaxial Dump Combustors," Combustion Science and Technology, Vol. 36, pp. 83-108, 1984.

8. Dowling, A.P. and Bloxsidge, G.J., "Reheat Buzz - An Acoustically Driven Combustion Instability," AIAA 9th Aeroacoustics Conference, AIAA Paper No. 84-2321, 1984.

9. Yang, V. and Culick, F.E.C., "Linear Theory of Pressure Oscillations in Liquid-Fueled Ramjet Engines," AIAA 21st Aerospace Sciences Meeting, AIAA Paper No. 83-0574, 1983.

10. Gaydon, A.G. and Wolfhard, H.G., "Flames: Their Structure, Radiation and Temperature," 4th Edition, John Wiley and Sons, N.Y., 1979.


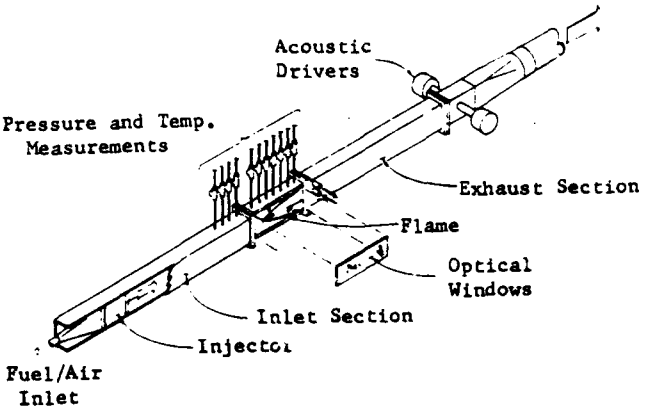


Fig. I Developed Experimental Set-up

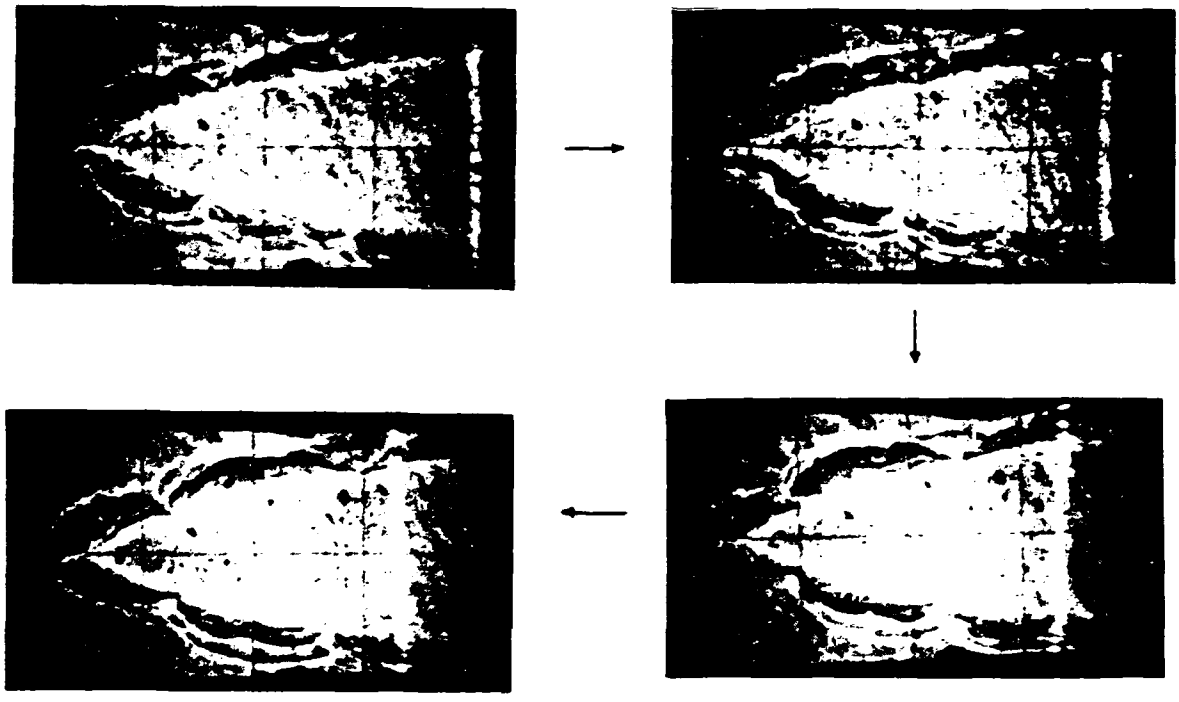

Fig. 2 Shadowgraph Film Sequence Showing Flamelet Shedding at a Preferred Frequency. Note Non-Negligible Thickness and Structure of Flame

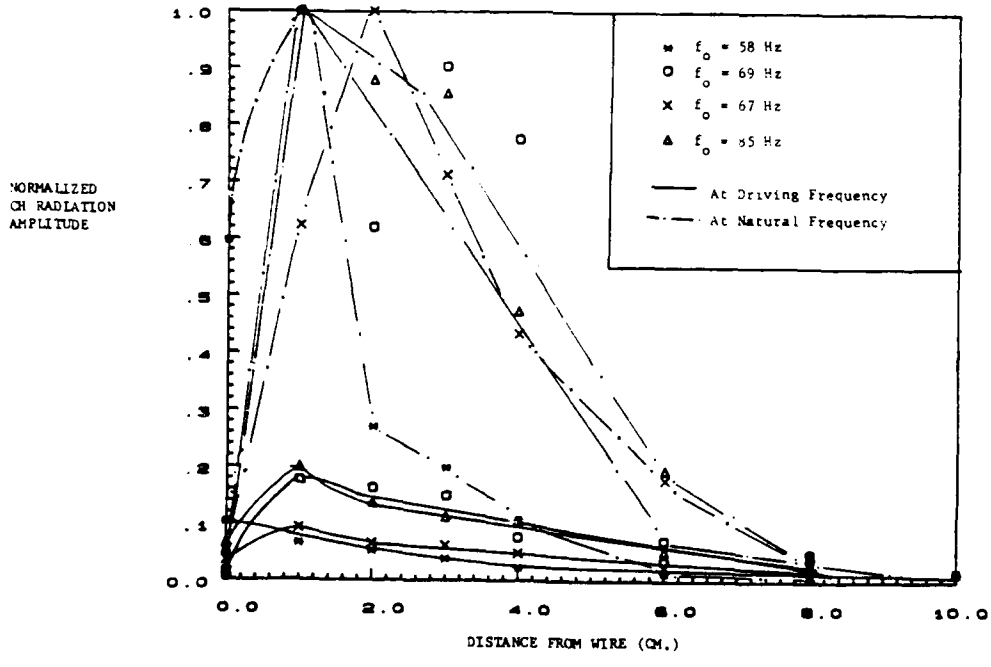


Fig. 3 Comparison of Emitted CH Radiation Amplitudes at First Natural Frequency and at Driving Frequency of 385 Hz. The Four Cases correspond to the Wire at a Maximum, a Minimum, Between a Minimum and Maximum and Between a Maximum and Minimum for the Standing Wave at 385 Hz.

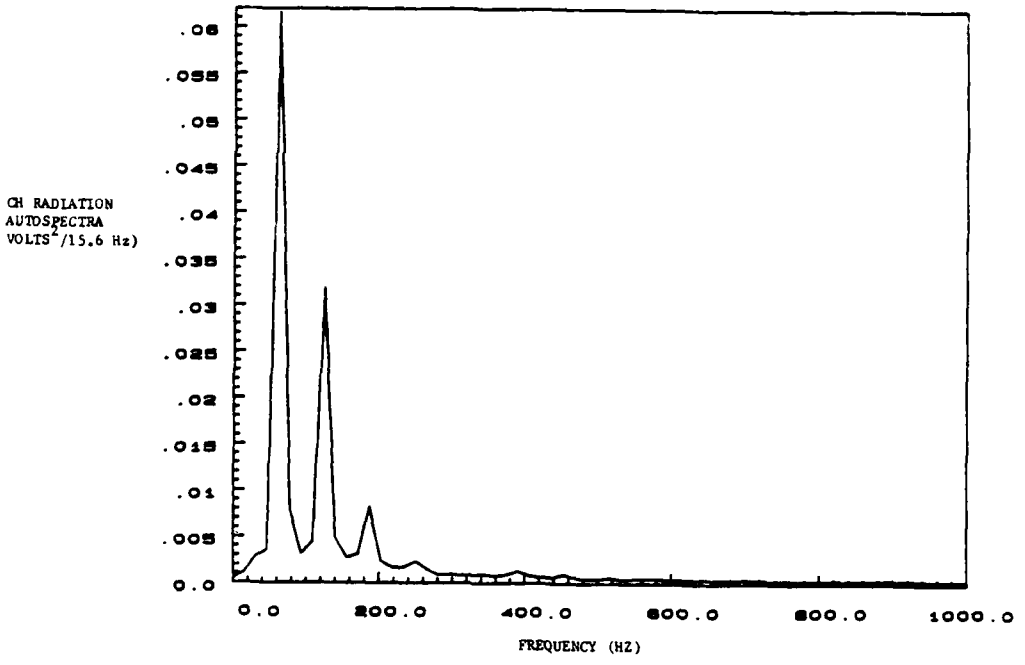


Fig. 4 Autospectrum of CH Radiation under Acoustic Excitation at 385 Hz.

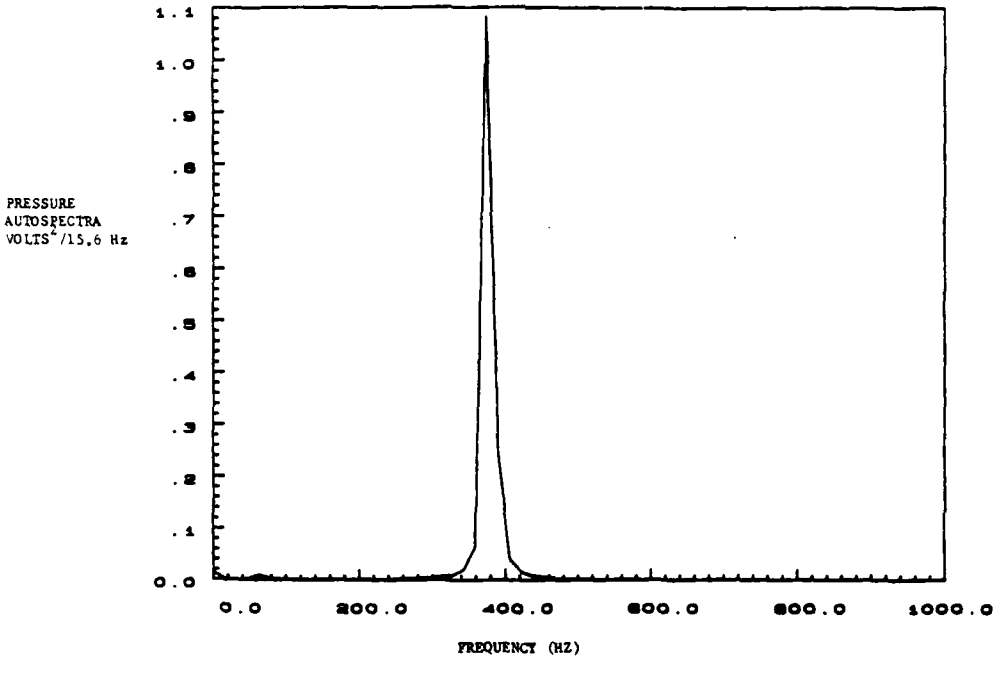


Fig. 5 Autospectrum of Pressure Fluctuations Under Acoustic Excitation at 385 Hz.

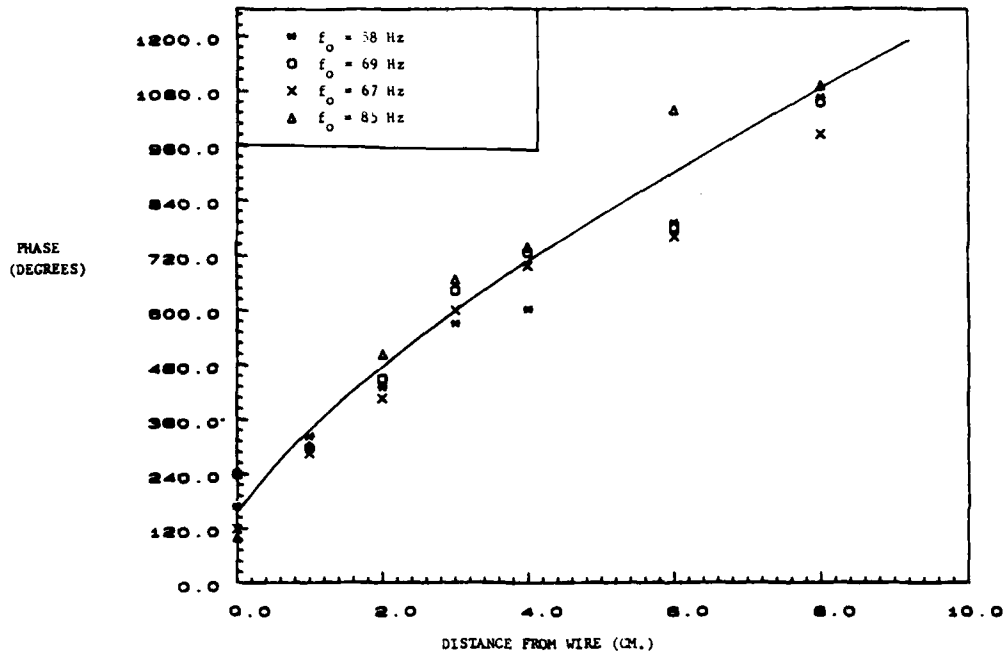


Fig. 6 Axial Variation of Phase of CH Radiation at first Natural Frequency under Acoustic Excitation at 385 Hz.

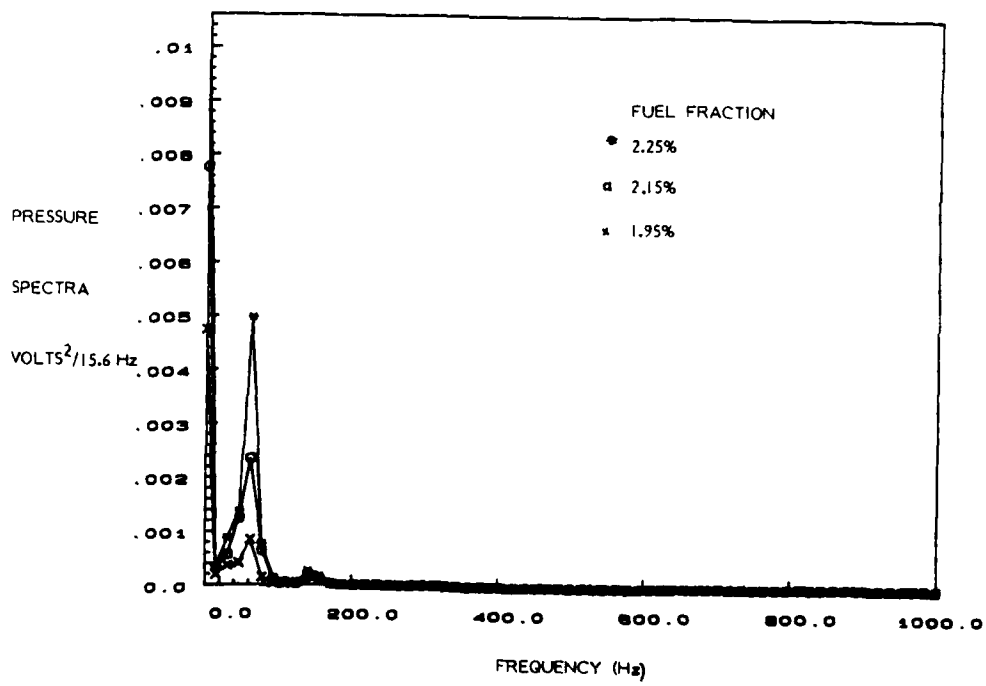


Fig. 7 Pressure Spectra of Unexcited Flame for Different Fuel-Air Ratios.

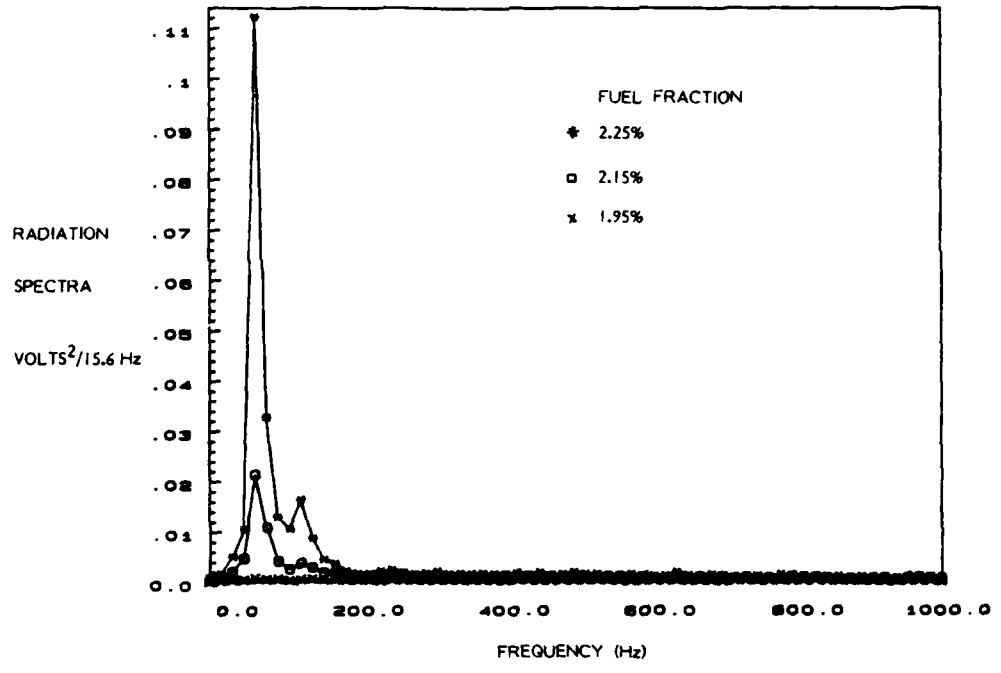


Fig. 8 CH Radiation Spectra of Unexcited Flame for Different Fuel-Air Ratios

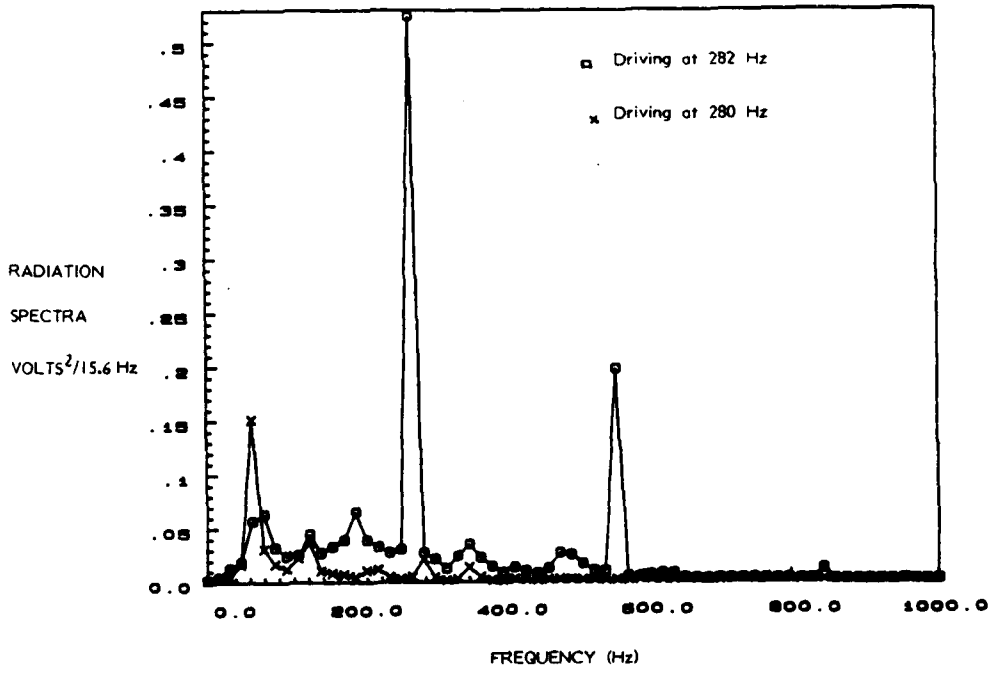


Fig. 9 CH Radiation Spectra under Acoustic Excitation at 282 Hz and 280 Hz. Note 282 Hz Corresponds to Third Natural frequency of set up.

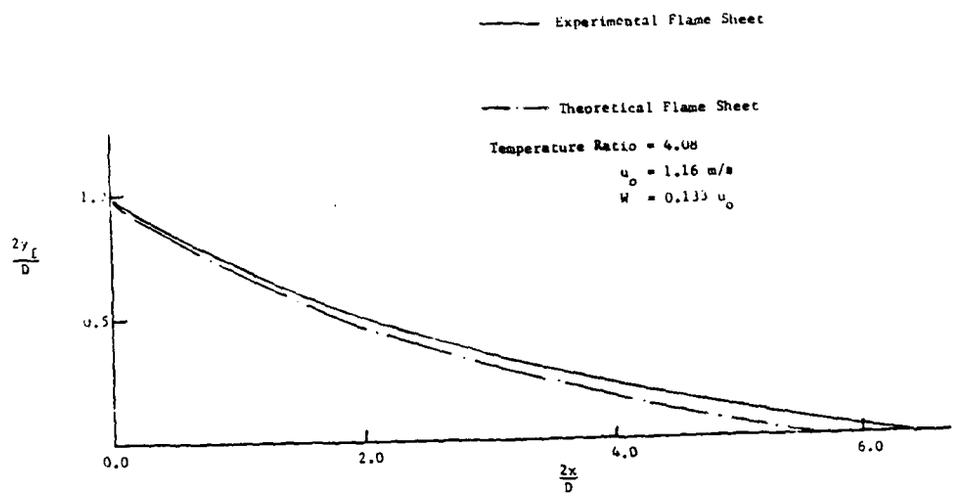


Fig. 10 Comparison of Theoretical and Experimental Flame Shape under Steady Conditions.

APPENDIX C

AIAA'87

AIAA-87-0216

# Fluid Mechanically Coupled Combustion-Instabilities in Ramjet Combustors

U. G. Hegde, D. Reuter, B. T. Zinn and B. R. Daniel, Georgia Institute of Technology, Atlanta, GA

**AIAA 25th Aerospace Sciences Meeting**

January 12-15, 1987/Reno, Nevada

# FLUID MECHANICALLY COUPLED COMBUSTION INSTABILITIES IN RAMJET COMBUSTORS*

U. G. Hegde[xx], D. Reuter[xxx], B. T. Zinn[†] and B. R. Daniel[††]

Georgia Institute of Technology
Atlanta, Georgia

## ABSTRACT

Combustion instability problems often occur in coaxial dump type ramjet combustors. A potentially severe type of instability is characterized by low frequency (in the range up to 500 Hz) pressure and velocity oscillations. This paper is concerned with this type of instability. It describes an investigation of the coupling between cone shaped flames, often encountered in dump type ramjet combustors and longitudinal acoustic fields associated with the low frequency instability. Specifically the unsteady behavior of a V-shaped flame, stabilized in a rectangular combustor, in various longitudinal acoustic fields is studied. A variety of experimental techniques, including high speed Schlieren and shadow photography, CH radiation emission and acoustic pressure measurements have been employed in this study. It is found that the shear layer formed by the flame exhibits a marked fluid dynamical instability at low frequencies resulting in the formation of burning vortical structures that are convected along the flame front. The resulting unsteady combustion process acts as a strong acoustic source resulting in longitudinal pressure oscillations. This problem, therefore, presents an intricate coupling among the three basic modes of fluid motion; that is, the vortical, acoustic and thermal modes. A simple model developed to predict flame generated acoustic spectra from measurements of the unsteady heat release rate yields the coupling between the thermal and acoustic modes. The unsteady vortical behavior of the flame is, however, extremely complicated and exhibits many nonlinear features, in particular the presence of subharmonics and harmonics of the main response frequency.

## INTRODUCTION

Recent developments of coaxial dump type ramjet engines have been hindered by occurrences of destructive combustion instabilities[1]. A potentially severe type of instability is characterized by low frequency (in the range of up to 500 Hz) pressure and velocity oscillations. This type of instability can interfere with the shock system in the ramjet inlet resulting in loss of engine performance as well as imposing excessive vibrational loads on the system. The present paper investigates this low frequency type of combustion instability.

In general, the unsteady combustion process provides the energy required for the excitation and maintenance of the observed oscillations. According to Rayleigh's criterion[2], driving of the pressure oscillations by the combustion process occurs if the oscillating heat release from the combustion process is in phase with the pressure oscillations. From this viewpoint, it becomes essential to determine the reasons and the events that conspire in a particular combustion instability problem to create an environment where Rayleigh's criterion is satisfied.

To date, a limited number of experimental studies of the coupling between the combustion processes and acoustic oscillations in a ramjet engine like environment have been conducted. Recent studies include those of Davis[3] and Heitor et al[4]. Davis used high speed photography to identify two modes of low frequency instability in dump type combustors. In the first mode, the entire combustion zone underwent a cyclic oscillation while in the second mode regular shedding of hot spots from the recirculation zone at the dump plane was observed. Heitor et al measured the frequency and strength of combustion induced oscillations for premixed methane air flames stabilized on baffles located on the axis of a closed-open pipe. They found that instability involving the fundamental acoustic mode (i.e., a quarter wave type) occurred for a wide range of fuel to air ratios. More recently, Smith and Zukoski[5] studied combustion instability involving a flame stabilized behind a rearward facing step. They report that under conditions of instability large vortical structures were formed downstream of the step at an acoustic resonant frequency. These were subsequently convected away from the step and the resulting unsteady combustion was found to feed energy into the acoustic oscillations. Keller et al[6] identified three modes of instability in a similar set up in an effort to understand the mechanisms responsible for flashback. They attributed this phenomenon to the action of vortices in the recirculation zone of the step. These studies indicate that the fluid mechanics of the flame stabilization region plays an important role in combustion instability.

The present study also confirms the importance of the fluid mechanics of the flame region. The experiments carried out and described later indicate the presence of a marked fluid dynamical instability of the flame region at low frequencies. This results in the formation of burning vortices that are shed from the flame holding region and are convected along the flame front. The resulting unsteady combustion acts as a strong acoustic source resulting in longitudinal pressure oscillations. The combustion instability problem in ramjets therefore involves an intricate coupling among the three basic modes of fluid motion; that is, the vortical acoustic and thermal modes[7].

## EXPERIMENTAL SET UP

The set up described in Fig. 1 has been developed. It consists of an inlet, combustor and exhaust sections. The inlet contains a movable injector through which a mixture of propane and air

---

* This work was performed under ONR Contract No. N00014-84-K-0470.

xx Research Engineer
xxx Graduate Research Assistant
† Regents' Professor. Associate Fellow AIAA
†† Senior Research Engineer

is introduced into the combustor. The flame is stabilized in the 7.5 x 5 $cm^2$ combustor section on a 0.8 mm diameter nichrome wire. The wire is attached to the combustor windows at half combustor height and it is heated electrically to improve the steadiness of the stabilized V-shaped flame. The exhaust section is equipped with two acoustic drivers which are used to excite a standing acoustic wave of desired amplitude and frequency in the set up. The movable injector provides a capability for "placing" the stabilizing wire on any part of the excited standing wave; that is, at a pressure maximum, minimum or in between. The maximum length, L, available between the injector face and the exhaust section exit plane is 3 meters. The flow approaching the stabilizing wire is parallel and uniform and disturbances are damped out by means of a fine wire mesh grid located 8 cm. upstream of the stabilizing wire. The cold flow Reynolds number is kept below 10,000 in the interest of maintaining a disturbance free flow. The combustor walls are water cooled enabling wall mounted pressure transducers to be used to monitor the acoustic pressure field. Capabilities for time and space resolved measurements of CH species radiation from the flame have also been developed. The concentrations of these species are a measure of the reaction rate[8] and, thus, the heat release rate and are useful in describing the unsteady combustion field.

The acquired pressure and radiation signals are digitized and stored in computer memory prior to their Fourier analyses. The developed Fourier analysis program yields both auto spectra and cross spectra of the signals. This facilitates determination of relationships between the pressure and the unsteady heat release including their relative phases. Also, capabilities for identifying specific frequency components and their amplitude and phase behavior have also been developed.

## EXPERIMENTAL RESULTS

The initial experiments performed including flow visualization (described in Ref. 9) had suggested a vortical instability of the flame characterized by the shedding of burning vortices from the flame holding wire around the first natural frequency, $f_o$, of the set up (ranging between 55-90 Hz for the different effective tube lengths employed). A representative frame from the high speed (6000 frames/second) shadowgraph movie is reproduced in Fig. 2. The non-negligible thickness and vortex like structure of the flame region should be noted. To classify this aspect, CH radiation emitted by the flame (representative of the unsteady heat release) was measured at different axial locations along the flame front.

Before describing the experiments, it is appropriate to consider some features of shear layer instability. This is a complex process, even in incompressible flows where a vast amount of data may be found in the literature.[10] These data indicate the presence of a favored frequency range (Strouhal number range) where instability occurs. Whereas the primary energy causing flow instability comes from the mean flow via interaction with the Reynolds stresses, nonlinear interactions, e.g., merging and breakup of the formed vortices also cause energy transfer among different frequency components. This results in the generation of harmonics and subharmonics of the primary instability frequency.

For the flame experiments, the preliminary investigation had shown that the preferred frequency for the flamelet shedding was around $f_o$. Hence, the Fourier analysis program for the radiation data was extended to pick out the frequency components not only at $f_o$ but also at

a) $f_o/2$ the first subharmonic of $f_o$

b) $2 f_o$ the first harmonic of $f_o$ and

c) $f_d$ the external driving frequency, if any.

A typical result is plotted in Fig. 3 which shows the dependence of the radiation amplitude upon the axial distance x from the flame holding wire. In this case there was no external driving and $f_o \cong 80$ Hz. Note the sharp increase in amplitude at all three frequencies (i.e., 80, 40 & 160 Hz) just downstream of the wire. Whereas the signal at 80 Hz is dominant, there is a strong signal also at 40 Hz. The increase in amplitude with progressing axial distance that is observed is characteristic of shear layer instability. The signals start decaying towards the end of the flame (i.e., x≈20 cm) which is probably due to the wall quenching effect on the flame since the flame meets the duct walls at its downstream end.

Figure 4 plots the phase of the radiation signal at 80 Hz with respect to the acoustic pressure as a function of x. Note the region of phase reversal in a small region just downstream of the wire. Since the phase curve slope is related to the convection velocity of the disturbance, the region of phase reversal indicates a negative convection velocity and hence represents the recirculation region downstream of the wire. Downstream of this region the phase increases smoothly and monotonically. The behavior of the phase distributions of the other low frequency component signals is similar. It is found also that the degree of phase variation over the flame is larger for the higher frequency components ($f_o$ and above) as may be expected, due to their smaller vortical wavelengths.

The convection velocity in the flame region for the radiation signal at $f_o$ is plotted in Fig. 5. Note the increase in the velocity with the axial distance due to the acceleration caused by the density gradients. The ratio of about 4.0 for the convection velocity at the downstream end to that at the upstream end is equal to the temperature ratio across the flame. Also, the value of the convection velocity (1.3 m/sec) at the upstream end is close to the cold flow velocity of 1.5 m/sec. This suggests that the vortical structures are basically convected at the average speeds of the hot and cold flows at any streamwise location, x, along the flame.

The radiation spectrum from the entire flame was also measured. A typical result is shown in Fig. 6. It is seen to be dominated by the low frequency components under $f_o$. Thus, at local stations along the flame front, the radiation signals at frequencies close to $f_o$ dominate but considering the radiation from the entire flame the low frequency components dominate. The reason for

this is that the radiation signals from different parts of the flame cancel out for the higher frequency components due to the larger phase variation of the signal over the flame. For the low frequency components, the phase variation is small so that cancellation effects are also small.

The effect of external acoustic excitation at a frequency $f_d$ may be categorized into the following classes:

a) $f_d = nf_o$ where n is an integer > 1. This corresponds to driving at a harmonic of $f_o$.

b) $f_d = f_o/n$. This corresponds to driving at a subharmonic of $f_o$ and

c) $f_d$ is arbitrary. This corresponds to driving at neither a harmonic nor a subharmonic of $f_o$.

To investigate Type (a) driving, $f_d$ was set at 160 Hz. To investigate Type (c) different frequencies were chosen; e.g., 385 Hz and 270 Hz. In these cases, tests were run so that the flame holding wire was on different locations of the excited standing wave; i.e., at a pressure maximum, a pressure minimum and in between. Unfortunately, Type (b) could not be run on the set up due to the inefficiency of the acoustic drivers at low frequencies.

For tests with $f_d$ of either Type (a) or Type (c) a very interesting phenomenon was observed. Figure 7 plots the radiation amplitudes vs. x at 80 Hz and 160 Hz when $f_d$ = 160 Hz. Note the sharp rise in the signal at 160 Hz just downstream of the wire. In fact for x < 2 cm, the signal at 160 Hz dominates the signal at 80 Hz (i.e., $f_o$). However, past this axial location, the 80 Hz (i.e., $f_o$) signal again dominates the 160 Hz signal. A similar behavior was observed in tests with Type (c) frequencies. It was found that independent of the location of the flame holding wire on the excited acoustic wave, the radiation signal very close to the wire was dominated by the driving frequency $f_d$. But past this initial region the signal at $f_o$ dominated. For example, Fig. 8 describes the radiation amplitudes at 80 Hz and 385 Hz. Just downstream of the wire the signal at $f_d$ dominates. The size of the region downstream of the wire where the signal at $f_d$ dominates the signal at $f_o$ depends on the amplitude of the driving (increasing with increasing amplitude of driving) and on $f_d$ itself (decreasing with increasing $f_d$).

Thus, the flame may be thought of as comprising two regions, i.e., a) a near wake region responsive to external excitation and b) a far wake region where the dominant frequency is $f_o$.

The effect of external driving on the behavior of the radiation signal at $f_o$ was also investigated. Figures 9 and 10 describe the amplitude and phase of the signal at 80 Hz ($f_o$) with and without driving at 160 hz. There does not appear to be any significant effects of the driving on the phase behavior at 80 Hz implying that the convection velocity of the disturbance is not altered. But the same cannot be said about the amplitude variation. While the trend of the signals in both cases is similar the levels are significantly different being much lower in the driving case. This emphasizes the nonlinear nature of the flamelet shedding phenomenon; that is, the effect of one frequency component of the radiation signal upon the other. Similar types of behavior have been reported in studies of coherent structures in nonreacting flows[10]. This nonlinearity has been attributed to vortex merging and pairing in the shear layer.

It is clear that in the reported experiments the flame is vortically unstable at the first natural frequency, $f_o$, of the set up. To maintain this instability a feedback mechanism through which disturbances at $f_o$ are "felt" by the flame must be present in the experimental set up. Since $f_o$ is the first natural acoustic frequency of the set up it is natural to seek an appropriate acoustic source in the set up instrumental in closing the feedback loop between the vortical instability and the duct acoustics.

According to Rayleigh's criterion, the unsteady heat release from the flame should be in phase with the acoustic pressure on the average over the entire flame if it is to drive the pressure oscillations. This criterion may be stated in the following form in the frequency domain:

$$\int_{\text{flame}} |S_{pq}| \cos \theta_{pq} \, dV_{\text{flame}} > 0 \qquad (1)$$

where $S_{pq}$ is the cross spectrum between the pressure and heat release (i.e., radiation) and $\theta_{pq}$ is the phase between the unsteady heat release and the pressure. If the criterion is satisfied, the feedback loop between the shear layer instability of the flame and the duct acoustics may be closed.

The integrand of Eq. (1) is plotted in Fig. 11 as a function of x for $f_o$ = 80 Hz in a no driving experiment. The value of the integral is found to be positive in accordance with the criterion. For other low frequency components below $f_o$ the criterion is also found to be satisfied indicating that the flame also drives the pressure oscillations at these frequencies.

The satisfying of the criterion, however, does not exclude the presence of other important acoustic sources in the set up. For example, impingement of the vortices against a solid surface (e.g., the duct walls) could also contribute to the generation of the duct acoustics as has been suggested to occur in segmented solid propellant rocket motors.[11] Thus, it becomes necessary to predict the acoustic pressure spectrum by considering the unsteady heat release as the primary acoustic source and comparing this prediction with the experimental pressure spectra. If satisfactory agreement is obtained, then the unsteady heat release rate may be taken to be the only important acoustic source. This prediction is described in the next section and it shows that this indeed appears to be the case.

## THEORETICAL CONSIDERATIONS

The experimental results described in the preceeding section demonstrate that combustion instability in the set up is connected with the vortical instability of the flame. The density jump across the flame causes sharp velocity gradients

resulting in an intense shear layer. This shear layer is vortically unstable in a certain frequency range depending upon the flow conditions. For the experimental conditions considered here, this range appears to be limited to frequencies below 100 Hz. Unsteady combustion in the vortices formed due to the shear layer instability can, in accordance with Rayleigh's criterion, generate an acoustic field. If the shear layer instability frequency range contains a natural acoustic frequency of the system, then the entire instability process is reinforced and may result in large pressure fluctuation levels.

A comprehensive theoretical analysis of this problem is still beyond the state of the art modelling techniques. Since the vortical structures appear to be quasi deterministic, traditional statistical analyses which assume randomness cannot reveal completely all the features of the flow. Recent trends have been towards a direct numerical simulation of vortical structures in mixing layers.[12,13] However, these methods are restricted to low or moderate Reynolds number because of the limited range of temporal and spatial scales that can be resolved with today's computers. As a result, only the global features of the flame may be reasonably modelled.

As a first step in this direction a simple model is developed to predict the pressure spectrum from the unsteady heat release rate spectrum. If satisfactory agreement is obtained it would also indicate that the unsteady heat release rate is the primary acoustic source in the set up as mentioned in the preceding section. In the analysis the unsteady heat release rate is specified by the unsteady CH radiation emitted by the flame (obtained experimentally). A future goal would be to predict the unsteady heat release rate also, perhaps from knowledge of the steady flow conditions.

The analysis considers only low frequencies (up to 300 Hz approximately). In this range, the flame zone may be assumed compact compared to the acoustic wavelength. Thus, the flame is assumed to be localized at $x = L_1$ (with $x = 0$ being the injector and $x = L$ the exhaust plane). The steady state temperature is assumed to be $\bar{T}_1$ in the region $0 < x < L_1$ and $\bar{T}_2$ (burned gas temperature) in the region $L_1 < x < L$. $\bar{T}_2$ is taken to be an average downstream temperature as there are some heat losses from the water cooled walls of the duct.

As only plane acoustic waves are of interest, only the one-dimensional wave equation for the acoustic pressure p' is considered. Moreover, steady flow velocity effects are neglected due to the extremely low Mach number of the flow (0.005 approximately). For axial temperature gradients with unsteady heat release q'(x) this wave equation may be written in the frequency domain as

$$\frac{d}{dx}\left(\bar{T}\frac{dp'}{dx}\right) + \bar{T}\frac{\omega^2}{c^2}p' = -\frac{i\omega}{C_p}q' \qquad (2)$$

where $\omega$, c and $C_p$ describe the angular frequency, speed of sound and specific heat at constant pressure.

The boundary conditions at $x = 0$ and $x = L$ may be written in terms of the respective specific acoustic impedances $Z_o$ and $Z_L$ at these two ends; that is,

$$\frac{dp'}{dx} + \frac{ik}{Z_o}p' = 0 \qquad \text{at } x = 0$$

$$\frac{dp'}{dx} + \frac{ik}{Z_L}p' = 0 \qquad \text{at } x = L$$

where $k = \omega/c$.

Equation (2) is solved by obtaining the Green's function G satisfying

$$\frac{d}{dx}\left(\bar{T}\frac{dG}{dx}\right) + \bar{T}\frac{\omega^2}{c^2}G = -\delta(x - x_o) \qquad (3)$$

with the same boundary conditions as for p'. This yields

$$p'(x) = \int_o^L \frac{i\omega q'}{C_p} G(x,x_o)\, dx_o$$

With the compact flame assumption

$$q' = q'(x)\ \delta(x - L_1)$$

so that

$$p'(x) = \frac{i\omega q'(L_1)}{C_p} G(x,L_1) \qquad (4)$$

$G(x,L_1)$ is obtained from Eq (3) by setting $x_o = L_1$. It may be constructed by standard methods.[14] The comparison with the experimental pressure spectrum will be made at the injector. The relevant Green's function $G(o,L_1)$ turns out to be

$$G(o,L_1) = -\frac{Z_o Z_L \cos k_2(L - L_1) + i \sin k_2(L - L_1)]}{\left\{k_1\bar{T}_1 Z_o \sin\alpha + i\cos\alpha][Z_L\cos\beta + i\sin\beta]\right.}$$

$$\left. - k_2\bar{T}_2[Z_L\sin\beta + i\cos\beta][Z_o\cos\alpha - i\sin\alpha]\right\} \qquad (5)$$

where $\alpha = k_1 L_1$ and $\beta = k_2(L - L_1)$

and $k_1 = \frac{\omega}{c_1}$ ; $k_2 = \frac{\omega}{c_2}$ and $c_1$ and $c_2$ are the average speeds of sound upstream and downstream of the flame respectively.

The pressure spectrum $S_{pp}$ is obtained by multiplying Eq. (4) by its complex conjugate and taking an ensemble average. The result is

$$S_{pp}(x = 0) = \frac{\bar{w}^2}{\bar{c}_p^2} |G(o, L_1)|^2 S_{qq}(x = L_1) \qquad (6)$$

where $S_{qq}$ is the net unsteady heat release spectrum from the entire flame. It is further assumed that

$$S_{qq} = B S_{rr} \qquad (7)$$

where $S_{rr}$ is the CH radiation autospectrum measured from the entire flame and B is a positive real constant relating the magnitudes of the two spectra.

A typical comparison of the predicted and measured pressure spectra is shown in Fig. 12. The agreement is good. It is also seen that while the spectrum shows a peak at $f_o$(80 Hz) as expected, there are also substantial pressure levels at lower frequencies indicating that the flame also drives at these lower frequencies. As noted in the previous section, Rayleigh's criterion is also satisfied at these lower frequencies.

It should be noted that the magnitude of the denominator of the Green's function G(Eq. 5) is minimized for the natural acoustic frequencies of the duct. This means that driving of the natural acoustic frequencies is favored as is expected. Thus, if high levels of unsteady heat release rate are obtained at a natural frequency of the duct, extremely large pressure oscillations may result as is evident from Eq. (6).

In the experiments described herein, it is believed that the fundamental acoustic frequency $f_o$ of the set up also belonged in the range of unstable frequencies for the flame shear layer instability. An interesting question that may be raised is whether the acoustic natural frequencies influence in some way the unstable frequency range for the shear layer instability by shifting, for example, this frequency range. To answer these types of questions it is planned to repeat some of the described tests in a shorter version of the developed set up. This will serve to increase the first natural acoustic frequency and, presumably, remove it from the unstable frequency range for the flame shear layer instability.

## CONCLUSION

The response of wedge shaped flames, similar to those often occurring in ramjet combustors, to acoustic excitation has been studied. The investigation has shown that the unsteady combustion in vortices shed from the flame holding region is the major cause of the observed pressure oscillations in the set up, and could also serve as the driving mechanism for low frequency ramjet instabilities. The vortical structures arise due to the instability of the shear layer formed by the flame. This instability and therefore the vortical structures are restricted to a limited frequency range. Thus, significant rates of unsteady heat release (and driving) are also confined to the same frequency range. Overlap of an acoustic resonant frequency with the frequency range of the flame shear layer instability can result in extremely large pressure oscillations and should be avoided. Better understanding of the origin and detailed structure of the vortices is the key to their control and, perhaps, the elimination of combustion instability in ramjets.

## REFERENCES


1. Waugh, R. C. and Brown, R. S., "A Literature Survey of Combustor Instability," CPIA Publication No. 375, pp. 1-13, April 1983.

2. Lord Rayleigh, "The Theory of Sound," Vol. II, Dover, pp. 224-235, 1945.

3. Davis, D. L., "Coaxial Dump Combustor Instabilities, Part I - Parametric Test Data," Aero Propulsion Laboratory, Air Force Wright Aeronautical Laboratories, Wright-Patterson AFB, Ohio, Interim Report, 1981.

4. Heitor, M. V., Taylor, A. M. K. P. and Whitelaw, J. H., "Influence of Confinement on Combustion Instabilities of Premixed Flames Stabilized on Axisymmetric Baffles," Combustion and Flame, Vol. 57, pp. 109-121, 1984.

5. Smith, D. A. and Zukoski, E. E., "Combustion Instability Sustained by Unsteady Vortex Combustion," AIAA/SAE/ASME/ASEE 21st Joint Propulsion Conference, AIAA Paper No. 85-1248, 1985.

6. Keller, J. O., Vanveld, L., Korschelt, D., Hubbard, G. L., Ghoneim, A. F., Daily, J. W. and Oppenheim, A. K., "Mechanism of Instabilities in Turbulent Combustion Leading to Flashback," AIAA Journal, Vol. 20, No. 2, pp. 254-262, 1982.

7. Chu, B. and Kovasznay, L. S. G., "Nonlinear Interactions in a Viscous Heat-Conducting Compressible Gas," J. Fluid Mechanics, Vol. 3, pp. 494-514, 1958.

8. Gaydon, A. G. and Wolfhard, H. G., "Flames: Their Structure, Radiation and Temperature," 4th Edition, John Wiley and Sons, N. Y., 1979.

9. Hegde, U. G., Reuter, D., Daniel, B. R. and Zinn, B. T., "Flame Driving of Longitudinal Instabilities in Dump Type Ramjet Combustors," AIAA 24th Aerospace Sciences Meeting, Paper No. 86-0371, 1986.

10. Ho, C. M. and Huerre, P., "Perturbed Free Shear Layers," Annual Review of Fluid Mechanics, Vol. 16, pp. 365-424, 1984.

11. Flandro, G. A. and Finlayson, P. A., "Nonlinear Interactions between Vortices and Acoustic Waves in a Rocket Combustion Chamber," Proceedings of the 21st JANNAF Combustion Meeting, September 1984.

12. Kailasanath, K., Gardner, J., Boris, J. and Oran, E., "Interactions between Acoustics and Vortex Structures in a Central Dump Combustor," AIAA/ASME/SAE/ASEE 22nd Joint Propulsion Conference, Paper No. 86-1609, June 1986.

13. McMurtry, P. A., Jou, W. H., Riley, J. J. and Metcalfe, R. W., "Direct Numerical Simulations of a Reacting Mixing Layer with Chemical Heat Release," AIAA Journal, Vol. 24, No. 6, pp. 962-970, 1986.

14. Morse, P. M. and Ingard, K. U., "Theoretical Acoustics," McGraw Hill, New York, 1968.

Fig. 2. Frame from High Speed Shadowgraph Film. Note Vortex Like Structures of Flame Region.

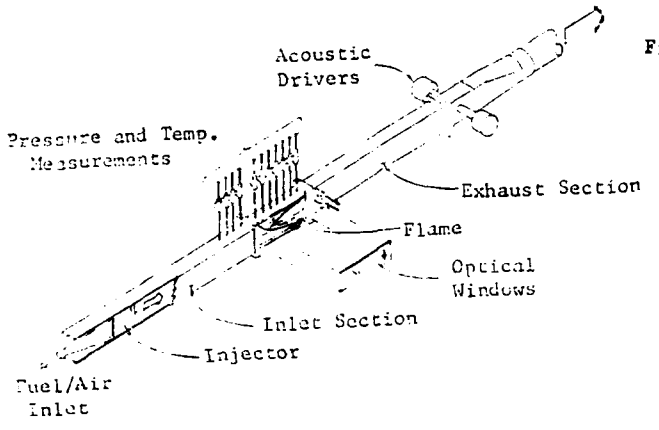


Fig. 1. Developed Experimental Set-Up.

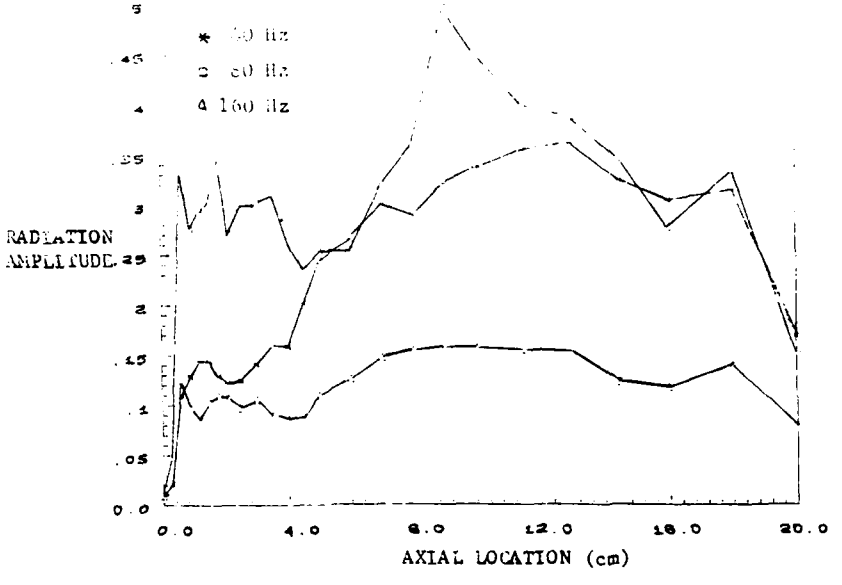


Fig. 3. Radiation Amplitude as a Function of Axial Distance from Flame Holding Wire. (no external driving).

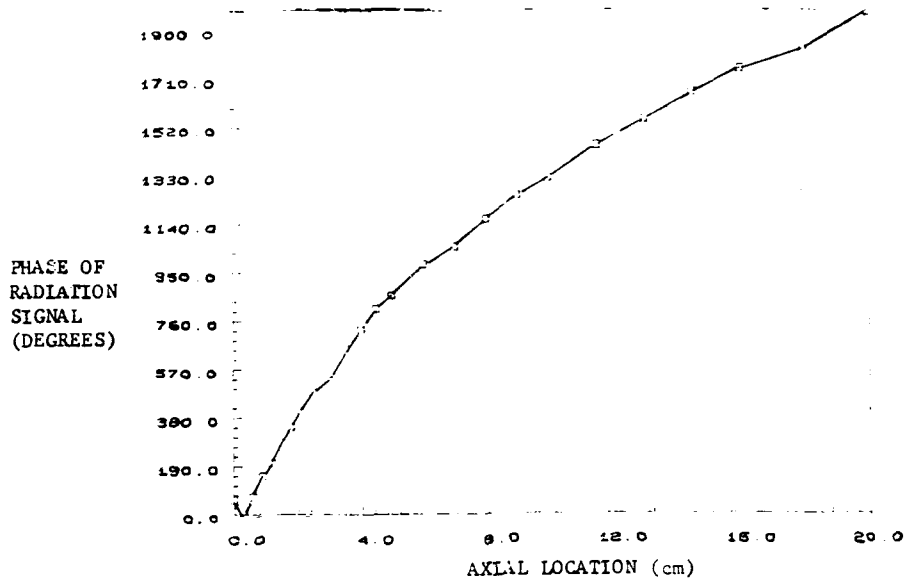


Fig. 4. Phase of Radiation Signal with Respect to Pressure (80 Hz) (no external driving).

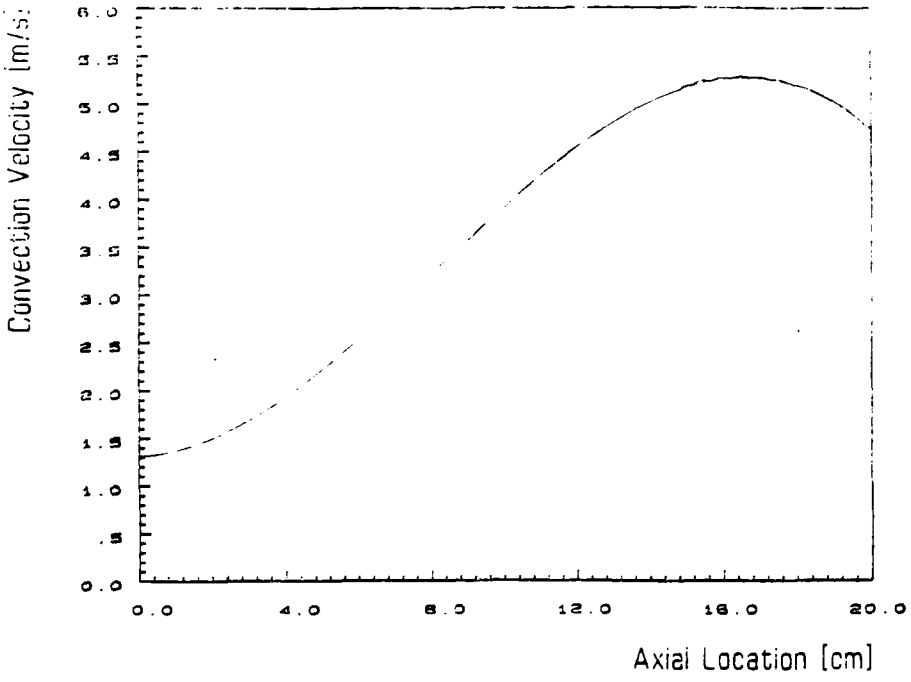


Fig. 5. Convection Velocity for Radiation (80 Hz.). Recirculation Region Not Shown. (no external driving).

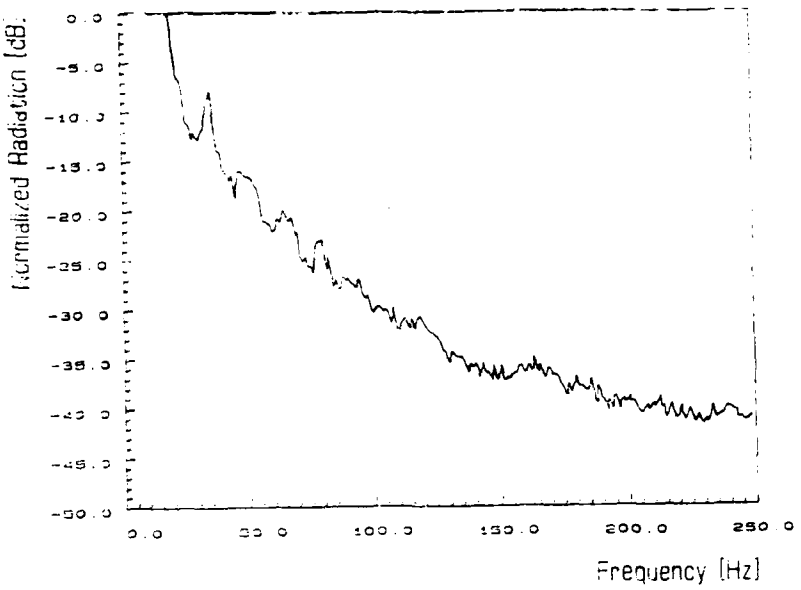


Fig. 6. Radiation Spectrum from Entire Flame. (no exter al driving).

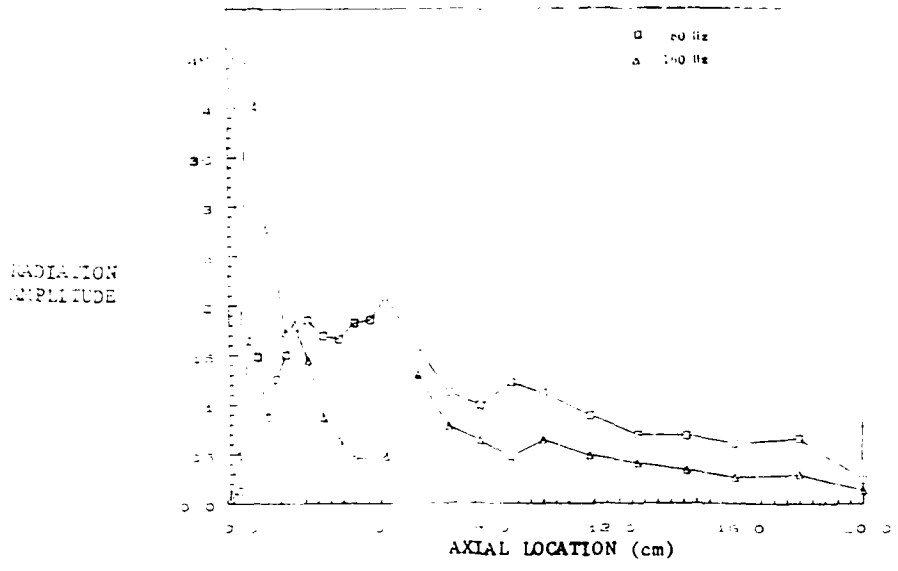


Fig. 7. Radiation Amplitude at 80 Hz and 160 Hz with Driving at 160 Hz.

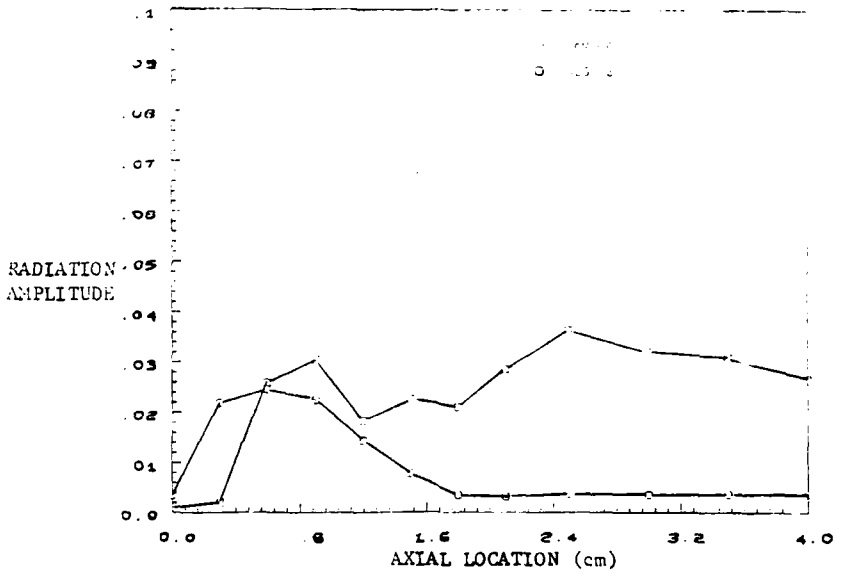


Fig. 8. Radiation Amplitude at 80 Hz and 385 Hz with Driving at 385 Hz.

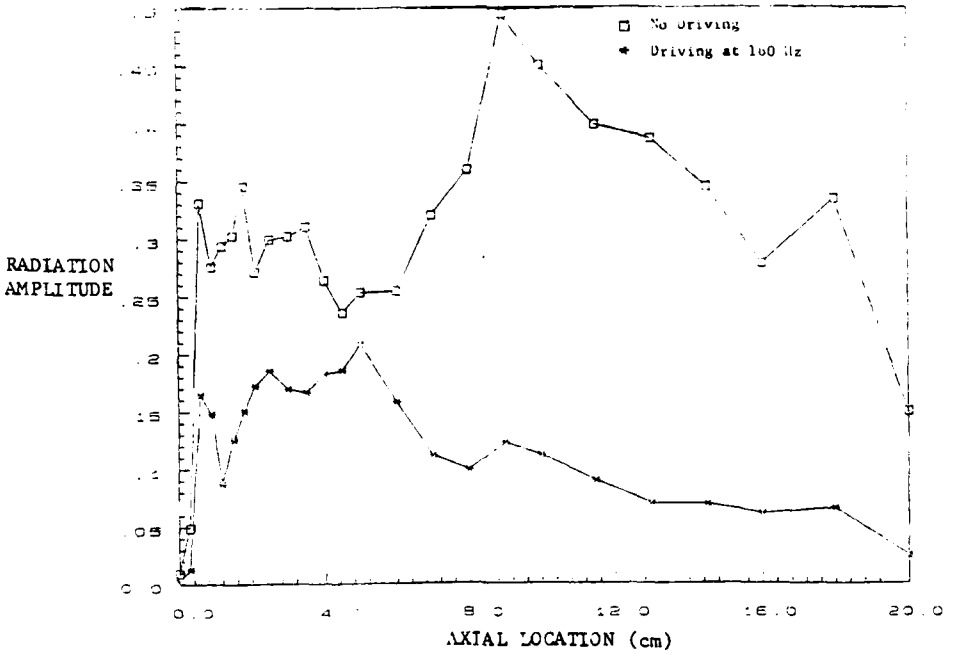


Fig. 9. Radiation Amplitude at 80 Hz with and without Driving at 160 Hz.

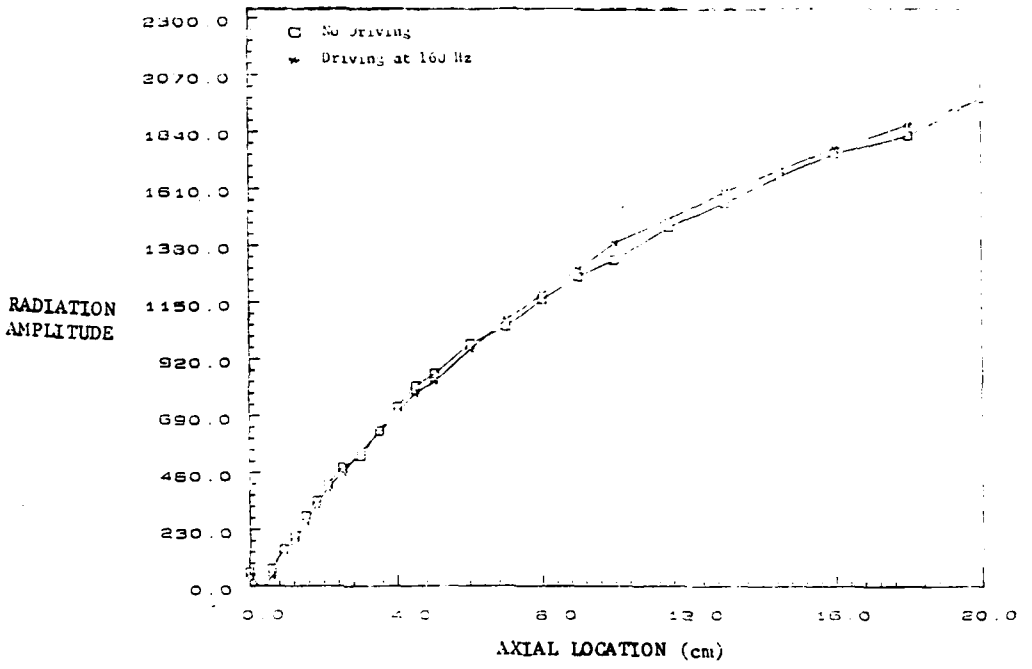


Fig. 10. Phase of Radiation at 80 Hz with and without Driving at 160 Hz.

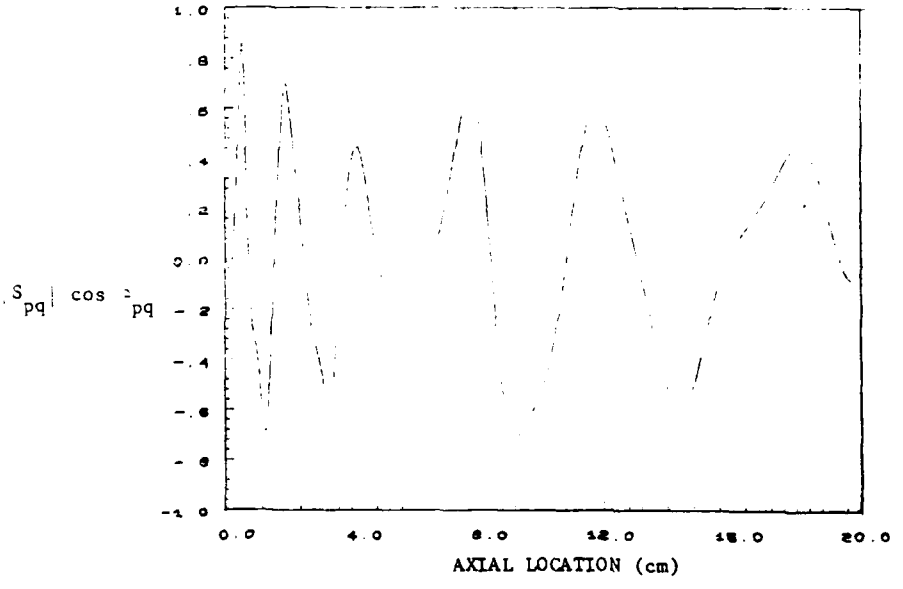


Fig. 11. Plot of the Integrand of Eq. (1) which Determine the Flame Driving at $f_o$ (80 Hz.) according to Rayleigh's Criterion.

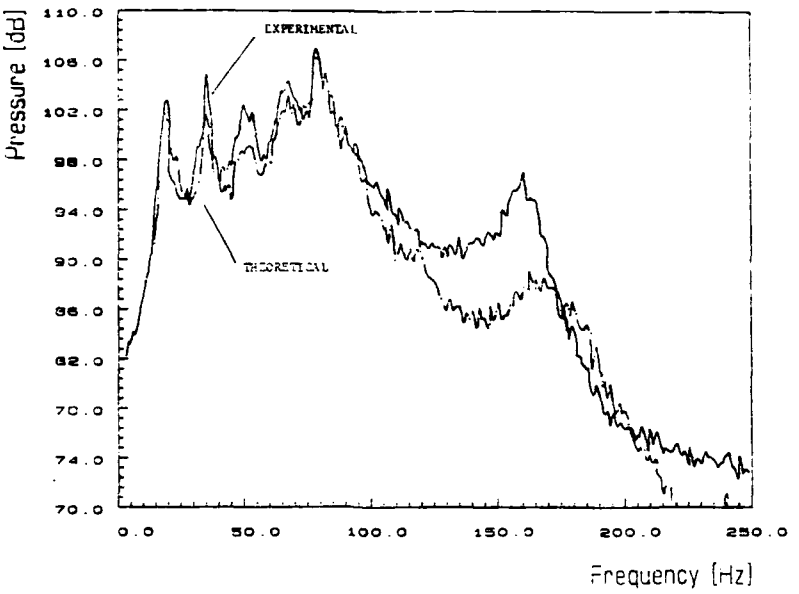


Fig. 12. Comparison of Predicted and Measured Pressure Spectra at Flow Injector.

APPENDIX D

# SOUND GENERATION BY DUCTED FLAMES

U.G. Hegde*, D. Reuter** and B.T. Zinn***

Georgia Institute of Technology

Atlanta, Georgia 30332

## ABSTRACT

The sound field established by a v-shaped flame confined in a rectangular duct is investigated both theoretically and experimentally. A theoretical model is developed to predict pressure spectra caused by the unsteady heat release from the flame. Comparisons between the theoretical and experimentally measured spectra confirm the validity of the model and are also reported. It is also found that changes in the flow field in the flame zone can significantly modify combustion rates. These modifications, in turn, affect the generated sound field and are important in determining the pressure levels in the duct. The results of this investigation are applicable to combustion noise and instability studies in a variety of burner and propulsion system configurations.

---

* Research Engineer, Member AIAA

** Graduate Research Assistant

*** Regents' Professor, Fellow AIAA

## NOMENCLATURE

| | |
|---|---|
| $a$ | duct width |
| $b$ | duct height |
| $B$ | constant defined by Eq. (17) |
| $B_1$ | constant defined by Eq. (18) |
| $c$ | speed of sound |
| $C_p$ | specific heat at constant pressure |
| $G$ | Green's function |
| $k_{oo}$ | modified wave number |
| $L$ | length of duct |
| $L_1$ | length of duct from entrance to flame zone |
| $\bar{M}_o$ | steady state Mach number at duct inlet |
| $\bar{M}_L$ | steady state Mach number at duct exit |
| $q$ | heat release rate per unit volume |
| $R$ | gas constant |
| $S_{pp}$ | pressure autospectrum |
| $S_{qq}$ | unsteady heat release rate autospectrum |
| $S_{rr}$ | CH radiation autospectrum |
| $t$ | time |
| $T$ | temperature |
| $\bar{T}_o$ | steady state cold gas temperature |
| $\bar{T}_f$ | steady state flame temperature |
| $u$ | velocity |
| $x, x_o$ | axial coordinate |
| $X$ | axial separation of flame holders |
| $y$ | vertical coordinate direction |
| $Y$ | vertical separation of flame holders |

$z$ transverse coordinate

$Z_o, \hat{Z}_o$ unmodified and modified specific acoustic impedances at entrance to duct

$Z_L, \hat{Z}_L$ unmodified and modified specific acoustic impedances at exit of duct

$\alpha$ defined by Eq. (14)

$\beta$ defined by Eq. (14)

$\psi$ specific acoustic admittance of duct side walls

$\delta$ Dirac delta function

$\gamma$ ratio of specific heats

$\omega$ angular frequency

$\chi$ wall loss factor (per unit length)

$\lambda$ acoustic wavelength

Superscripts

$\bar{}$ time or ensemble average

$'$ time dependent part (fluctuation)

$*$ complex conjugate

Subscripts

$\omega$ Fourier component

1 relating to the region upstream of the combustion zone

2 relating to the region downstream of the combustion zone

$\rightarrow$ vector quantity

Other

$\langle\ \rangle$ cross section average

# INTRODUCTION

Sound generated by unsteady combustion processes is of interest in several applications including propulsion devices, industrial furnaces, burners, heaters and so on. In the majority of cases, the generated sound is undesirable, as for example, in ramjet engines where the problem may become so severe that unstable operation of the engine may occur[1]. In some cases, however, as in pulse combustors, sound pressure variations are essential to maintain operation[2].

Unsteady combustion processes generate sound as a result of unsteady expansion of the fluid undergoing reaction. Depending upon the nature of the flow field and the combustion process, unsteady combustion may arise in different ways. For example, the injection of fuel or combustible mixture may be unsteady, the flow field may be turbulent or there may be feedback of the acoustic motions on the flame.

It is convenient for the purposes of this paper to categorize confined flames as those burning in an enclosure and unconfined flames as those burning in a free space. The distinction is important in characterizing the generated sound field. Thus, for unconfined flames, the radiated sound field is, generally, non directional and monopole in character[3]. For confined flames, on the other hand, reflections from the boundaries and wave guide effects can cause preferred directionality of the acoustic motions as well as sustain discrete frequency or narrow band excitation around the natural frequencies of the enclosure.

There have been several recent investigations of combustion generated sound. Strahle[3,4] has developed a general theory of combustion generated noise for free flames in the low frequency limit and shown that the radiated

sound pressure is related to the time derivative of the heat release rate averaged over the combustion region. The generated sound in such cases is generally broadband with a frequency content related to the temporal variations in volume of the combustion region. Experimental verification of the theory has been obtained by Sivasankara et al[5].

Sound generated by confined flames have been studied in relation to combustion instabilities in rocket motors and ramjets. A review is provided by Barrere and Williams[6]. A recent experimental investigation of noise sources in a ramjet like combustor is presented by Poinsot et al[7]. The investigation presented here is also part of a larger research effort on combustion instabilities in dump type ramjet combustors[8].

In this paper, a theory for predicting the sound generated by flames enclosed in a duct is developed. Knowledge of the unsteady combustion field is presumed and attention is focused on longitudinal wave motions. This is presented in the Theoretical Considerations Section. The theory is tested in an experimental set up in which a v-shaped flame is stabilized in a rectangular duct. Measurements are made of the unsteady heat release from the flame, in terms of emitted radiation, for input into the model. The calculated pressure spectra in the duct are then compared with experimentally measured spectra to test the theory. The results are presented in the Experimental Efforts Section. In addition, the relationship between the frequency content of the unsteady combustion and the generated sound is investigated. It is also shown that the combustion rates are sensitive to changes in the flow field in the flame region and, in turn, affect the generated sound levels.

## THEORETICAL CONSIDERATIONS

Consider a rectangular duct similar to the one in Fig. 1. The x-axis is parallel to the duct axis and the cross sectional dimensions are a and b. The length of the duct is L. A combustible mixture is introduced at x=0 and the combustion occurs in a region $\Delta L_1$ around $L_1$. The mach number of the flow is assumed to be small(i.e., $\bar{M}_o^2 << 1$). A typical axial temperature profile which might be present in the duct is also shown in Fig. 1. Due to heat conduction upstream of the combustion region there is a gradual rise in temperature from the cold temperature $\bar{T}_o$ at x=0. A sharp rise in temperature occurs in the combustion zone to the flame temperature $\bar{T}_f$ . Downstream of the combustion region the temperature may again drop due to heat losses to the duct walls.

The wave equation for the pressure fluctuations in the duct will be briefly formulated. The pressure fluctuations will be assumed to be small with respect to the mean (i.e., steady state) pressure levels allowing the application of the linearized conservation equations to obtain the required solutions. In addition, the actual details of the mean velocity field in the duct will be ignored. There are two reasons why this is permissible. First, the mach number is taken to be small so that convective effects in the wave equation may be ignored. Secondly, although the flow field is instrumental in determining the combustion rates, the actual details of this process is not considered herein and the needed reaction rates will be assumed known. This means that it is expected that the effects of the flow field on the generated sound will be obtained implicitly through the unsteady combustion process and there will be no significant effects on the sound field only by virtue of changes in the flow field which do not affect the reaction rates. This approach is justified by the fact that unsteady combustion is a monopole type

of acoustic source and is a much more efficient sound source than pure flow noise sources which are either quadropole or dipole in character[9]. In addition, experimental results obtained as part of this investigation, and discussed in the next section, are in agreement with the model predictions.

Neglecting viscous and heat conduction effects (although mean temperature and density gradients are allowed) and assuming a perfect gas behavior, the linearized conservation equations can be expressed in the following form:

Continuity:

$$\frac{\partial \rho'}{\partial t} + \bar{\rho}\ \nabla \cdot \underrightarrow{u}' + \underrightarrow{u}' \cdot \nabla \bar{\rho} = 0 \tag{1}$$

Momentum:

$$\bar{\rho}\ \frac{\partial \underrightarrow{u}'}{\partial t} = -\nabla p' \tag{2}$$

Energy:

$$\bar{\rho}\ C_p \left[ \frac{\partial T'}{\partial t} + \underrightarrow{u}' \cdot \nabla \bar{T} \right] = \frac{\partial p'}{\partial t} + q' \tag{3}$$

State:

$$p' = R\bar{T}\ \rho' + R\bar{\rho}\ T' \tag{4}$$

Equation (1) may be rewritten in terms of p',u' and q' by substituting for $\rho'$ and T' from equations (4) and (3) and making use of the steady state equation of state

$$\bar{p} = R\,\bar{\rho}\,\bar{T} \tag{5}$$

yielding

$$\frac{1}{c^2}\ \frac{\partial p'}{\partial t} + \bar{\rho}\ \nabla \cdot \underrightarrow{u}' = \frac{q'}{C_p \bar{T}} \tag{6}$$

where $c^2 = \gamma R\bar{T}$

Taking the divergence of Eq.(2) and subtracting the partial time derivative of Eq.(6) one obtains

$$\nabla.(\bar{T}\,\nabla p') - \frac{\bar{T}}{c^2}\,\frac{\partial^2 p'}{\partial t^2} = \frac{-1}{C_p}\,\frac{\partial q'}{\partial t} \qquad (7)$$

Equation (7) is the relevant wave equation for the pressure taking into account the heat release from the combustion process and the spatial variations of the temperature. Harmonic motion is considered so that the fluctuations may be written in the form

$$p' = p_\omega\, e^{i\omega t} \text{ and } q' = q_\omega\, e^{i\omega t}$$

Substituting these solutions into Eq. (7) one obtains

$$\nabla.(\bar{T}\,\nabla p_\omega) + \bar{T}\,\frac{\omega^2}{c^2}\,p_\omega = \frac{-i\omega}{C_p}\,q_\omega \qquad (8)$$

Attention is now focussed only on longitudinal wave motion. The axial wave equation may be obtained by integrating Eq.(8) over the duct cross section. Noting that $\bar{T}/c^2$ is independent of the location, it will be assumed that it may be replaced by $\langle \bar{T}\rangle/\langle c^2\rangle$. Also, for longitudinal wave motions, it is permissible to replace

$$\frac{\partial}{\partial x}\,\frac{1}{ab}\iint \bar{T}\,\frac{\partial p_\omega}{\partial x}\,dy\,dz \quad \text{by} \quad \frac{d}{dx}\langle\bar{T}\rangle\,\frac{d\langle p_\omega\rangle}{dx}$$

as $p_\omega \cong \langle p_\omega \rangle$

Then, for longitudinal wave motion Eq.(8) may be expressed as follows:

$$\frac{d}{dx}<\bar{T}>\frac{d}{dx}<p_\omega> + <\bar{T}><k_{oo}^2><p_\omega> = \frac{-i\omega}{C_p}<q_\omega> \tag{9}$$

where, $<k_{oo}^2> = \left[\frac{\omega^2}{<c^2>} - i\frac{2\omega}{<c>}\psi\frac{(a+b)}{ab}\right]$

and $\psi$ is the specific acoustic admittance of the side walls of the duct and is assumed to be independent of location along the duct. For rigid walled ducts, this admittance is zero. For nearly rigid walls, as is considered here, the admittance remains small and the modified wave number $<k_{oo}>$ may be approximated by[10]

$$<k_{oo}> = \frac{\omega}{<c>} - i\chi$$

where $\chi$ is known as the wall loss factor.

Removing the now superfluous < >, Eq. (9) may be written as

$$\frac{d}{dx}\bar{T}\frac{dp_\omega}{dx} + \bar{T}k_{oo}^2 p_\omega = \frac{-i\omega}{C_p}q_\omega \tag{10}$$

where it is now understood that cross sectional averages of quantities are under consideration.

The boundary conditions at x=0 and x=L may be written in terms of the specific acoustic impedances $Z_o$ and $Z_L$ at these two planes. It should be noted that although convection effects may be negligible in determining the wave structure at low mach numbers, convection losses at the end planes may be important in determining the amplitudes of the motions. This may be incorporated as shown in Ref. 11 and the relevant boundary conditions are

at x=0:

$$\frac{dp_\omega}{dx} + \frac{i\,k_{oo}}{Z_o + M_o}\, p_\omega = 0$$

at x=L:

$$\frac{dp_\omega}{dx} + \frac{i\,k_{oo}}{Z_L + M_L}\, p_\omega = 0$$

The solution to Eq.(9) may be obtained in terms of the Green's function $G(x,x_o)$ satisfying

$$\frac{d}{dx}\,\bar{T}\,\frac{dG}{dx} + \bar{T}k_{oo}^2 G = -\,\delta(x - x_o) \tag{11}$$

along with the same boundary conditions as for $p_\omega$. The solution for $p_\omega$ may then be written as

$$p_\omega(x) = \int_o^L \frac{i\omega q_\omega}{C_p}\, G(x,x_o)\, dx_o \tag{12}$$

An analytical solution will now be obtained for the important case when the length of the combustion zone, $\Delta L_1$, is much smaller than the acoustic wavelength, $\lambda$. In such cases, the combustion zone may be treated as a discontinuity at $x = L_1$ as far as the acoustics are concerned. The unsteady heat release rate $q_\omega(x)$ may then be written as

$$q_\omega = q_\omega(x)\,\delta(x - L_1)$$

and the corresponding solution for $p_\omega$ becomes

$$p_\omega(x) = \frac{i\omega q_\omega(L_1)\, G(x,L_1)}{C_p} \tag{13}$$

The Green's funnction $G(x,L_1)$ may be obtained from Eq.(11) by setting $x_o = L_1$. The required jump conditions across the discontinuity at $L_1$ are (i) G is continuous at $L_1$ and

(ii)

$$\bar{T}\left.\frac{dG}{dx}\right]_{L_{1+}} - \bar{T}\left.\frac{dG}{dx}\right]_{L_{1-}} = -1$$

The second condition is obtained by integrating Eq.(11) across $L_1$.

In general, most of the steady state temperature change will occur in the combustion region as shown in Fig. 1. This change is accounted for in the matching conditions across the flame zone. The changes in the steady state temperature away from the combustion zone will now be accommodated in an approximate fashion to simplify the computations. Upstream and downstream of the combustion zone, constant (although different) average temperatures will be prescribed. Thus, in the region $0 < x < L_1$, the steady state temperature is taken to be $\bar{T}_1$ (approximately equal to the cold gas temperature) and in the region $L_1 < x < L$, the steady state temperature is taken to be $\bar{T}_2$ (approximately equal to $\bar{T}_f$, the flame temperature, provided heat losses to the walls are not significant).

The comparison with the experimental pressure spectrum will be made at $x = 0$. The Green's function $G(0,L_1)$ may be obtained by standard methods[10] and it turns out to be

$$G(0,L_1) = \frac{-[\hat{Z}_o][\hat{Z}_L \cos\beta + i \sin\beta]}{k_1\bar{T}_1[\hat{Z}_o \sin\alpha + i\cos\alpha][\hat{Z}_L\cos\beta + i\sin\beta] - k_2\bar{T}_2[-\hat{Z}_L\sin\beta + i\cos\beta][\hat{Z}_o\cos\alpha - i\sin\alpha]} \tag{14}$$

where $\alpha = (k_{oo})_1 L_1$ , $\beta = (k_{oo})_2 (L_2 - L_1)$ , $k_1 = (k_{oo})_1$ , $k_2 = (k_{oo})_2$

with $(k_{oo})_1$ and $(k_{oo})_2$ being the relevant wave numbers upstream and downstream of the flame region and the modified impedances $\hat{Z}_o$ and $\hat{Z}_L$ are given by

$$\hat{Z}_o = Z_o + \bar{M}_o \quad \text{and} \quad \hat{Z}_L = Z_L + \bar{M}_L$$

The pressure spectrum $S_{pp}$ is obtained by multiplying Eq.(13) by its complex conjugate and taking an ensemble average. The result is (for x = 0)

$$S_{pp}(x=0) = \frac{\bar{w}^2}{C_p^2} \; |G(o_1 L_1)|^2 \; S_{qq}(x=0) \tag{15}$$

where $S_{qq}$ is the spectrum of the unsteady heat release from the combustion region.

The natural frequencies of the duct may be obtained by minimizing the magnitude of the denominator of the Green's function. For example, consider the case of a rigid walled duct with no convection losses, which is acoustically rigid at x=0 (i.e., $\hat{Z}_o = \infty$) and open at the end x = L (i.e., $\hat{Z}_L = 0$). In this case, the natural frequencies are given by the relation

$$\cos(\alpha + \beta) + \left[\sqrt{\frac{\bar{T}_2}{\bar{T}_1}} - 1\right][\cos\alpha \cos\beta] = 0 \tag{16}$$

## EXPERIMENTAL EFFORTS

The experimental set up used is shown in Fig. 2. It consists of a rectangular duct three meters long. It has a 7.5 x 5 $cm^2$ cross section and consists of an inlet, combustor and exhaust sections. The inlet contains an injector whose face is made of sintered stainless steel. A mixture of propane and air is introduced into the set up via the injector.A v-shaped flame is stabilized in the combustor section on a 0.8 mm diameter nichrome wire. The wire is attached to the combustor windows at half combustor height and it is heated electrically to improve its flame holding characteristics. The windows are made of quartz and allow optical access of the flame zone.

The flow approaching the stabilizing wire is parallel and uniform and a fine wire mesh grid located 8 cm upstream of the stabilizing wire acts as a flame arrestor in case of a flashback. The cold flow Reynolds number is kept below 10,000 in the interest of maintaining a disturbance free flow. Typical cold flow velocities considered are in the range of 1-2 m/sec. The combustor walls are water cooled enabling wall mounted pressure transducers to be used to monitor the acoustic pressure field. In addition, temperature measurements are carried out by means of thermocouple junctions.

Capabilities for measuring spontaneous CH species radiation from the flame have also been developed. The concentrations of these species are a measure of the reaction rate[12] and , thus, the heat release rate and are useful in describing the unsteady combustion field. Thus, the autospectrum of the unsteady heat release rate is proportional to that of the radiation and the following relation is assumed to hold

$$S_{qq} = B\, S_{rr} \tag{17}$$

where B is a positive, real constant.

The radiation signal was measured from the entire flame to obtain the net unsteady heat release spectrum from the combustion zone. The autospectrum of a typical measurement is shown in Fig. 3. According to Eqs. (15) and (17) this spectrum may be regarded as the source for the corresponding pressure fluctuations. Note that the spectrum is dominated by low frequency components. Detailed investigations of the flame region are presented in Ref. 8 where it is shown that this pattern occurs due to the dominating influence of large scale structures in the flame region.

Measurements of the radiation signal from the flame were carried out under several different conditions. The fuel fraction was changed between approximately 2.1 % to 2.4 %. Measurements at higher fuel fractions could not be made due to the appearance of combustion instability in the system which resulted in flame flash back (see Ref. 8). Measured flame temperatures were in the 1250 - 1400$^{o}$K range. Experiments were also run in a shortened version of the set up shown in Fig. 2 by removing the exnaust section. This had the effect of increasing the natural frequencies of the set up. In addition, some experiments were performed in the presence of an additional flame holder in the combustor section. This served to modify the flow field in the flame region and addressed the question whether the flow field influences the sound generation process in a direct fashion (i.e, is the sound field changed appreciably by the flow field even without changes in the unsteady heat release rate). It will be discussed shortly.

To carry out the theoretical calculations of the pressure spectra, the values of $\hat{Z}_o$, $\hat{Z}_L$, the wall loss factor $\chi$ and the constant B (Eq.(17)) must be known. Impedance measurements in cold flow (i.e., flow without combustion) tests using an impedance tube technique and an available computer program

indicated that the set up behaved to a good approximation as an acoustically closed-open duct. Thus, $\hat{Z}_L$ and $1/\hat{Z}_o$ were both set to zero. The wall loss factor $\chi$ was modelled, following Pierce,[13] as

$$\chi = B_1 \omega^{0.5} \tag{18}$$

where $B_1$ is a constant, independent of the frequency and depends only upon the characteristics of the duct walls.

To estimate $B_1$ and B, a trial and error technique was used. A sample pressure and corresponding radiation spectrum were chosen. Using Eqs. (15) and (17), theoretical pressure spectra corresponding to different values of $B_1$ and B were calculated. The values of $B_1$ and B yielding the best fit with the experimental pressure spectrum were determined. Once determined, $B_1$ and B are known for all the tests run on the experimental set up since they depend only upon the duct and radiation data acquisition system characteristics (which remained same in all the tests).

The comparison between the theoretical and experimental pressure spectra corresponding to the radiation spectrum in Fig. (3) is shown in Fig.(4). Using the same values of B and $B_1$ (recall the wall loss factor is defined for unit length and remains the same), a comparison between the theoretical and experimental pressure spectra for the shortened duct case is shown in Fig. 5. The unsteady radiation spectrum measured for this case is shown in Fig. 6. The agreement in both these cases and for all the other cases tried (but not shown here for brevity) is very good and serves to verify the theory. Note that the comparison is made only in the low frequency range (up to approximately 250 Hz). In this frequency range, the flame zone length (of the order of 20 cm) is an order of magnitude smaller than the relevant acoustic wavelengths.

Some comments are in order regarding the connection between the frequency content of the source ( the unsteady heat release rate) and the pressure fluctuations. The unsteady heat release is broadband in nature (see Figures 3 and 6) with low frequency components dominating (frequencies less than approximately 100 Hz in the considered experiments). As shown in Ref. 8, this behavior is due to the presence of large scale structures in the flame region. For an unenclosed flame, this frequency content is reflected in the resulting pressure fluctuations which also are broadband in nature[3]. For enclosed flames, however, such as those considered herein, the pressure spectrum is modified by the presence of the duct natural frequencies. Theoretically, this may be explained in terms of the Green's function G and the requirement that the frequency spectrum of the time rate of variation of the heat release rate (the source for the pressure fluctuations, see Eq. (7)) be bounded. The latter requirement implies that $\overline{(\frac{\partial q}{\partial t})(\frac{\partial q}{\partial t})^*}$ varies approximately as $\omega^{-n}$ where n is a positive number. This implies that $\omega^2 S_{qq}$ also varies as $\omega^{-n}$. Thus, the frequency dependence of the pressure spectrum may be given by (see Eq. (15))

$$S_{pp} \sim \omega^{-n} |G|^2$$

As noted earlier, the Green's function G is maximized at the natural frequencies of the duct. However, the presence of $\omega^{-n}$ ensures that the pressure fluctuations also exhibit an upper cutoff and it will be only the first few natural frequencies that will be significant in the spectrum.

The theory constructed herein is valid for any flame shape in the combustion region, as long as this region is compact compared to the relevant acoustic wavelength. The flame shape is largely dependent upon the nature of the flow field in the combustion region. In the theory, the flow effects are

not included directly but are included implicitly in the unsteady heat release (which is controlled by the flow to a large extent) which is presumed known. Thus, it is assumed that the sound pressure fluctuations are mainly affected by changes in the unsteady heat release and are not directly modified by the flow field (i.e., the effect of the flow field is indirect via the unsteady heat release). To check this assumption , the flame shape was changed by introducing a second flame holder into the combustion region as shown in Fig. 7. This second flame holder was a cylindrical rod, 5 mm in diameter and its introduction resulted in the formation of a double v-shaped flame. The position of this flame holder could be adjusted with respect to the original flame holder (i.e., the wire). Thus, several different combustion zones could be investigated.

As an example consider a set of experiments in which the vertical displacement Y between the flame holders was held fixed while the axial displacement X was varied. It was found that depending upon the distance, X, the pressure levels measured at $x = 0$ varied between 100 to 140 db. However, in all cases, the changes in the pressure levels were linearly related to the changes in the radiation levels. This is shown in Fig. 8, which plots the obtained pressure levels as a function of the corresponding radiation levels at the first natural frequency. The predicted pressure spectra were also found to be in good agreement with the experimentally measured spectra in all cases. These experiments, therefore, verify the assumption inherent in the theoretical model, that changes in the flow field affect the generated sound mainly by changing the associated combustion rates and not in a direct manner.

## CONCLUSION

A theoretical model capable of predicting the sound generated by confined flames has been developed and verified by comparison with experimental data. The relationship between the frequency contents of the unsteady flame heat release and the generated pressure spectra has been shown to depend upon the natural frequencies of the duct enclosing the flame. Finally, it has been shown experimentally that for low velocity situations the flow field influences the sound field only indirectly through its influence upon the combustion process.

## REFERENCES


1. Waugh, R. C. and Brown, R. S., "A Literature Survey of Combustion Instability," CPIA Publication No. 375, pp. 1-13, April 1983.

2. Zinn, B. T., "Pulsating Combustion," Mechanical Engineering, pp. 36-41, August 1985.

3. Strahle, W. C., "A More Modern Theory of Combustion Noise," in Recent Advances in the Aerospace Sciences (Editor: C. Casci), Plenum Press, New York, pp. 103-114, 1985.

4. Strahle, W. C., "On Combustion Generated Noise," J. Fluid Mechanics, Vol. 49, pp. 399-414, 1971.

5. Shivashankara, B. N., Strahle, W. C. and Handley, J. C., "Evaluation of Combustion Noise Scaling Laws by an Optical Technique," AIAA Journal, Vol. 13, pp. 623-627, 1975.

6. Barrere, M. and Williams, F. A., "Comparison of Combustion Instabilities Found in Various Types of Combustion Chambers," 12th Symposium (International) on Combustion, 1969.

7. Poinsot, T. Hosseini, K., Le Chatlier, C., Candel, S. H. and Esposito, E., "An Experimental Analysis of Noise Sources in a Dump Combustor" in Dynamics of Reactive Systems Part I: Flames and Configurations (Editors: Bowen, J. R., Leyer, J. C. and Soloukhin, R. I.), Vol. 105, Progress in Astronautics and Aeronautics, AIAA, New York, pp. 333-345, 1986.

8. Hedge, U. G., Reuter, D., Zinn, B., T. and Daniel, B. R., "Fluid Mechanically Coupled Combustion Instabilities in Ramjet Combustors," AIAA Paper No. 87-0216, 1987.

9. Goldstein, M. E., "Aeroacoustics," McGraw Hill, New York, 1976.

10. Morse, P. M. and Ingard, K. U., "Theoretical Acoustics," McGraw Hill, New York, N.Y., 1968.

11. Hegde, U. G. and Strahle, W. C., "Sound Generation by Turbulence in Simulated Rocket Motor Cavities," AIAA Journal, Vol. 23, No. 1, pp. 71-76, 1985.

12. Gaydon, A. G. and Wolfhard, H. G., "Flames: Their Structure, Radiation and Temperature," 4th Edition, John Wiley and Sons, N.Y., 1979.

13. Pierce, A. D., "Acoustics," McGraw Hill, N.Y., 1981.

## LIST OF FIGURES

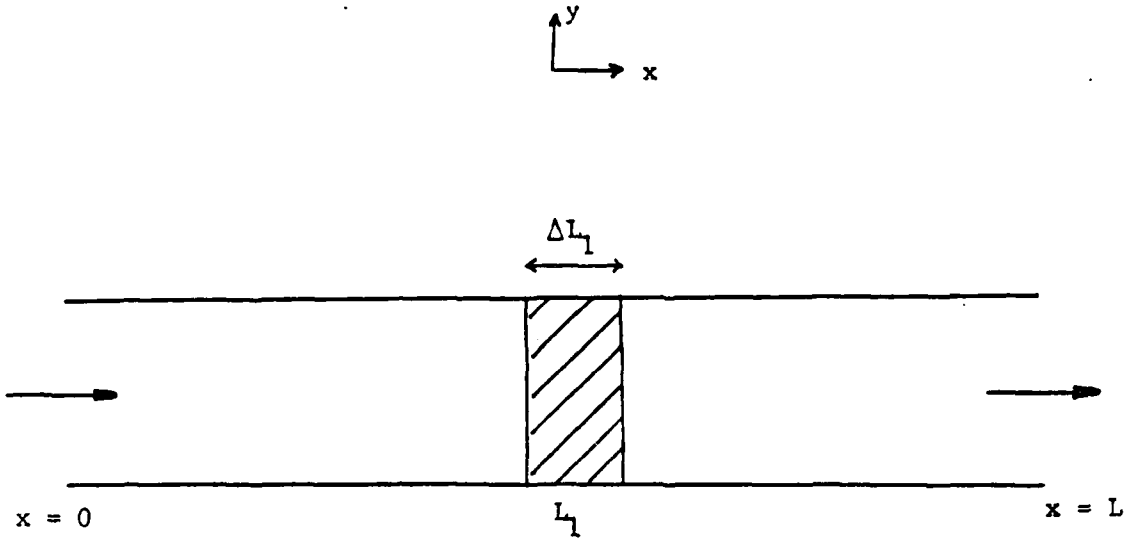


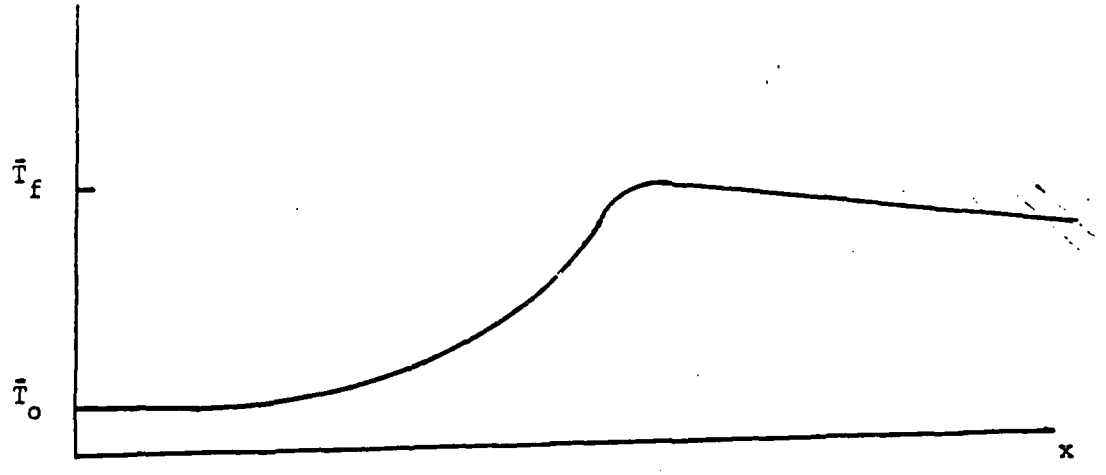


Fig. 1

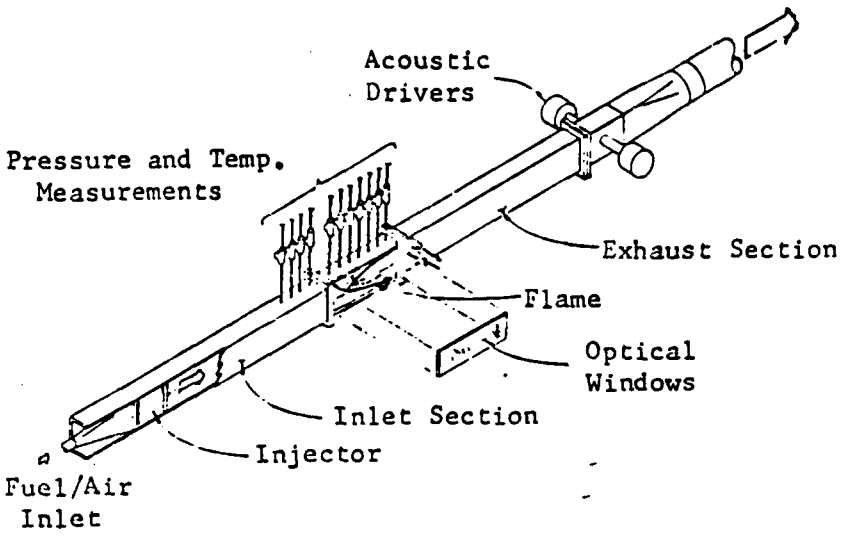
Acoustic
Drivers
Pressure and Temp.
Measurements
Exhaust Section
Flame
Optical
Windows
Inlet Section
Injector
Fuel/Air
Inlet

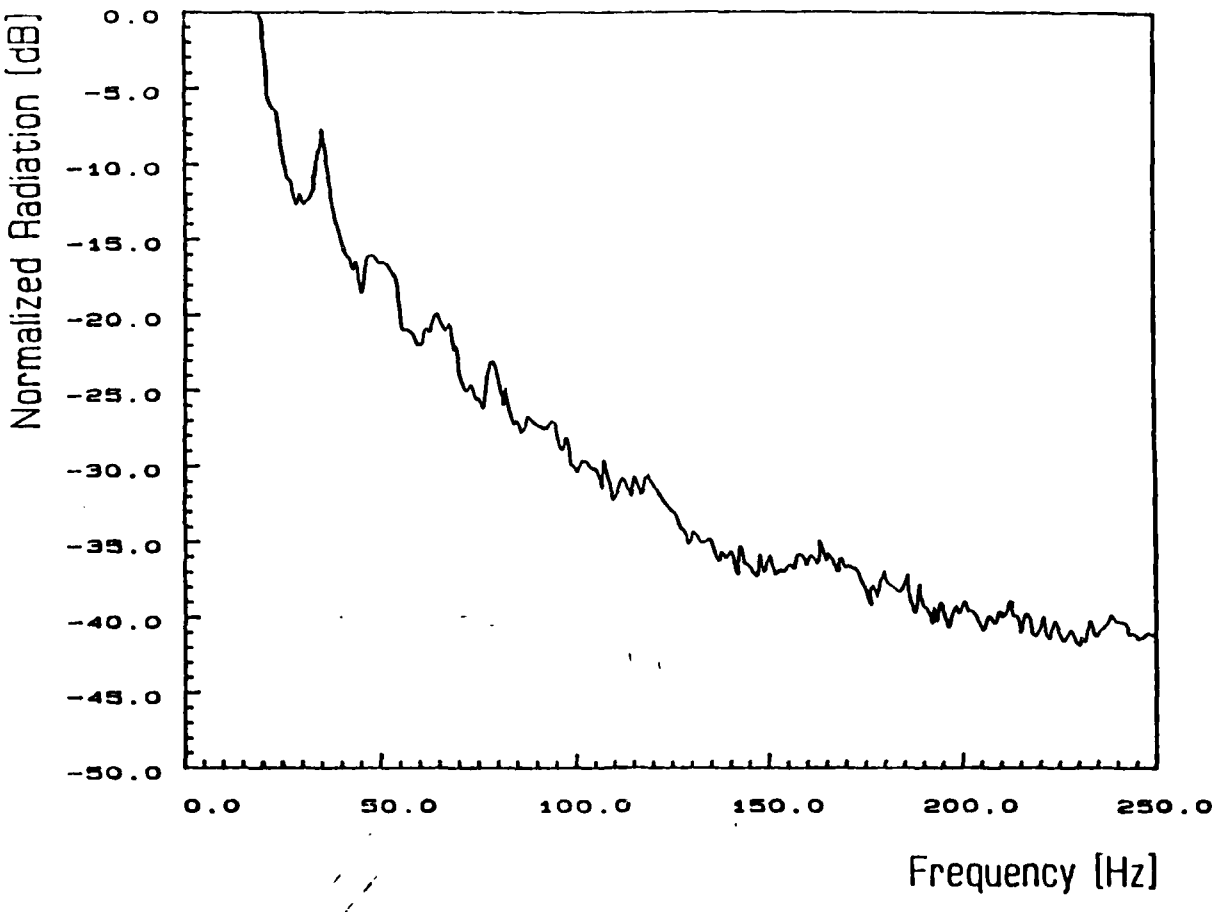
Normalized Radiation [dB]
0.0
-5.0
-10.0
-15.0
-20.0
-25.0
-30.0
-35.0
-40.0
-45.0
-50.0
0.0
50.0
100.0
150.0
200.0
250.0
Frequency [Hz]

Fig 3

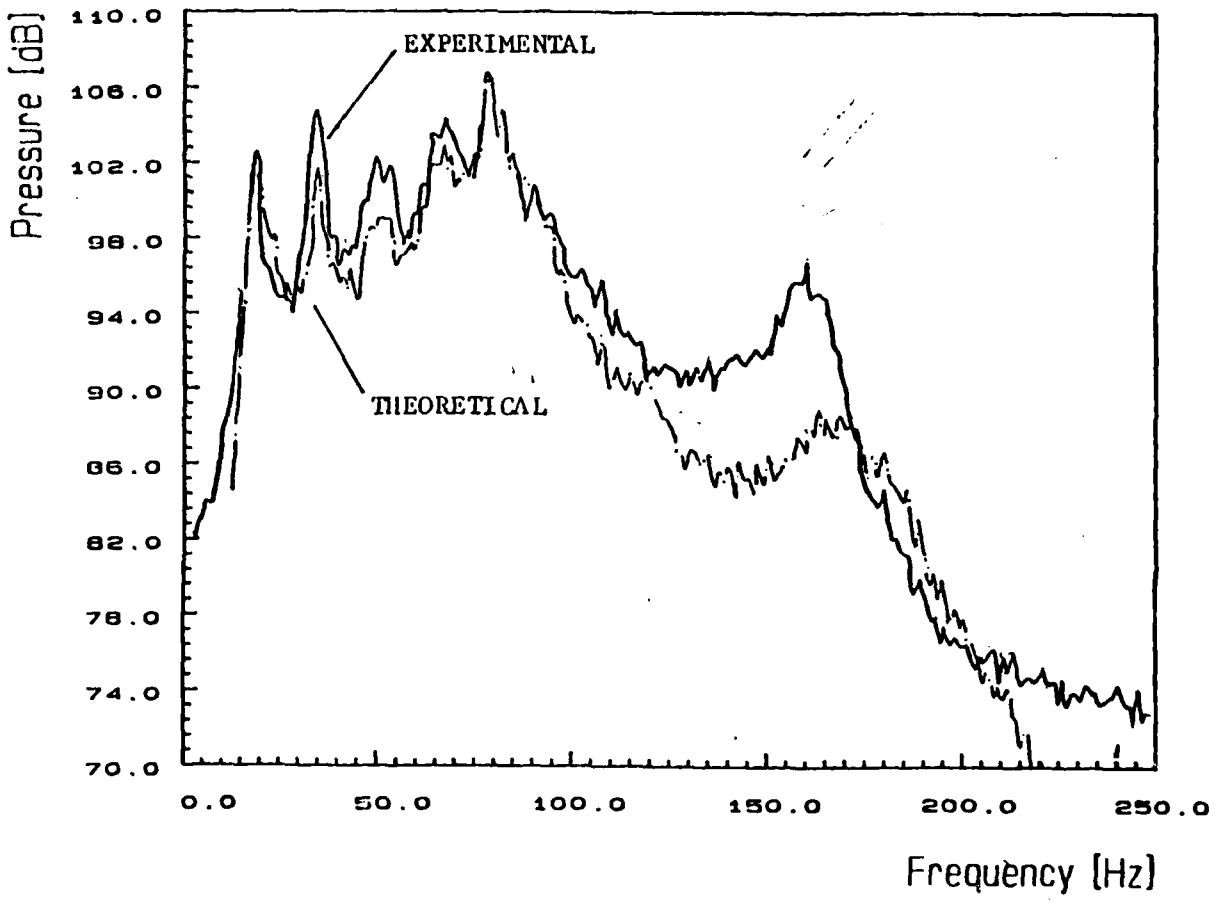
Pressure [dB]
110.0
106.0
102.0
98.0
94.0
90.0
86.0
82.0
78.0
74.0
70.0
EXPERIMENTAL
THEORETICAL
0.0
50.0
100.0
150.0
200.0
250.0
Frequency [Hz]

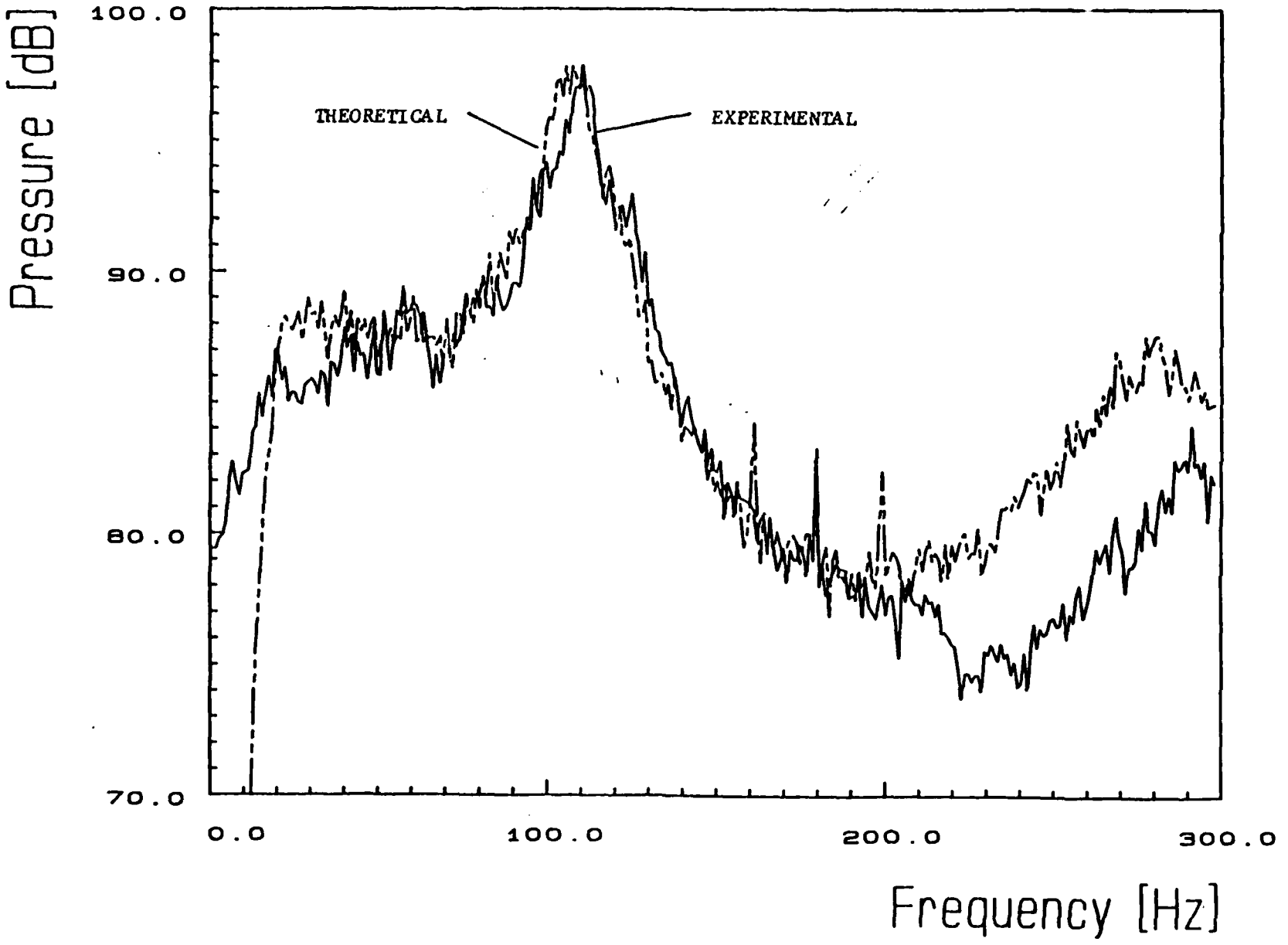
Pressure [dB]
100.0
90.0
80.0
70.0
THEORETICAL
EXPERIMENTAL
0.0
100.0
200.0
300.0
Frequency [Hz]

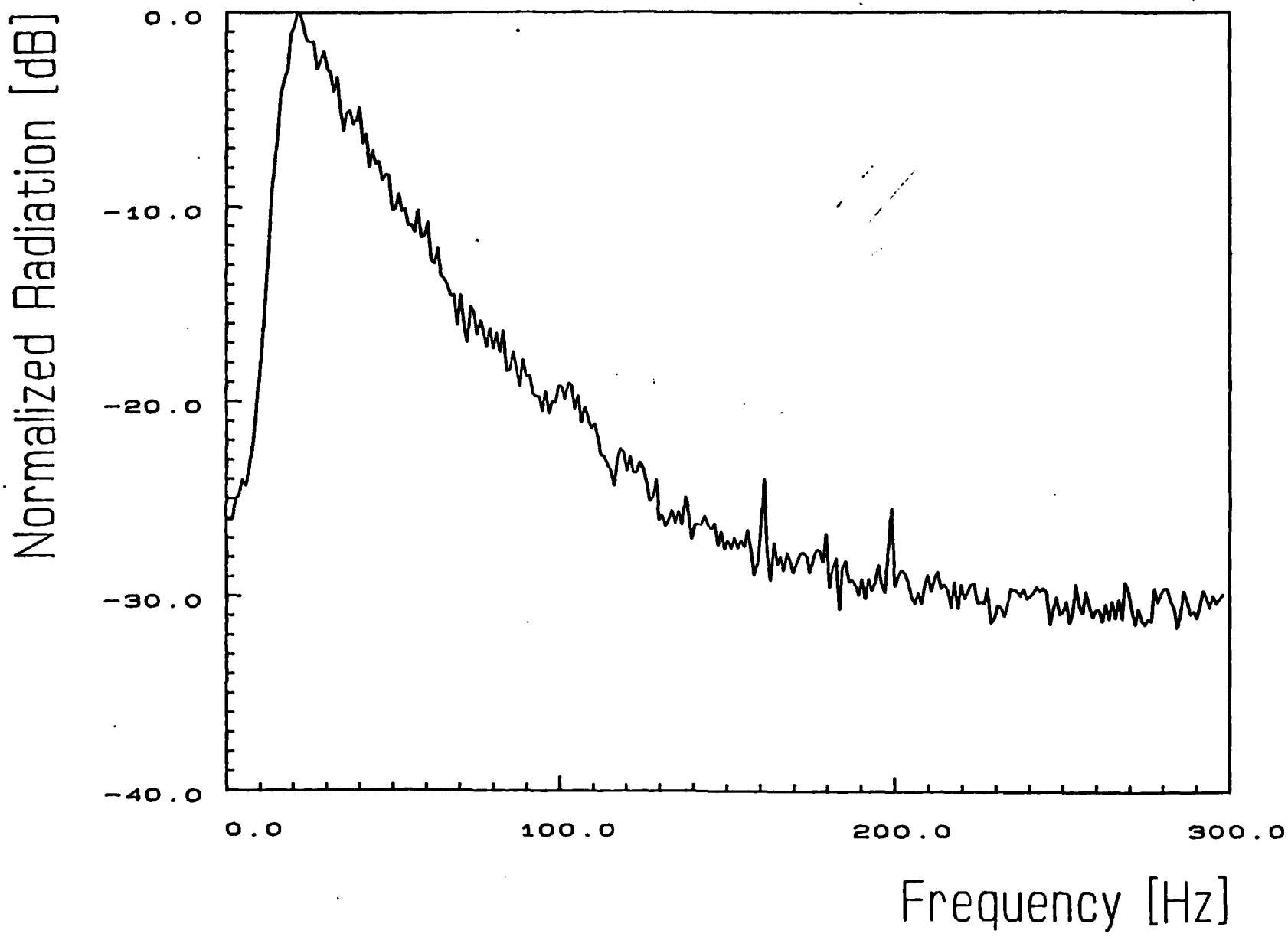
Normalized Radiation [dB]
0.0
-10.0
-20.0
-30.0
-40.0
0.0
100.0
200.0
300.0
Frequency [Hz]

PART II

(7/1/87 - 2/29/88)

AIAA'88

# AIAA-88-2855
# Flowfield Measurements in an Unstable Ramjet Burner

D.M. Reuter, U.G. Hegde and B.T. Zinn, Georgia Institute of Technology, Atlanta, GA

**AIAA/ASME/SAE/ASEE 24th JOINT PROPULSION CONFERENCE**

July 11-13, 1988/Boston, Massachusetts

# Flowfield Measurements in an Unstable Ramjet Burner

D. M. Reuter#, U. G. Hegde## and B. T. Zinn###
Georgia Institute of Technology
Atlanta, Georgia 30332

## Abstract

This paper investigates the flow field in the flame region of an unstable laboratory ramjet burner. The steady and unsteady components of the velocity field are obtained using a conditional sampling laser-Doppler velocimetry (LDV) technique. The vorticity field is also derived from the measured velocity field. It is shown that combustion instability in the ramjet burner is accompanied by unsteady vortex shedding at the flame holding region. The vortex shedding occurs at the frequency of instability and it periodically distorts the flame front causing a cyclic variation of the flame area. This variation in the flame area results in a strong unsteady heat release rate capable of driving the longitudinal instabilities in the system.

## Introduction

Combustion instabilities often occur in coaxial, dump type ramjet combustors. These instabilities are characterized by either low frequency (i.e., rumble) or high frequency (i.e., screech) pressure and velocity oscillations. The low frequency pressure and velocity oscillations are encountered in the range of 50 - 500 Hz and involve longitudinal acoustic oscillations at a natural frequency of the combustor. These oscillations are undesirable because their interaction with the inlet shock system of the ramjet may result in inlet unstarting and loss of engine performance. In addition excessive vibrational loads on the system may result. This paper investigates the mechanisms controlling the low frequency instability by studying the flowfield in the combustion zone of a laboratory ramjet burner.

Previous studies [1,2] of this problem have suggested that these low frequency instabilities are driven by unsteady combustion in vortical structures shed at the flame holding region in the ramjet combustor. Unstable modes of the shear layer formed in the wake of the flame holder are believed to interact with the unstable acoustic mode of the combustor at the frequency of instability [3] to give rise to the vortex shedding process. This paper describes a continuation of the above mentioned studies and presents results of experimental measurements of the unsteady combustor flow field. These measurements provide a detailed description of the velocity field in the ramjet flame region as well as yield insights into the vortex shedding process. The measurements also show that the shed vortices affect the flame structure and cause an oscillatory heat release rate capable of sustaining the acoustic instability.

The following *Experimental Set-Up* section briefly describes the ramjet simulator specifically developed for this investigation and the velocity measurement technique. The *Experimental Results* section presents measurements of the unsteady velocity and the shear layer structure and provides details of the vortex shedding process. The effects of the unsteady vortex structures on the ramjet flame are also discussed.

## Experimental Set-Up

A schematic of the basic experimental apparatus, described in detail in earlier papers [1], is shown in Figure 1. It consists of a sintered stainless steel injector through which a mixture of propane and air is introduced into a 7.5 x 5 $cm^2$ rectangular duct which is 3 m long. A W-shaped premixed flame, see Figure 2, is stabilized in the combustor section by means of two 6 mm diameter steel cylinders which are held in position perpendicular to the flow by two thin support wires. Figure 2, which is drawn to scale, shows the geometry of the flame arrangement. This configuration results in strong acoustic oscillations of the order of 140 dB at the first natural frequency, $f_0$, of the duct, and is therefore appropriate for investigating the instability mechanisms. The side walls of the combustor section are made of quartz to enable optical access to the flame region. In addition pressure transducers and thermocouples are used to characterize the acoustic pressure field and the temperature rise across the flame.

The flow entering the combustion chamber is parallel and uniform. The cold flow velocity is 1.9 m/s resulting in a Reynolds' number, based on the duct height, of the order of 10,000. Any residual turbulence or large scale velocity fluctuations in the inlet section of the duct is suppressed at the entrance of the combustor by means of a 63 mm long honey comb section which suppresses the measured turbulence to a value of 2% of the free stream velocity. A low free stream turbulence level is important because large random velocity fluctuations may mask the periodic velocity changes associated with the instability.

Velocity measurements have been carried out by means of laser-Doppler velocimetry (LDV). The LDV system used in the present investigation has been installed in the two component dual beam arrangement in the forward scatter mode and provides measurements of the axial and normal velocities. Both channels of the LDV are frequency shifted for the detection of possible reversed flows. The laser light source provides approximately 5 watt continuous power output. The photomultiplier signal from the LDV is analyzed by counter type signal processors. The data is digitally transferred to the core memory of a computer where it is stored on disk and subsequently analyzed.

Gas phase LDV measurements depend on seeding particles which are small enough to follow the flow. The arrangement used here introduces titanium dioxide seed

# Graduate Research Assistant. Member AIAA
## Research Engineer. Member AIAA
### Regents Professor. Fellow AIAA

particles of an average size of 0.19 μm into the flow upstream of the flame. This seeding material has been previously tested by DeGroot [6] and shown to be able to follow highly turbulent flows at frequencies up to 1 kHz. The developed seeding arrangement provides dense seeding only in the vertical center plane of the combustor and therefore reduces the rate at which particles agglomerate on the optical windows.

The major focus of this investigation is on the unsteady velocity components in the flame region of the combustor which are associated with the instability. These velocities have been obtained by conditional (phase locked) sampling [4,5,6]. This technique determines the phase of each velocity data point with respect to a reference signal. Since the acoustic instability is expected to be synchronized with the oscillations of the velocity field, a trigger pulse generated electronically from the pressure signal has been used to start each sample period which therefore spans one cycle of the pressure oscillation. Each sample period is divided in the present investigation into 16 subintervals each of which may be "tagged" with a phase, Ø, relative to the pressure. Data is collected over a number of sample periods (approximately 3000 data points are typically obtained. A phase averaging technique described next, is then used to obtain the steady state and phase dependent components of the velocity vector. The velocity vector, v, is written as

$$v = Ui + Vj$$

where U and V are the axial and normal components respectively. The data in each phase subinterval for each component (U or V) is first averaged. This results in sixteen averaged velocity data points (for each velocity component) spanning one cycle of the pressure oscillation. A least squares cosine curve is the employed to "fit" the measured velocity as a function of the phase angle Θ. For example,

$$U = \bar{U} + U' \text{ where}$$
$$U' = U_0 \cos \Theta$$

where $\bar{U}$ is the steady state or phase independent component of U and $U_0$ is the amplitude of the phase dependent component $U'$. The component, V, is dealt with in a similar fashion so that finally,

$$v = Ui + Vj = \bar{v} + v' = (\bar{U} + U')i + (\bar{V} + V')j$$

The experimental set-up is mounted on a linear, two axis translating system. Two stepper motors, controlled by the same host computer that collects the data from the LDV, are used to actuate each axis of the system. Here the axial coordinate is denoted by X and the normal coordinate is denoted by Y. Hence, the experiment is moved in the X and Y coordinate directions while the probe volume of the LDV remains stationary. The domain of the velocity measurements comprises a rectangle in a vertical plane centered between the two quartz windows of the combustor (Figure 2). The zero reference point is located 7.7 mm downstream of the center of the lower flame holder. The boundaries of the measured rectangular domain extend in axial direction from the reference point to a location 69 mm downstream of the reference point. The limits of the vertical boundaries extend from 16.5 mm below to 21.6 mm above the reference point. The measurement points are the nodes of a 26x21 staggered rectangular grid with a high density of points in the wake of the flame holder where the grid spacing is reduced to 1.3 mm in both axes from spacings of ΔX (in X) of 7.6 mm and a ΔY (in Y) of 2.5 mm at the upper and lower limit of the downstream boundary. It should also be pointed out that the vertical arrangement of the grid is not symmetric with respect to the reference origin. The grid spacing is more dense above the center line from Y=0 to Y=0.4 inch. This implies that more details of the flow field is revealed in the upper half plane and that the lower points merely serve to confirm the symmetry of the shedding process.

## Experimental Results

The velocity field of the W-shaped premixed symmetrical flame (Figure 2) has been measured. As noted earlier, this configuration resulted in an instability of the fundamental longitudinal mode ($f_0$=80Hz) of the duct. Figure 3 shows a vector plot of the steady state velocity field in the domain of measurement. The length of each vector scales with the magnitude of the velocity and the orientation of the arrow shows the direction of the local flow. The mean flow accelerates from 1.9 m/s at the inflow boundary to an average of about 9.0 m/s at the outflow boundary. The velocity profile is parallel and uniform with the exception of a velocity deficit in the wake of the flame holding cylinder. The burned gas temperature has been calculated based on mass conservation of the flow in the duct and the calculated result of 1150°C is close to the result obtained from thermocouple measurements.

The mean axial velocity profile is shown in Figure 4 as a function of Y for several axial locations. The plot shows that the flow behind the cylinder accelerates quickly due to the decrease in density of the burned combustion products. Therefore the velocity deficit in the wake of the cylinder disappears at about X = 0.3 inch and causes a reversal in the shear layer velocity gradients. The implications of this behavior is further discussed shortly. Figure 5 shows the mean U- velocity component as a function of X for several vertical Y locations. This plot also clearly shows the axial acceleration of the flow as well as the velocity deficit in the wake of the cylindrical flame holder.

The remainder of the paper will be focused mainly on the unsteady velocities and their effect on the flame structure. The phase of the pressure oscillation is denoted by Ø. A phase of Ø=0° represents the phase of maximum acoustic pressure during a cycle. Figure 6 shows the superimposed vector plot of the unsteady velocities for Ø=0° and Ø=180°. The velocity vectors fall very much on top of each other over much of the flow region with the exception of the wake flow behind the cylinder which indicates that the unsteady component of the velocity vector, $v'$, is small compared to the mean velocity vector, $\bar{v}$ over most of the measurement domain. For example, at a typical location (X=(1.0,-0.45)) the magnitude of the mean velocity is $|\bar{v}|$=3.47 m/s whereas the amplitude of the unsteady velocity is $|v'|$ = 0.24 m/s. It should be noted, however, that a steep increase in the standard deviation, σ, of the phase averaged velocity is observed as the measurements progress from the cold to the burned region of the flow. For example, typical values measured are:

$X_1$ = (0.1,-0.45): $|\bar{v}|$ = 1.84 m/s σ = 0.25 m/s
$X_2$ = (1.6,-0.45): $|\bar{v}|$ = 5.20 m/s σ = 1.0 m/s

This increase in the measured standard deviation of the velocity signal is most likely due to an increased turbulence

level caused by the combustion process as has been reported in the literature [7]. However, it is possible that changes in the flow field which are periodic at frequencies other than the frequency of instability could also cause the observed increase in the standard deviation of the velocity signal.

The steady vorticity, $\bar{\omega}$, of the flow is given by:

$$\bar{\omega} = \frac{\partial \bar{V}}{\partial X} - \frac{\partial \bar{U}}{\partial Y}$$

where $\bar{U}$ and $\bar{V}$ are the steady velocity components in the X (axial) and Y (normal) directions. The steady vorticity may be experimentally determined by finite differencing the above equation using the measured steady velocity components $\bar{U}$ and $\bar{V}$. Similarly, the unsteady vorticity, $\omega'$, may be calculated from the unsteady velocity components $U'$ and $V'$. The steady vorticity of the flow is shown in Figure 7. The plot shows equivorticity lines with an increment of 3 rad/sec. The figure shows a counter rotating vortex pair (A+ and A- in Figure 7) directly in the wake of the flame holder. This is caused by the velocity deficit of the wake. A second large pair of vortices (B+ and B- in Figure 7) is located further downstream of the first pair. This second pair is of opposite sign in comparison to the first one which is a manifestation of the accelerated flow downstream of the flame holders and the resulting reversal in the shear layer velocity gradients noted earlier in connection with Figure 4.

Figures 8 to 11 show the unsteady vorticity at Ø=0°, 90°, 180° and 270°. The velocity measurements reveal pairs of counter rotating vortices shed at the frequency of instability. During one period of the instability two pairs of vortices of opposite sign appear in the wake on both the top and bottom surfaces of the flame holder. As these vortices are accelerated by the mean flow field they also undergo stretching and lose intensity. The convection velocity of the structures is estimated as 1.0±0.5 m/s at X=0.2 inch and 4.0±0.5 m/s at X= 1.0 inch. These results confirm that the unsteady vortical structures are convected with approximately the mean flow velocity as suggested by earlier studies[1].

Figures 8 to 11 also show the instantaneous flame front superimposed on the unsteady vorticity. The location of the flame front has been obtained by means of a phase locked shadow photography technique described elsewhere [9]. Note that the scale of the abscissa differs from the scale of the ordinate and therefore the flame shape and the thickness of the vorticies are distorted. These figures suggest that the unsteady vortices cause the flame front perturbations which are observed in the shadowgraphy pictures. For example, at Ø=0° the "kinks" at X=0.7 inch in the flame (branch A and B in Figure 8) are believed to be caused by the adjacent counter rotating vortex pair. The "kinks" (branch A and B in Figure 9 at X=0.75 inch) continue to grow in size and the flame fronts are simultaneously rolled up by vortical structures marked A+ and B-. As the reaction fronts move closer together all the reactants between the two fronts is consumed and the "kinks" collapse as evident from Figure 10 where the remainder of the "kinks" are labelled A and B. The process repeats itself in a new cycle. For example, the first occurrence of flame perturbations are marked C and D at the inflow boundary of Figure 11. Therefore it is evident that that the vortex shedding causes a periodic distortion of the flame front.

This distortion of the flame front results in a cyclic variation of the flame area [2]. Since the reactants are consumed at the flame surface, the instantaneous flame surface area (the flame length in the two dimensional approximation) is a measure of the instantaneous reaction rate and, hence, the instantaneous heat release rate. The flame length has been determined experimentally as a function of the phase of the pressure oscillation by means of shadow photography [2]. The measured variation in flame length is shown in Figure 12 together with the acoustic pressure levels as a function of the phase of the pressure oscillation. The flame length is seen to be approximately in phase with the pressure. This finding suggests that the unsteady combustion and heat release rates are in phase with the pressure. It should be noted that this is consistent with Rayleigh's criterion [10] for the driving of acoustic waves by heat addition (i.e., the flame). Hence, the obtained flow field measurements demonstrate that the vortex shedding at the flame holders results in an unsteady heat release rate capable of driving the observed combustion instability in the burner.

## Conclusions

The role of the fluid mechanics of the flame region on the driving of combustion instabilities in a ramjet engine has been studied. Extensive measurements of the unsteady flow field have been carried out to characterize the interaction between the ramjet flame and the unsteady vortical field downstream of the flame holders. These measurements show that symmetric vortex shedding occurs in the wake of the flame holder at the frequency of instability. These vorticies periodically distort the flame front and cause oscillatory changes in the heat released rate which are capable of driving the observed instabilities.

## References


[1] Hegde, U. G., Reuter, D., Daniel, B. R. and Zinn, B. T., "Flame Driving of Longitudinal Instabilities in Dump Type Ramjet Combustors," Combustion Science and Technology, Vol. 55, No. 4-6, p. 125.

[2] Hegde, U. G., Reuter, D. and Zinn, B. T., "Combustion Instability Mechanisms in Ramjets," AIAA Paper No. 88-0150, January 1988.

[3] Flandro, G. A. and Finlayson, P. A., "Nonlinear Interactions between Vortices and Acoustic Waves in a Rocket Combustion Chamber," 21st JANNAF Combustion Meeting, 1984.

[4] Bell, W.A. and Lepicovsky, J., "Conditional Sampling with a Laser Velocimeter," AIAA 8th Aeroacoustics Conference, AIAA Paper No. 83-0756.

[5] Sankar, S.V., Investigation Of The Flame-Acoustic Wave Interaction During Axial Solid Rocket Instabilities, PhD thesis, Georgia Institute of Technology, Atlanta, Georgia 1987.

[6] Lepicovsky, J., "Laser Velocimeter Measurements of Large-Scale Structures in a Tone-Excited Jet," AIAA Journal, Vol. 24, No. 1, pp. 27-31, 1986.

[7] DeGroot, W. A., Laser Diagnostics of the Flow Behind a Backward Facing Step, PhD thesis, Georgia Institute of Technology, Atlanta, Georgia 1985.

[8] Ballal, D.R. and Chen, T-H., "Turbulence-Combustion Interaction in Practical Combustion Systems," AIAA/ASME/SAE/ASEE 22nd Joint Propulsion Conference, AIAA Paper No. 86-1607, 1986.

[9] Hegde, U. G., Reuter, D. and Zinn, B. T., "Driving Mechanisms in Unstable Ramjet Combustors," 16th ICAS Congress, August 1988. (to appear)

[10] Lord Rayleigh, The Theory of Sound, pp. 224 - 235, Vol. II, Dover Publications, 1945.

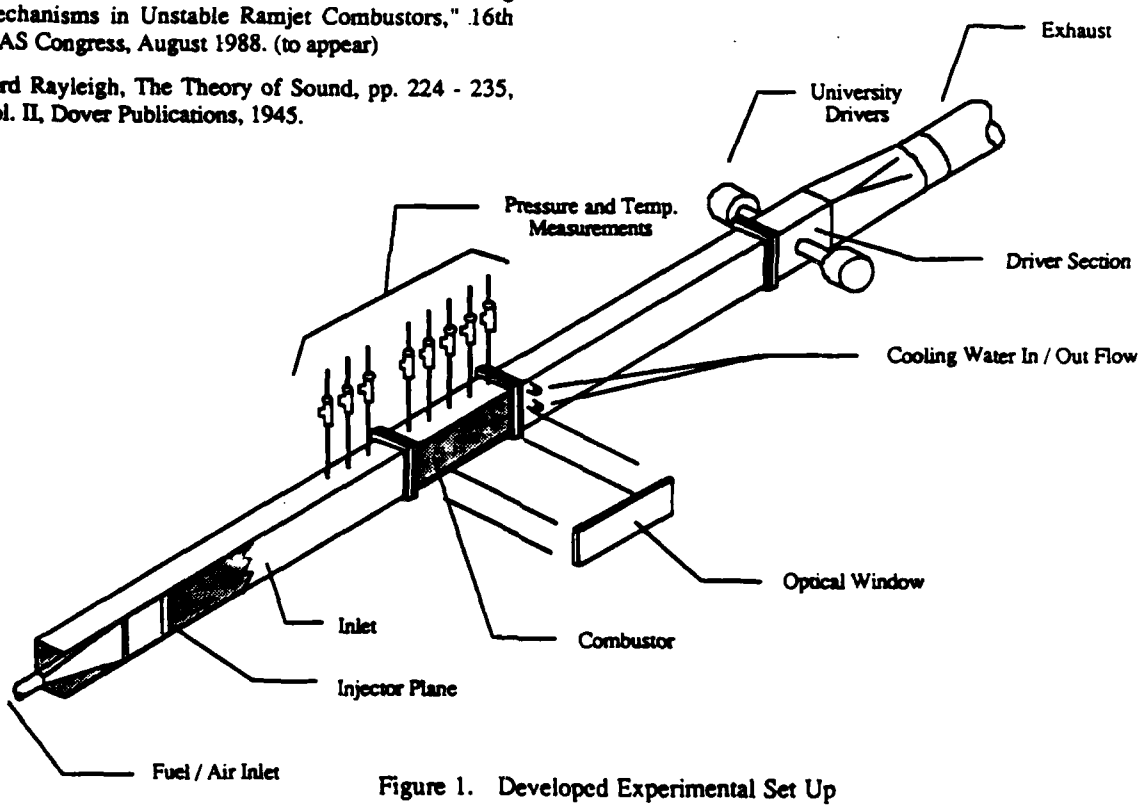


Figure 1. Developed Experimental Set Up

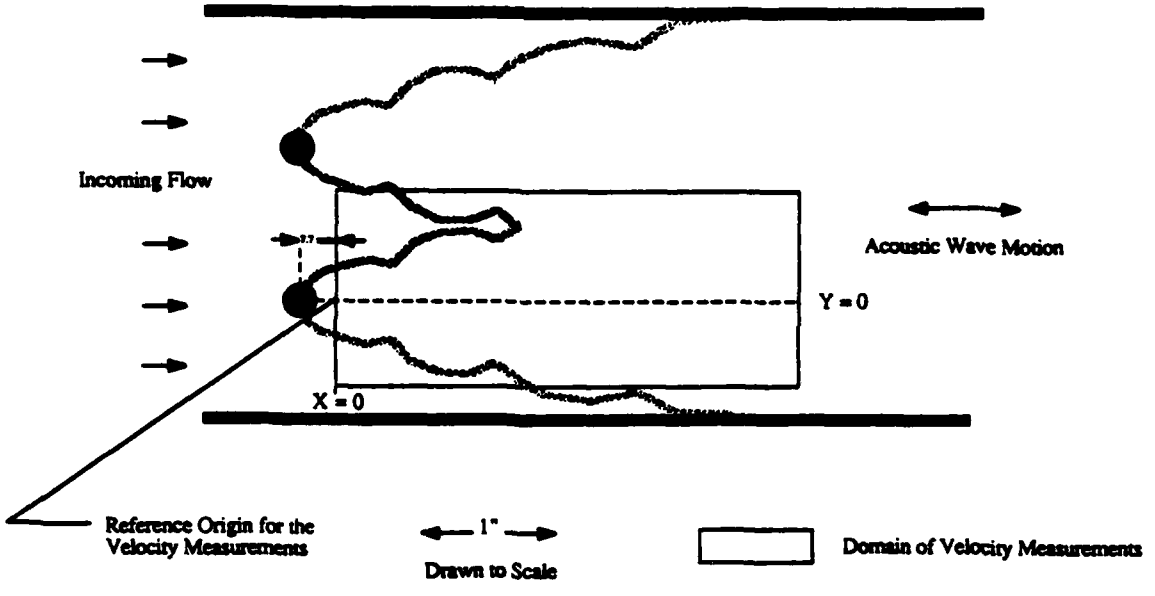


Figure 2. Schematic of Double Flame Set-Up

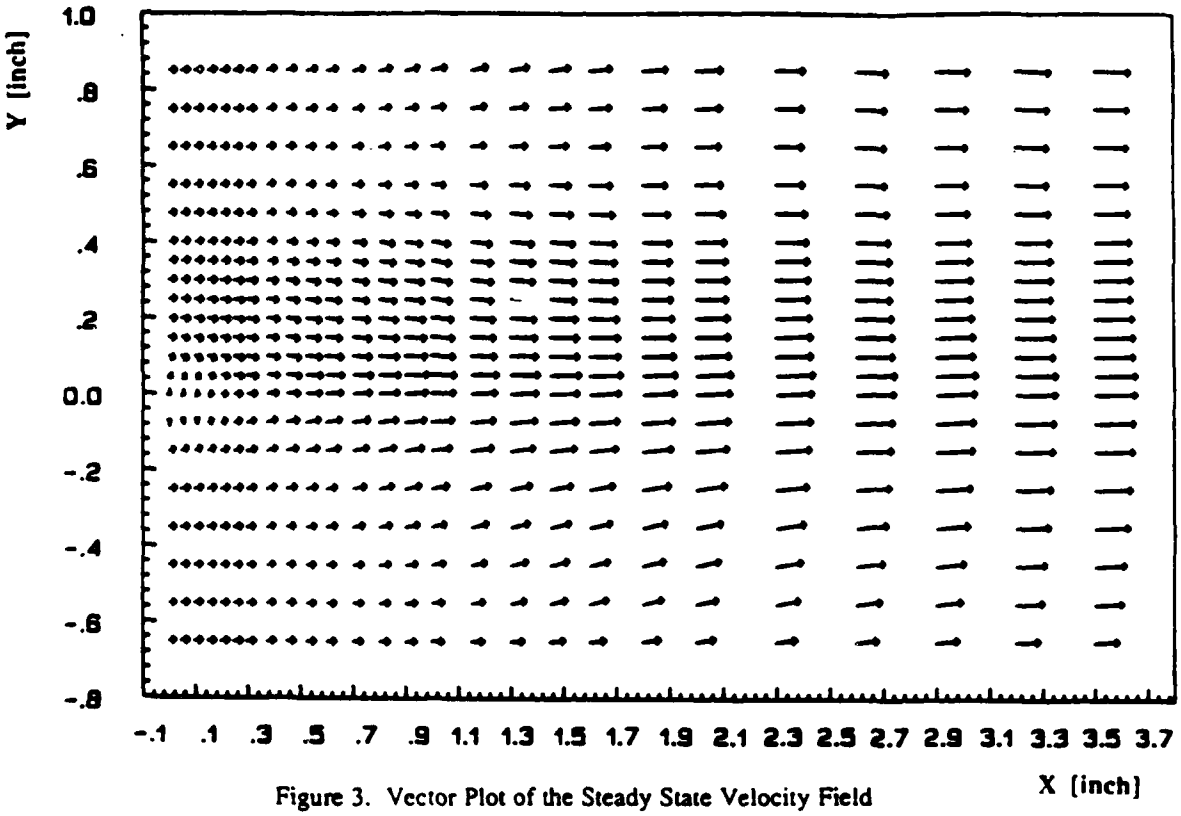


Figure 3. Vector Plot of the Steady State Velocity Field

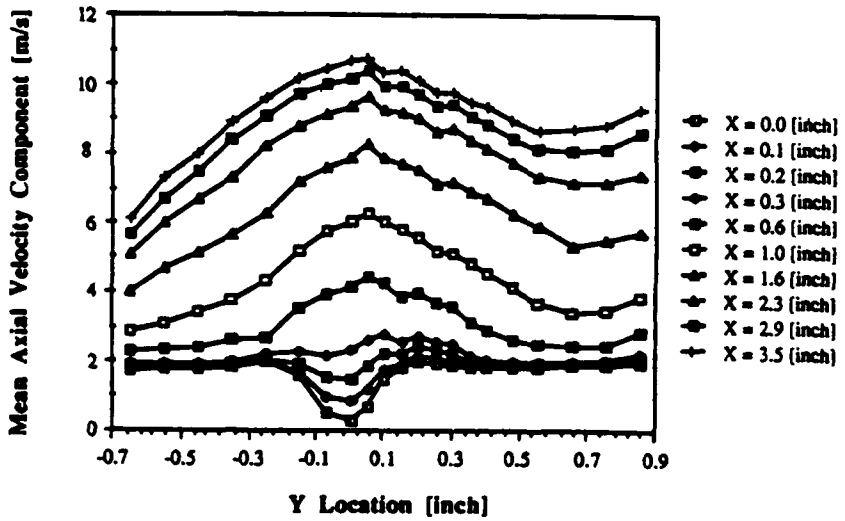


Figure 4. Mean Axial Velocity as a Function of Vertical Coordinate Y

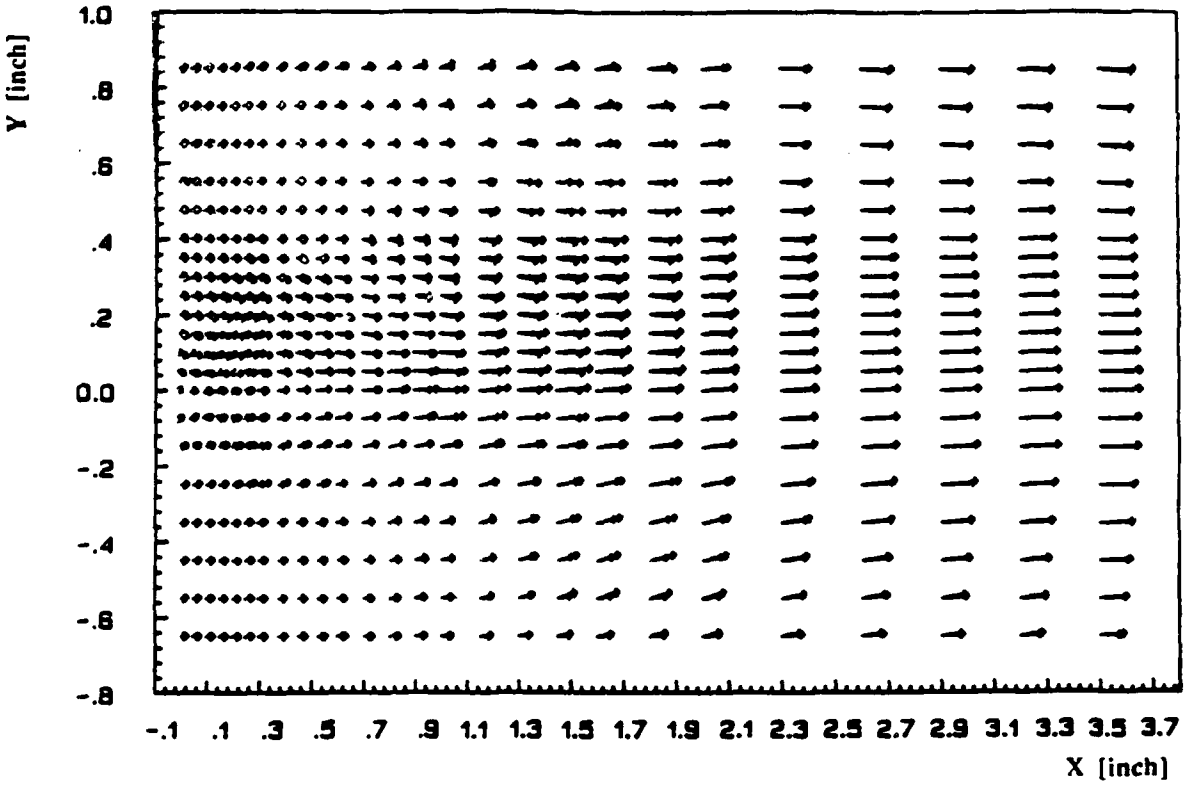


Figure 6. Superimposed Instantaneous Velocities at Ø=0° and Ø=180°

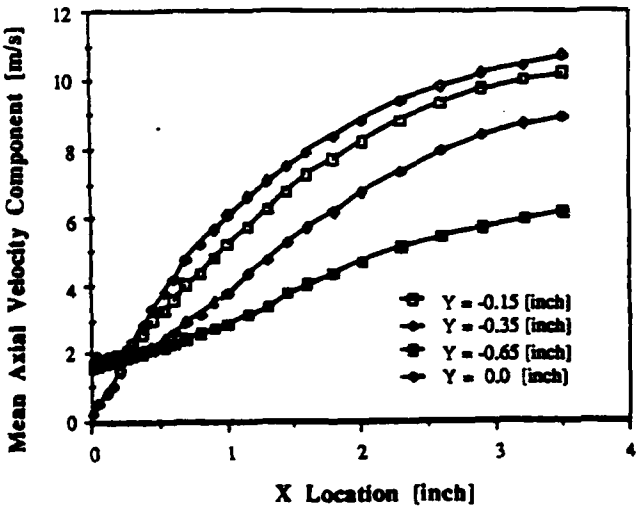


Figure 5. Mean Axial Velocity as a Function of Axial Coordinate X

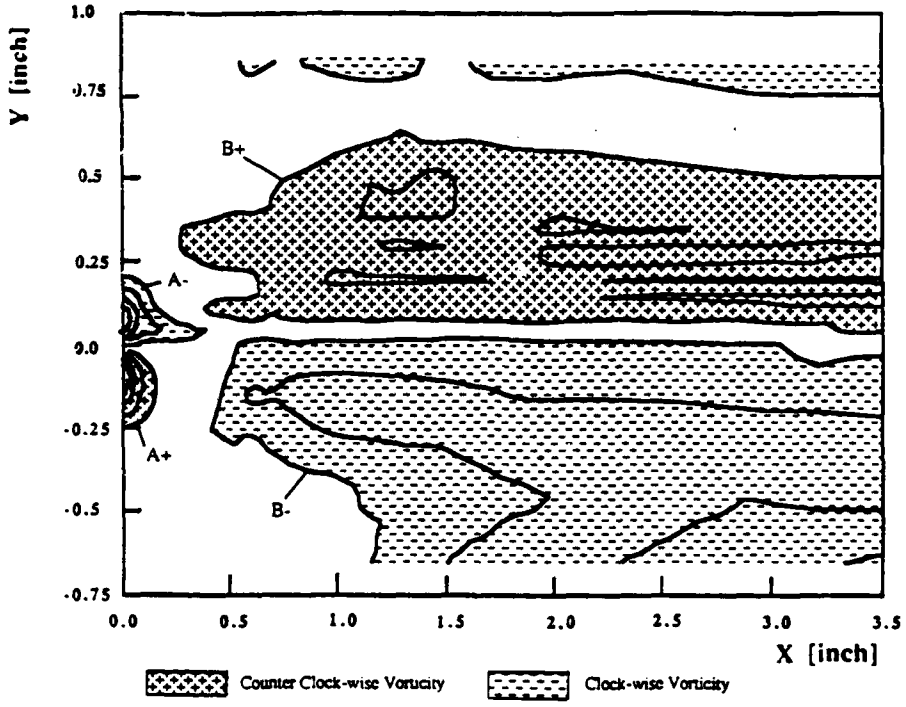


Figure 7. Mean Vorticity

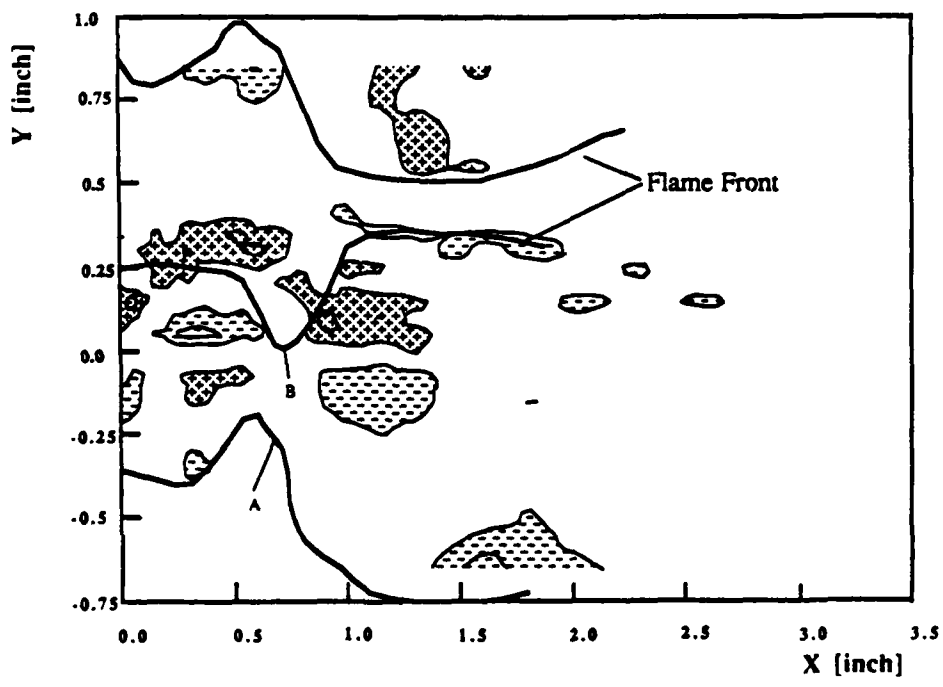


Figure 8. Unsteady Vortical Field for Phi = 0°

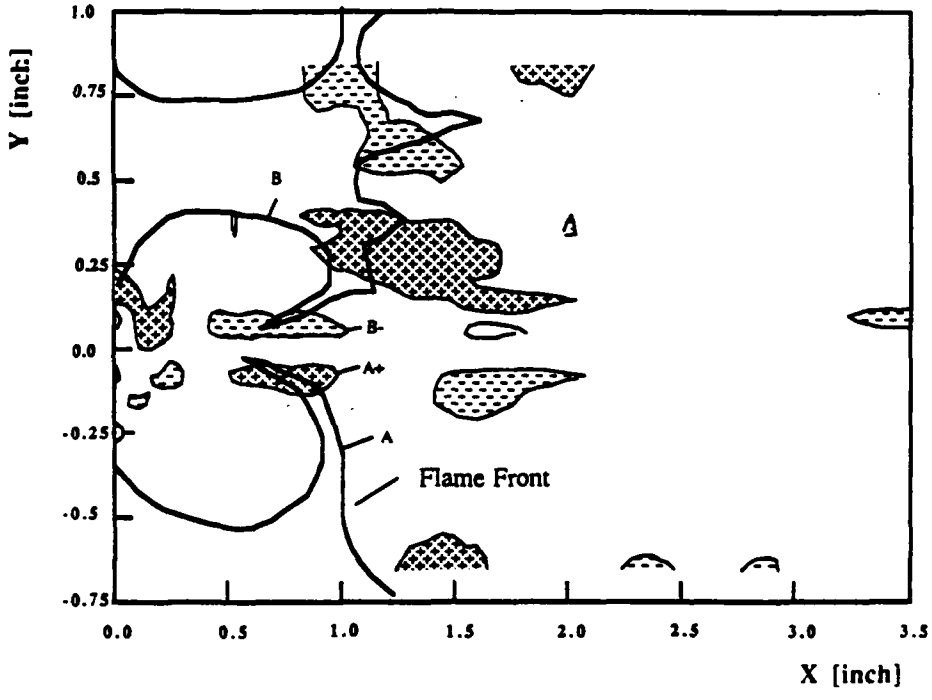


Figure 9. Unsteady Vortical Field for Phi = 90°

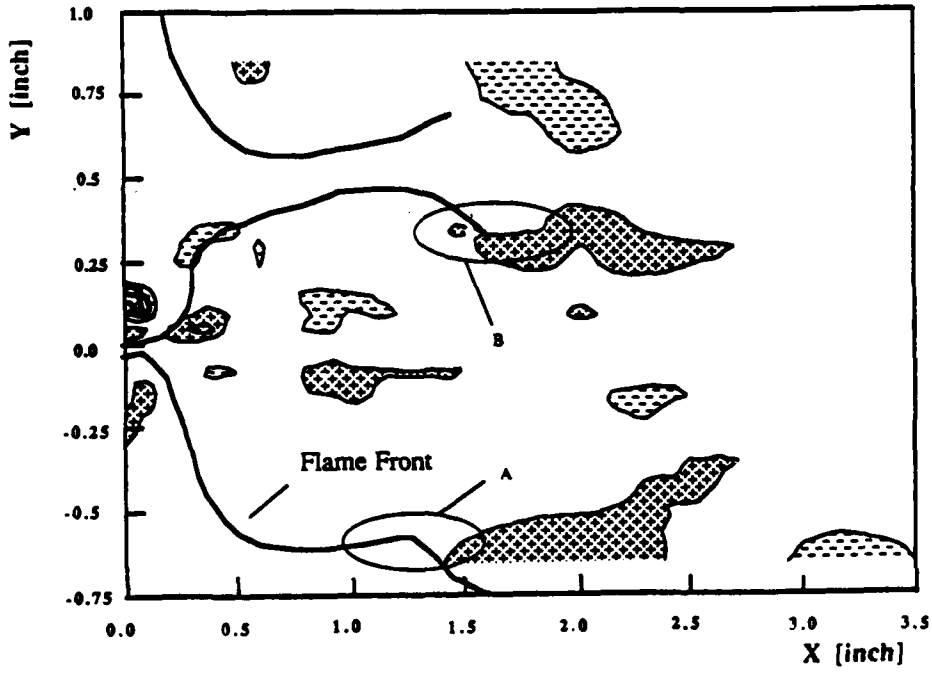


Figure 10. Unsteady Vortical Field for Phi = 180°

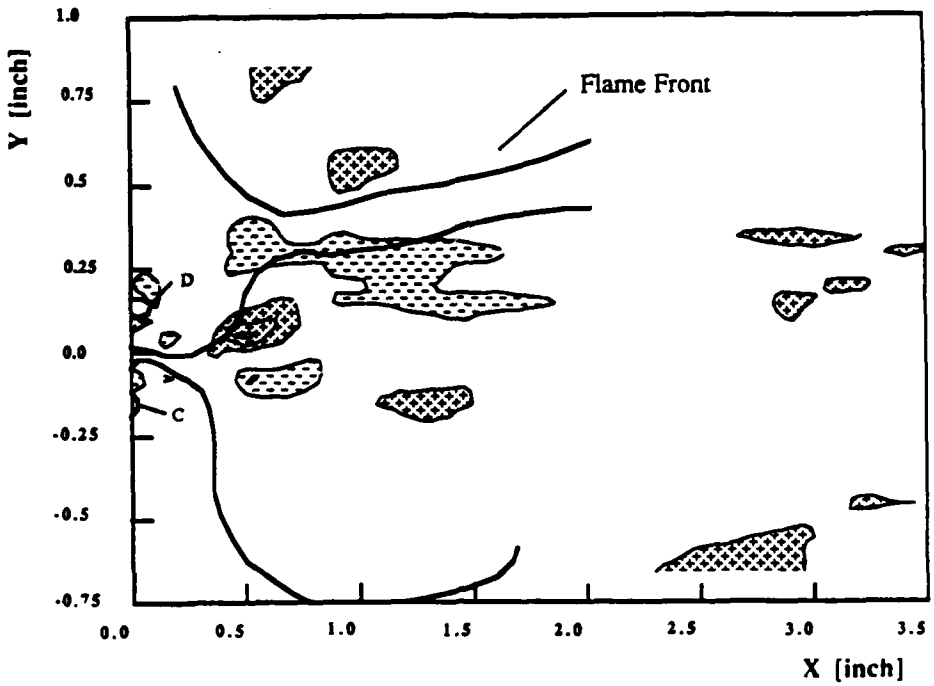


Figure 11. Unsteady Vortical Field for Phi = 270°

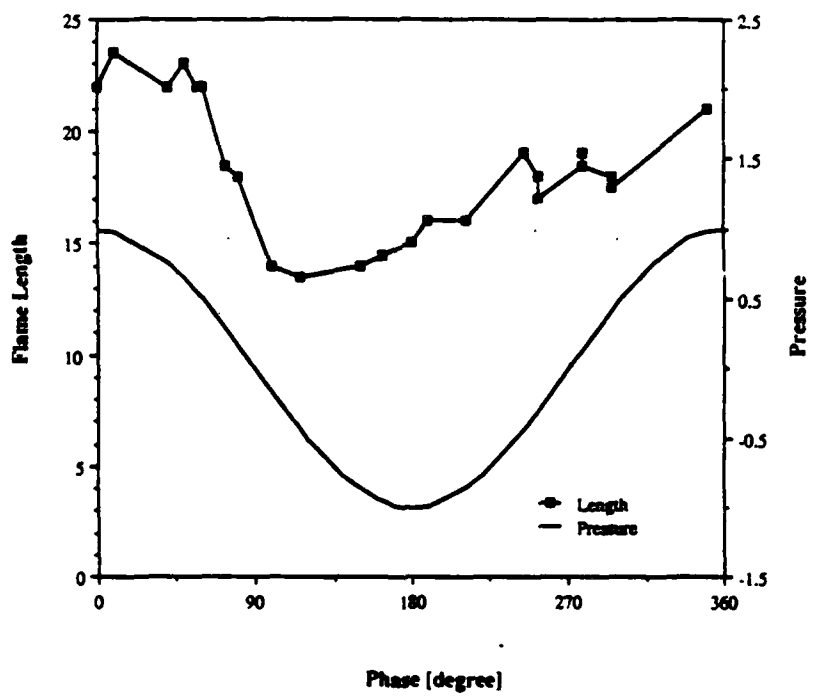


Figure 12. Flame Length and Pressure vs. Phase Angle